Signaltransduktion in membran-gebundenen Adenylatcyclasen

Dissertation

der Mathematisch-Naturwissenschaftlichen Fakultät

der Eberhard Karls Universität Tübingen

zur Erlangung des Grades eines

Doktors der Naturwissenschaften

(Dr. rer. nat.)

Vorgelegt von

Julia Grischin

aus Frunse (Kirgisien)

Tübingen

2020

Gedruckt mit Genehmigung der Mathematisch-Naturwissenschaftlichen Fakultät der Eberhard Karls Universität Tübingen.

Tag der mündlichen Qualifikation:	03. Juli 2020
Dekan:	Prof. Dr. Wolfgang Rosenstiel
1. Berichterstatter:	Prof. Dr. Joachim E. Schultz
2. Berichterstatter:	Prof. Dr. Peter Ruth

Danksagung

Mein besonderer Dank gilt meinem Doktorvater, Herr Prof. Dr. Joachim E. Schultz, für die Übergabe dieses überaus interessanten Themas und die sehr gute Betreuung während meiner Promotion. Er stand mir stets mit guten Ideen und wissenschaftlichen Diskussionen zur Seite und ermöglichte mir auch die Teilnahme an Kongressen, die meine Sicht auf das Forschungsgebiet erweiterten.

Bei Herr Prof. Dr. Peter Ruth bedanke ich mich sehr herzlich für die freundliche Übernahme des Zweitgutachtens meiner Dissertation und die Abnahme meiner Promotionsprüfung.

Herr Prof. Dr. Andrei Lupas danke ich sehr für die finanzielle und wissenschaftliche Unterstützung durch anregende Diskussionen und die Möglichkeit, das Projekt bei den Group Meetings vorzustellen, sowie für die Abnahme meiner Promotionsprüfung.

Für die erfolgreiche und produktive Kooperation bedanke ich mich bei Prof. Dr. Gottfried Unden und Juliane Wissig.

Des Weiteren bedanke ich mich bei Dr. Jens Baßler für die erfolgreiche und freundliche Zusammenarbeit und seinen bioinformatischen Beitrag zu dem Projekt.

Bei Anita Schultz möchte ich mich für ihre Hilfe und die Bereitstellung der Konstrukte sowie ihr Fachwissen bei jeglichen Fragen zur Klonierung bedanken.

Meinen derzeitigen und ehemaligen Kolleginnen und Kollegen Frau Ursula Kurz, Frau Anubha Seth, Herr Manuel Finkbeiner, Frau Dr. Stephanie Beltz und Prof. Dr. Klaus Hantke bedanke ich mich herzlich für das angenehme Arbeitsklima, die freundliche Aufnahme in die Arbeitsgruppe und die vielen fachlichen Diskussionen.

Allen Mitarbeitern der Arbeitskreise Drews, Lukowski und Ruth danke ich für die freundliche Atmosphäre und die nette Zusammenarbeit.

Meiner Familie und meinen Freunden danke ich besonders herzlich für ihre ermunternden Worte und Unterstützung in allen Lebenslagen.

Die experimentelle Tätigkeit für diese Arbeit erfolgte im Zeitraum 07/2016-11/2019.

Inhaltsverzeichnis

Abkürzungen

AC(n)	Adenylatcyclase(n)
hAC1-10	humane Adenylatcyclase Isoform 1-10
AS(n)	Aminosäure(n)
BSA	Bovines Serumalbumin
C1, C2	Katalytische Domänen in Mammalia-Adenylatcyclasen
CAP	Catabolite Activator Protein
CAI-1	*Cholera* Autoinducer-1
CqsS	*Cholera* Quorum-Sensing Sensor
CRE	cAMP Response Element
CTE	Cyclase-Transducing-Element
$CyaC_{Sm}$	Adenylatcyclase aus *Sinorhizobium meliloti*
DPBS	Dulbecco's Phosphate Buffered Saline
DTT	Dithiothreitol
EPAC	Exchange Protein Activated by cAMP
F-6-P	Fructose-6-Phosphat
FBS	Fetales Bovines Serum
FSK	Forskolin
G-6-P	Glucose-6-Phosphat
GLP-1	Glucagon-like Peptide 1
GLUT	Glucosetransporter
GPCR(s)	G-Protein gekoppelte(r) Rezeptor(en)
GTP	Guanosintriphosphat
HS	Humanserum
HSA	Humanserumalbumin
LAI-1	*Legionella* Autoinducer-1
LqsS	*Legionella* Quorum-Sensing Sensor
PKA	Proteinkinase A
Q_0	Chinon
Q_0H_2	Chinol
SQOR(s)	Succinat:Chinon-Oxidoreduktase(n)
TM	Transmembranhelix

Summary

Class III adenylate cyclases are important transmitters for external signals into the intracellular second messenger cAMP. According to sequence similarities, they are classified into four distinct classes, IIIa-d. Among them, the classes IIIa and IIIb stand out the most not only for being present in both prokaryotic and eukaryotic cells but also for carrying a large hexahelical membrane anchor with a potential regulatory function. Previous work on membrane-bound adenylate cyclases has indicated the ability to perceive extracellular signals through the similarly structured quorum sensors CqsS and LqsS from *V. harveyi* and *L. pneumophila*. However, a possible regulatory mechanism by the membrane anchors has not been defined yet.

One of 26 cyclases from *S. meliloti*, $CyaC_{Sm}$, shows a noteworthy similarity to succinate:quinone oxidoreductases regarding its membrane anchor.

It is a monomer consisting of one 6TM domain, a ferredoxin domain, and a catalytic domain. According to UV-Vis measurements, four highly conserved histidine residues are binding two heme B molecules as a prosthetic group in the first four α-helices of the membrane anchor. Hence, specifically replacing these residues by alanine demonstrated that these histidines are responsible for binding of heme B. Subsequently, *in vivo* and *in vitro* measurements of these mutants indicated a significant decrease in AC activity. The hypothesis of AC regulation by the quinone Q_0 and its reduced counterpart Q_0H_2 has been confirmed in this work. Experiments have shown a nearly threefold increase in cyclase activity under reduced (addition of Q_0H_2) to oxidized (addition of Q_0) conditions.

The formation of cAMP in mammalian cells is mainly regulated by GPCRs through the binding of the dissociated G protein subunit $G_s\alpha$ to the intracellular catalytic dimer. So far, direct regulation by an extracellular ligand for these adenylate cyclases has not been shown.

First *in vitro* experiments on the effect of several hormones and neurotransmitters on the human adenylate cyclase isoform 5 showed no significant changes in the amount of produced cAMP after activation with $G_s\alpha$.

Only the addition of heat-inactivated human serum resulted in a significant inhibition of the $G_s\alpha$-stimulated cyclase. This observation not only indicated the structural ability of the catalytic domains to recognize external signals, but also emphasizes the existence of a ligand in blood serum. The identification of ligands provides the basis for future research.

Zusammenfassung

Adenylatcyclasen der Klasse III sind wichtige Übersetzer externer Signale in den intrazellulären sekundären Botenstoff cAMP. In Anbetracht ihrer Sequenzähnlichkeiten lassen sich diese in vier alleinstehende Unterklassen, IIIa-d, unterteilen. Dabei wird den zwei Klassen IIIa und IIIb besondere Bedeutung zuteil; nicht nur, weil sie sowohl in Eukaryoten als auch in Prokaryoten vertreten sind, sondern auch aufgrund der oftmals großen hexahelikalen Membrananker mit einer naheliegenden regulatorischen Funktion. Bisherige Arbeiten über membrangebundene Adenylatcyclasen haben bewiesen, dass diese Enzyme die strukturelle Voraussetzung haben, extrazelluläre Signale mittels der strukturähnlichen Quorum-Sensing Rezeptoren CqsS und LqsS aus *V. harveyi* und *L. pneumophila* wahrzunehmen. Jedoch ist für membrangebundene Adenylatcyclasen bisher kein regulatorischer Mechanismus über den Membrananker beschrieben.

Eine von 26 Cyclasen aus *S. meliloti*, $CyaC_{Sm}$, weist in Bezug auf ihren Membrananker eine bemerkenswerte Ähnlichkeit zu Succinat:Chinon-Oxidoreduktasen auf. Dabei handelt es sich um ein Monomer bestehend aus einer 6 TM Domäne, einer Ferredoxin-Domäne und einer katalytischen Domäne. UV-Vis-Messungen zufolge binden vier hochkonservierte Histidinreste zwei Häm-B-Moleküle als prosthetische Gruppe innerhalb der ersten vier α-Helices des Membranankers. Daher zeigte der gezielte Austausch dieser Reste durch Alanin, dass diese Histidinreste für die Häm-B-Bindung verantwortlich sind. Anschließende *in vivo* und *in vitro* Messungen zeigten, dass das Enzym ohne Häm-B nur eine sehr geringe AC-Aktivität hat. In dieser Arbeit bestätigte sich die Hypothese einer Regulierbarkeit von $CyaC_{Sm}$ durch das Chinon Q_0 und das reduzierte Pendant Q_0H_2. In den Versuchen wurde eine beinahe dreifache Steigerung der Aktivität vom reduzierten (Q_0H_2-Zugabe) zum oxidierten Zustand (Q_0-Zugabe) gemessen.

Die Bildung von cAMP in Säugetierzellen wird überwiegend über GPCRs reguliert, indem die dissoziierte G-Protein-Untereinheit intrazellulär am

katalytischen Dimer bindet. Bisher steht der Beweis einer direkten Regulierung durch einen extrazellulären Liganden aus.

Erste *in vitro* Versuche, in denen die Wirkung ausgewählter Hormone und Neurotransmitter auf die humane Adenylatcyclase Isoform 5 untersucht wurde, zeigten nach Aktivierung durch $G_s\alpha$ keine signifikante Änderung des cAMP-Gehalts der Proben.

Allein die Zugabe von hitzeinaktiviertem Humanserum zeigte einen deutlich inhibierenden Effekt auf die durch $G_s\alpha$ stimulierte Cyclase. Dies weist nicht nur auf die mögliche Fähigkeit der katalytischen Domänen hin, Signale von außen wahrzunehmen, sondern auch auf die Existenz von Liganden im Blutserum. Die Identifizierung der Liganden bildet die Basis zukünftiger Forschung.

1. Einleitung

Die Viabilität von Zellen hängt von der Fähigkeit ab, wechselnde Umweltbedingungen und äußere Reize zu erkennen und darauf physiologisch adäquat zu reagieren. Durch die Abgrenzung des Zellinneren zur Außenwelt mithilfe der Zellmembran können nur wenige Stoffe die Lipiddoppelschicht frei passieren. Daher bedienen sich viele regulatorische Systeme eines Signalwegs mittels sekundärer Botenstoffe. Ein Großteil der primären Botenstoffe (darunter Hormone, Neurotransmitter und Zytokine) aktivieren membrangebundene Rezeptoren, die intrazelluläre Signale generieren und dadurch eine Zellantwort auslösen. Die nachgeschaltete Signalweiterleitung innerhalb der Zelle erfordert die Bildung eines sekundären Botenstoffs wie cAMP. cAMP ist an vielen Prozessen zur Zelldifferenzierung, Zellproliferation, Anpassung an den Nährstoffgehalt in der Umgebung, Aufrechterhaltung der Homöostase, etc. beteiligt (1).

Die Zyklisierung von ATP zu cAMP unter Abspaltung eines Pyrophosphatrestes erfolgt durch die sowohl in prokaryotischen als auch in eukaryotischen Zellen vorhandenen Adenylatcyclasen, die anhand ihrer Sequenz und Struktur in die sechs Klassen I-VI unterteilt werden. Zur Klasse I gehören Adenylatcyclasen vieler gram-negativer Bakterien der Familie Enterobacteriaceae wie *E. coli*. In Klasse II finden sich pathogene Bakterien wie *B. anthracis*, *P. aeruginosa* und *B. pertussis* (2), deren ACn sezerniert werden und als extrazelluläre Toxine fungieren, indem sie in Wirtszellen eindringen und durch Überproduktion zelltoxische cAMP-Spiegel aufbauen (3). In den bisher wenig erforschten Klassen IV-VI finden sich nur wenige, bakterielle Vertreter (4). In der zahlenmäßig größten Klasse III befinden sich hingegen sowohl prokaryotische als eukaryotische ACn (5). Diese Gruppe wird aufgrund konservierter Sequenzmotive in der katalytischen Domäne in vier Subklassen, IIIa-IIId, eingeteilt (3,5).

1.1 Bakterielle Adenylatcyclasen

Die für diese Arbeit interessanten bakteriellen ACn bestehen aus einer hexahelikalen TM-Domäne, an die sich C-terminal die katalytische Domäne anschließt. Jedes Monomer verfügt über sechs an der Katalyse beteiligte Aminosäuren (Abb. 1.1 rechts). Lysin und Aspartat gewährleisten die Substratspezifität. Zwei Aspartatreste binden bivalente Kationen (Mg^{2+} oder Mn^{2+}) als Kofaktoren für den nukleophilen Angriff an der 3‘-Hydroxylgruppe der Ribose von ATP, während Arginin und Asparagin den Übergangszustand stabilisieren (3,6). Durch die Bildung eines Homodimers nach der Aktivierung entstehen zwei katalytische Zentren (3).

Die Regulierung der Aktivität bakterieller ACn hat in der Forschung bisher nur wenig Interesse erfahren. Es gibt lediglich einige wenige Vertreter, deren Regulation nachweislich über den pH-Wert, Fettsäuren und CO_2 erfolgt (7-10).

Die Änderung der cAMP-Konzentration hat in Bakterien viele Auswirkungen. Gut erforscht ist hierbei die Katabolitrepression (11,12). Dieser Vorgang ermöglicht der Zelle ein schnelles Wachstum, indem Energie aus möglichst leicht verfügbaren Kohlenstoffquellen bezogen wird (12). Ausführlich untersucht wurde dabei die durch Glucose vermittelte *lac*-Repression im gramnegativen Bakterium *E. coli*. Dieses verfügt über eine einzige Adenylatcyclase CyaA aus der Klasse I und bevorzugt Glucose als Energiequelle. Erst wenn diese Kohlenstoffquelle erschöpft ist, bildet die Zelle Enzyme, die Zuckerquellen wie Lactose verstoffwechseln können (13). Diese Regulierung setzt nicht nur das Vorhandensein von Lactose in der Zelle voraus, sondern beruht auch auf einem rasanten Anstieg der cAMP-Konzentration, der durch das Fehlen von Glucose im Nährmedium ausgelöst wird (14).

In Bakterien vermittelt cAMP seine Wirkung größtenteils über eine direkte Bindung an das cAMP Response Element (CRE) (13,15). Der dimere cAMP-CAP-Komplex (cAMP-Catabolite-Activator-Protein-Komplex) wirkt als Aktivator für die Expression kataboler Operons, beispielsweise des *lac*-Operons, indem es sequenzspezifisch an DNA bindet (13). Dadurch wird die Bildung von β-Galactosidase initiiert, wodurch dem Bakterium Lactose zur Energiegewinnung zur Verfügung steht.

1.2 Eukaryotische Adenylatcyclasen

In Säugetieren wurden zehn Adenylatcyclase-Gene entdeckt, die für eine lösliche (AC10) und neun membrangebundene (AC1-9) Isoformen codieren. Die Expression der Isoformen ist teilweise gewebsspezifisch. AC10 (Subklasse IIIb) findet sich überwiegend in Spermatozoen und wird pH-unabhängig durch Bicarbonat aktiviert (16). Die Regulierung der Isoformen AC1-9 (Subklasse IIIa) ermöglicht eine weitere Unterteilung anhand ähnlicher Aminosäuresequenzen und funktioneller Eigenschaften. So sind AC1, AC3 und AC8 durch Ca^{2+}-Calmodulin aktivierbar, während AC2, AC4 und AC7 durch die Untereinheit $G_{\beta\gamma}$ reguliert werden können. Die Aktivität von AC5 und AC6 hingegen lässt sich mittels Ca^{2+} und $G_i\alpha$ hemmen. Anders als alle anderen ACn zeigte AC9 in vielen Arbeiten keine Stimulierung durch das pflanzliche Diterpen Forskolin (17-19) und steht somit allein. Jedoch besteht neueren Untersuchungen zufolge eine bedingte Stimulierbarkeit in Anwesenheit von $G_s\alpha$ (20,21).

Der Aufbau der Isoformen AC1-9 ist einheitlich, die Verankerung in der Membran erfolgt über 2 x 6 α-Helices. Die erste hexahelikale Transmembrandomäne (TM1) befindet sich am N-Terminus, an die sich die katalytische Domäne C1a anschließt. Über eine Linkerregion (C1b) ist diese mit der zweiten Transmembrandomäne (TM2) verbunden, auf die wiederum eine katalytische Domäne (C2a) mit abschließendem C-Terminus C2b folgt. Die cAMP-Synthese erfolgt durch die Bildung eines Pseudoheterodimers mittels der beiden hochkonservierten katalytischen Domänen C1a und C2a, wodurch zwei Bindetaschen geformt werden (2,4). An der katalytisch aktiven Bindestelle wird ATP zu cAMP umgewandelt, während an der katalytisch inaktiven Bindestelle Forskolin (FSK) die Aktivität der ACn erhöht (6,22).

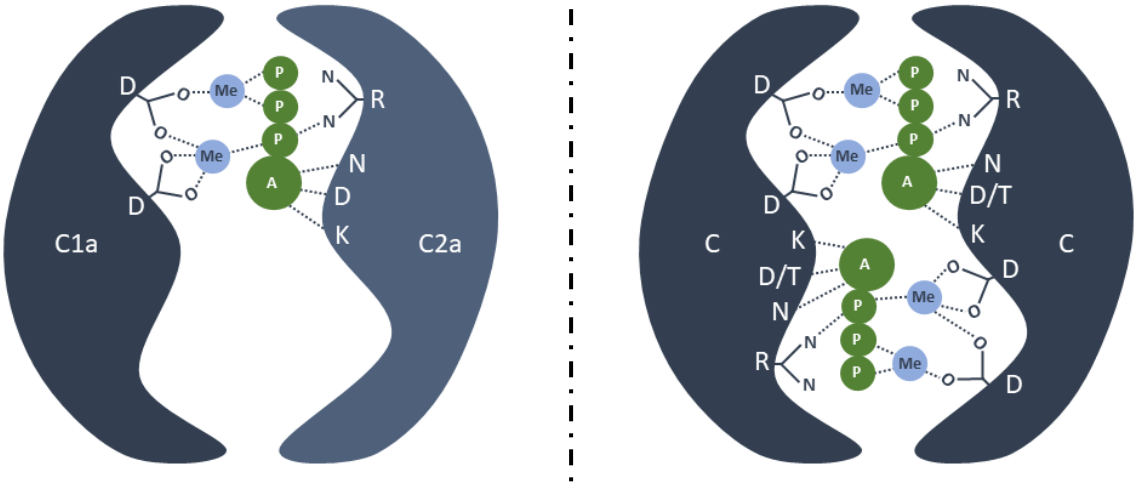

Abb 1.1 *Schematische Darstellung katalytischer Domänen in ACn mit den sechs an der Katalyse von ATP zu cAMP beteiligten Aminosäuren (ASn) im Einbuchstabencode. Darstellung des Substrats in Grün: A = Adenosin, P = Phosphatgruppe. Me = bivalentes Metallkation.* ***Links:*** *Eukaryotische ACn, die ein Pseudoheterodimer mit einem aktiven Zentrum bilden, während in dem inaktiven Zentrum FSK gebunden werden kann (nicht dargestellt).* ***Rechts:*** *Bakterielle ACn, die durch die Bildung eines Homodimers zwei katalytische Zentren aufweisen. Adaptiert nach (3).*

In Säugetierzellen wird die Bildung von cAMP über die größte Familie der Zelloberflächenrezeptoren, den G-Protein-gekoppelten-Rezeptoren (GPCRs), reguliert, die eine intrazelluläre Signalkaskade auslösen (Abb. 1.2). Dabei handelt es sich um Transmembranproteine mit heptahelikaler Struktur. Im Grundzustand binden heterotrimere GTP-bindende Proteine (G-Proteine) an einer intrazellulären Andockstelle der GPCRs. Diese G-Proteine bestehen aus einer α-Untereinheit und einer βγ-Untereinheit, wobei im inaktiven Zustand GDP an Gα gebunden vorliegt. Durch Aktivierung der GPCR durch Katecholamine, Peptidhormone, Aminosäuren etc., kommt es zu einer Konformationsänderung und der Rezeptor wirkt als Guaninnucleotid-Austauschfaktor, indem die Affinität für GDP gemindert und der Austausch gegen GTP erleichtert wird. Daraufhin dissoziiert der Komplex in die zwei aktiven Einheiten Gα-GTP und Gβγ. Diese wiederum beeinflussen die Synthese von cAMP durch Bindung am katalytischen Zentrum der Adenylatcyclasen (23). Durch die intrinsische GTPase-Aktivität der Gα-Untereinheit wird GTP in GDP + P_i gespalten, was zur Re-Assoziation der

beiden Untereinheiten und zur Bindung des nun wieder vollständigen trimeren Komplexes an den GPCR führt.

In Eukaryoten vermittelt cAMP seine Wirkung über die Bindung an cAMP-regulierte Kationenkanäle (24), EPAC (Exchange Protein activated by cAMP) oder als allosterischer Modulator der cAMP-abhängigen Proteinkinase A (PKA), durch deren katalytische Untereinheit die Transkription von etwa 105 Genen, die über das cAMP Response Element (CRE) verfügen, reguliert wird (23,25).

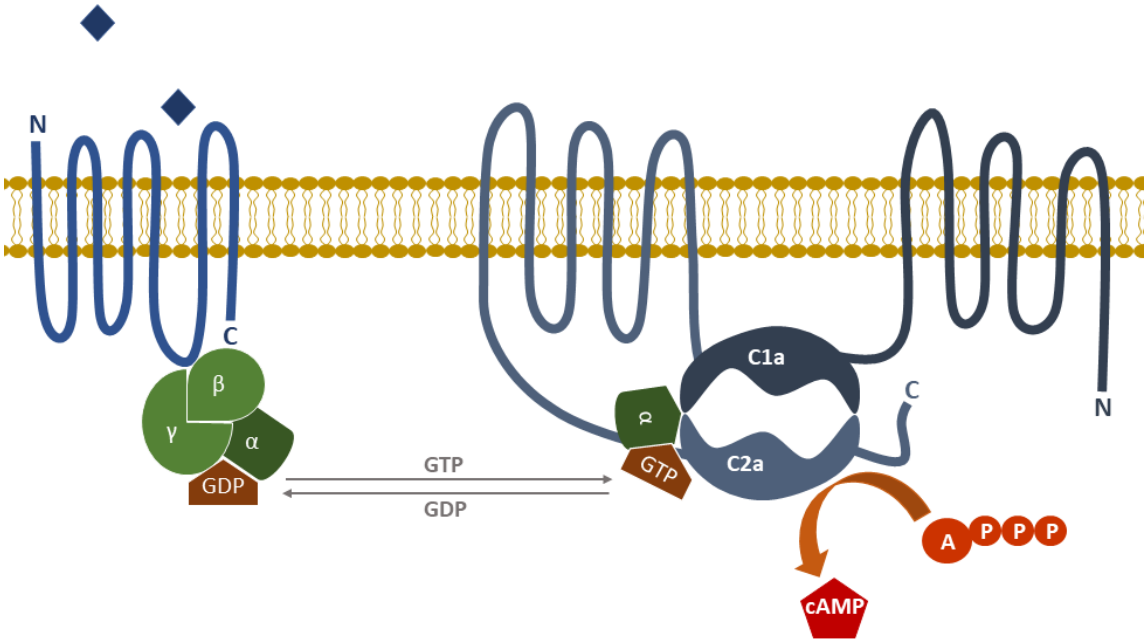

Abb. 1.2 *Regulierung membrangebundener Adenylatcyclasen (mACn, rechts) durch G-Protein gekoppelte Rezeptoren (GPCR, links). Im inaktiven Zustand ist GDP an das trimere G-Protein gebunden. Sobald ein Ligand (Raute) an den GPCR bindet, erfolgt der Austausch von GDP gegen GTP. Die Gα- und Gβγ-Untereinheiten dissoziieren, wobei Gα durch Bindung an C1a und C2a der mAC die aktive Form der katalytischen Domäne stabilisiert. Die cAMP-Bildung nimmt daraufhin zu und der sekundäre Botenstoff reguliert weitere intrazelluläre Mechanismen.*

1.3 Die Adenylatcyclase CyaC aus *Sinorhizobium meliloti*

Das Gram-negative Bodenbakterium *Sinorhizobium meliloti* ist durch seine symbiotische Beziehung zu Hülsenfrüchtlern von agrarwissenschaftlichem Interesse. Dabei bilden sich an den Wurzelenden der Stickstofffixierung dienende Wurzelknöllchen aus, die das Pflanzenwachstum fördern. Anhand von Sequenzanalysen wurden im Genom des Bakteriums über 26 Cyclasegene ermittelt, was eine ungewöhnlich hohe Anzahl dieser Enzyme darstellt (26).
Eines dieser Cyclasegene wurde in einer separaten Arbeit und in einem anderen wissenschaftlichen Zusammenhang identifiziert (27). Die Clusteranalyse der 6TM Domänen eukaryotischer und bakterieller ACn mit den 6TM Domänen der Quorum-Sensing Rezeptoren CqsS zeigte eine Aufteilung von ACn in fünf Gruppen (27). Neben der erwarteten Trennung in eukaryotische TM1/TM2 (IIIa), bakterielle TM (IIIa), bakterielle TM (IIIb) ohne HAMP und bakterielle TM (IIIb) mit HAMP, fand sich eine getrennte Gruppe mit Ferredoxin-haltigen ACn (IIIb), die auch eine AC aus *S. meliloti* ($CyaC_{Sm}$) umfasste (27).
Weitere Sequenzanalysen ergaben Ähnlichkeiten zu der Cytochrom b Untereinheit von Succinat:Chinon-Oxidoreduktasen (SQOR) (27). Dabei handelt es sich um Proteine der Atmungskette (28). Durch die Reduktion von Chinon zu Chinol ermöglichen sie den Elektronentransport über die mitochondriale Membran (29,30). Genau wie die Chinon-abhängigen Oxidoreduktasen enthält $CyaC_{Sm}$ vier konservierte Histidinreste in den TM1-4, die zwei Häm-Moleküle als prosthetische Gruppe binden (31). $CyaC_{Sm}$ hat einen modularen Aufbau, bestehend aus einer hexahelikalen Transmembrandomäne, einem an TM6 anschließenden Eisen-Schwefelcluster (2Fe2S) und einer C-terminalen Cyclasedomäne (31).

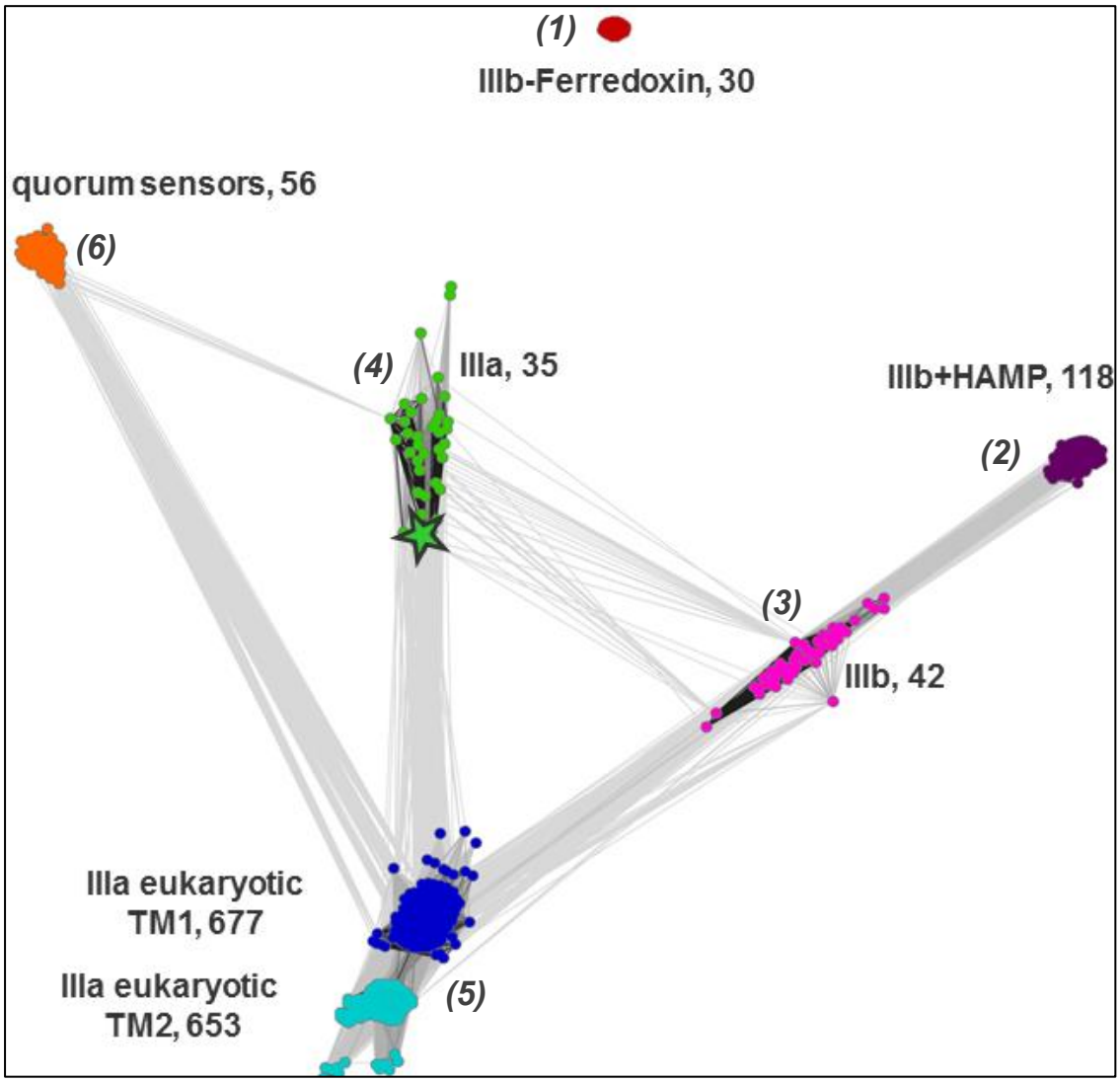

Abb. 1.3 *Clusteranalyse der 6TM Domänen von ACn und CqsS-ähnlichen sensorischen Rezeptoren aus 408 eukaryotischen und 1456 bakteriellen Sequenzen. Ausreißer wurden entfernt. Es bilden sich fünf getrennte Gruppen mit hohen Sequenzähnlichkeiten: (1) Membrananker bakterieller Klasse IIIb ACn mit zytosolischer Ferredoxindomäne (30 Sequenzen); (2) Membrananker bakterieller Klasse IIIb ACn mit einer HAMP-Domäne (118 Sequenzen); (3) Membrananker bakterieller Klasse IIIb ACn ohne HAMP-Domäne (42 Sequenzen); (4) Membrananker bakterieller Klasse IIIa ACn (35 Sequenzen); (5) Membrananker Pseudoheterodimerer eukaryotischer Klasse IIIa ACn (TM1 677, TM2 653 Sequenzen); (6) 6TM Domänen sensorischer Histidinkinasen ähnlich denen von CqsS (56 Sequenzen) (27).*

1.4 Signaltransduktion in membrangebundenen Mammalia-Adenylatcyclasen

Bisher geht man bei der Regulierung eukaryotischer Adenylatcyclasen von einem Zwei-Komponenten-System aus. Die Signalerkennung selbst erfolgt an den GPCRs, woraufhin intrazellulär die G-Protein-Untereinheiten Gα und Gβγ als Regulatorproteine dissoziieren. Diese regulieren sodann die ACn durch Bindung an der katalytischen Domäne. Der Vorgang lässt sich als horizontale Signaltransduktion bezeichnen, Gα bzw. Gβγ wirken intrazellulär direkt an der katalytischen AC Domäne. Isoformspezifisch erfolgt an dieser Stelle auch eine Regulierung durch zellinterne Botenstoffe wie Calmodulin und Ca^{2+}. Allerdings gibt es Hinweise, die im Folgenden erläutert werden, dass ACn auch zu einer vertikalen Signaltransduktion fähig sind. Die Position der katalytischen Domänen zueinander kann vermutlich durch Strukturänderungen, ausgelöst durch Ligandenbindung an der Membran, beeinflusst werden. Hinweise darauf finden sich in der Literatur (5,20,27,32).

In früheren Arbeiten ist es gelungen, funktionsfähige chimäre Proteine zwischen dem Quorum-Sensing Rezeptor CqsS aus *Vibrio harveyi* und der bakteriellen 6TM AC Rv1625c aus *Mykobakterium tuberculosis* zu bilden (27). Die 6TM Domäne von CqsS ähnelt mit den über kurze Linker verbundenen α-Helices auffallend stark der membrangebundener ACn. Das Effektorprotein von CqsS selbst ist allerdings eine Histidinkinase, die wie ACn nach Aktivierung ein Homodimer bildet (27,33,34). Die Chimäre CqsS-Rv1625c ließ sich durch den Quorum-Sensing Liganden CAI-1 (**C**holera **A**uto**I**nducer-**1**, (S)-3-hydroxytridecan-4-on) spezifisch und konzentrationsabhängig aktivieren (27).

Bei der Konstruktion einer ähnlichen Chimäre bestehend aus dem Quorum-Sensing Rezeptor LqsS aus *Legionella pneumophila* und der katalytischen Domäne von Rv1625c wurde als idealer Verbindungspunkt das N-terminale Ende der AS-Sequenz des Cyclase-Transducing-Elements (CTE) beschrieben (32). Beim CTE handelt es sich um eine hochkonservierte 19 ASn lange Region, die sich in ACn der Klassen IIIa und IIIb vor den katalytischen Domänen befindet und an die Coiled-Coil Struktur der TM-Domäne anschließt (32). In Kristallstrukturen zeigt es die Form zweier Helices, die durch einen 45° Winkel unterbrochen werden (5). Lag der Verknüpfungspunkt nicht am Beginn des CTE oder wurde

dieses ganz weggelassen, wurde die Signalweiterleitung innerhalb des chimären Proteins unterbrochen, was für eine zentrale Rolle dieser Region in der Regulation von ACn spricht (5,32). Es wird angenommen, dass das CTE durch Änderungen in der TM-Domäne eine ausgestreckte Konformation einnimmt und dadurch die katalytischen Domänen auf Abstand hält (32).

Des Weiteren scheint das Azol-Antimykotikum Miconazol die AC9 direkt zu stimulieren und AC1 und AC2 zu inhibieren (35). Im Falle der Aktivierung der AC9 lassen weitere Untersuchungen zu dem möglichen Mechanismus dieser Regulierung eine intrazelluläre Bindung an der katalytischen Domäne, wie sie für FSK, $G_i\alpha$ oder $G_s\alpha$ bekannt ist, unwahrscheinlich erscheinen (20,35). Allem Anschein nach befindet sich die Bindestelle innerhalb der Transmembrandomäne (20).

Die strukturellen Voraussetzungen für eine Signaltransduktion von der Membrandomäne zur katalytischen Domäne sind einer kryo-elektromikroskopischen Analyse zufolge gegeben (21). TM6 und TM12 von AC9 ragen 40 ASn lang in das Cytosol und bilden eine helikale Domäne (HD) in Form einer Coiled-Coil, bestehend aus HD1 und HD2, die für die korrekte Anordnung der beiden katalytischen Domänen unentbehrlich ist (21).

1.5 Die Rolle der hAC5 in der Insulinfreisetzung

Diabetes mellitus ist eine Erkrankung, deren Ursache auf einem absoluten (Typ 1) oder relativen (Typ 2) Insulinmangel beruht. Weltweit leidet mehr als 8% der Bevölkerung an dieser häufigsten und hinsichtlich der Folgen bedeutsamsten Form der Stoffwechselstörung (36). Während bei Typ 1 Diabetes eine Schädigung der Bauchspeicheldrüse vorliegt, wird bei Typ 2 nicht ausreichend Insulin aus den β-Zellen des Pankreas ausgeschüttet, obwohl es weiterhin synthetisiert wird. Genau wie die gesundheitlichen Folgen eines manifesten Diabetes sind auch die Entstehung dieser Erkrankung und die Mechanismen einer regelkonformen Insulinfreisetzung mannigfaltig und von zahlreichen Faktoren abhängig.

Die Insulinausschüttung ist direkt an die Glucosekonzentration im Blut gekoppelt und verläuft zweiphasig, wobei beiden Phasen unterschiedliche Mechanismen zugrunde liegen (37-42). Zunächst gelangt Glucose durch den insulin-unabhängigen Glucosetransporter 2 (GLUT2) (43), einigen dem widersprechenden Arbeiten zufolge allerdings nur durch die ebenfalls insulin-unabhängigen Transporter GLUT1 und GLUT3 (44), in die β-Zellen und wird umgehend durch die Glucokinase in Glucose-6-Phosphat (G-6-P) umgewandelt. G-6-P wird zur Energiegewinnung in den Zellen weiter zu ATP abgebaut (45). Durch den Anstieg der ATP-Konzentration erhöht sich das Verhältnis von ATP/ADP, was zur Schließung der ATP-abhängigen Kaliumkanäle führt (46). Die dadurch ausgelöste Depolarisation der β-Zellen fördert einen vermehrten Einstrom an Ca^{2+}-Ionen, indem spannungsabhängige Calciumkanäle geöffnet werden (47), was die Freisetzung von gespeichertem Insulin aus den Sekretionsgranula einleitet (37,43,48,49).

Besonders deutlich wird der zweiphasige Verlauf, wenn man die jeweiligen Freisetzungsgeschwindigkeiten betrachtet. Die auf dem Calciumeinstrom beruhende erste Phase der Insulinfreisetzung dauert etwa 10 min und hat eine maximale Freisetzungsgeschwindigkeit von etwa 1.4 nmol/min. Anschließend geht die Ausschüttung in die zweite, länger andauernde Phase mit einer langsameren Ausschüttungsgeschwindigkeit von etwa 0,4 nmol/min und einer

pulsierenden Insulinfreisetzung über (50), die hauptsächlich durch andere amplifizierende Signale innerhalb der Zelle getragen wird (51).

cAMP ist neben Ca^{2+} der wichtigste Effektor für die Insulinausschüttung aus den β-Zellen, da es die elektrische Aktivität der Zelle steigert und das Ca^{2+}-Signal verstärkt, die Bereitstellung neuer Granula fördert und die Exocytose stimuliert (52,53). Zusätzlich vermittelt es über die PKA und EPAC wichtige Signale in der Gentranskription, indem es nicht nur die Zelldifferenzierung und -proliferation reguliert, sondern auch Zellen vor Apoptose schützt (54,55).

Auf der Suche nach genetischen Risikofaktoren für die Entstehung eines Typ 2 Diabetes wurden zahlreiche Punktmutationen beschrieben, unter anderem rs11708067 im 3. Intron der hAC5 (56,57). Zudem ist einigen mRNA-Screenings zufolge die Expressionsrate dieser Isoform im Vergleich zu allen anderen hACn in den β-Zellen am höchsten, d.h. etwa doppelt so hoch wie die der hAC1 und fünffach höher als hAC6 (58).

Obwohl alle Isoformen der hACn im Pankreas vertreten sind, scheint die Stilllegung des Gens für hAC5 die durch Glucose stimulierte Insulinsekretion stark zu hemmen (58).

Da die große Mehrheit der Untersuchungen zur Rolle von cAMP in der Entstehung von Diabetes Typ 2 bisher mit Langerhans-Inseln oder im Tiermodell durchgeführt wurden, kommen zahlreiche zugrundeliegende Mechanismen wie interzelluläre Kommunikation (zwischen den β-Zellen oder α/γ- und β-Zellen) oder der Einfluss von GPCRs und deren Aktivierung durch Glucagon oder GLP-1 infrage. Von Interesse für diese Arbeit war die Möglichkeit einer Regulation der hAC5 oder anderer hACn durch im Humanserum zirkulierende Bestandteile wie Insulin, Glucagon, C-Peptid oder Glucose.

2. Zielsetzung

Seit der Sequenzierung einer AC-Primärsequenz aus bovinen Gehirnzellen wurde vermutet, dass es sich bei den ACn um Proteine mit Transporter- oder Ionenkanalfunktion handeln könnte (59). Nicht nur die geladenen ASn innerhalb der sechs α-Helices, welche die Membran durchspannen, zeugen von einer gewissen Ähnlichkeit gegenüber anderen Transportproteinen, sondern auch die schiere Größe der Membrananker lässt auf eine weitere Funktion abseits der bloßen Verankerung schließen (59). Strukturen weiterer integraler Membranproteine zeigen, dass eine Ankerfunktion bereits mit 1-2 TM Domänen erreicht werden kann. Die beiden 6TM Domänen hingegen nehmen über 30% der Enzymgröße in Anspruch und zeigen eine vergleichsweise hohe Sequenzkonservierung zwischen den Isoformen verschiedener Spezies (5,60). Innerhalb einer Spezies unterscheiden sich die Membrananker der Isoformen allerdings gravierend, was auch eine Voraussetzung für eine individuelle Regulierung über isoformspezifische Liganden sein könnte (5,60).

Durch die Omnipräsenz von cAMP als sekundärer Botenstoff in allen Zellen würde die Entdeckung solcher Liganden großes wissenschaftliches und therapeutisches Potential bergen (20). Aufgrund der größten Anzahl an Vertretern und einer hohen Diversität in Bezug auf Struktur und Funktion sind die ACn der Klasse III von besonderem pharmakologischem Interesse (5). Betrachtet man eine Clusteranalyse der 6TM Domänen der Klasse III ACn, wird eine Unterteilung in fünf Gruppen deutlich (Abb. 1.3).

Erkennbar sind dabei einige nennenswerte Aspekte. TM1 und TM2 eukaryotischer Klasse IIIa ACn (darunter auch alle humanen Isoformen AC 1-9) bilden zwei stark miteinander verbundene Gruppen, während Klasse IIIb ACn mit einer Ferredoxingruppe wie $CyaC_{Sm}$ keinerlei Ähnlichkeit zu den restlichen TM Domänen aufweisen und somit eindeutig von SQOR abstammen (5).

Ziel dieser Arbeit war die Beschreibung einer Signaltransduktion durch Liganden, die an der TM Domäne humaner ACn, speziell der Isoform 5, bzw. der AC $CyaC_{Sm}$ binden und dadurch die Aktivität der katalytischen Domäne regulieren können.

Während hAC5 in die Klasse IIIa eingeordnet wird, gehört die bakterielle AC $CyaC_{Sm}$ zur Klasse IIIb. Durch die grundlegend verschiedene Domänenstruktur der beiden ACn und der Tatsache, dass sie aus Pro- bzw. Eukaryoten stammen, ergaben sich auch unterschiedliche Herangehensweisen für die Suche nach einer Regulierbarkeit über die Membrandomänen.

2.1 Die AC $CyaC_{Sm}$ aus Sinorhizobium meliloti

Die bereits durch J. Wissig in *E. coli* BTH101 *ΔcyaA* klonierte $CyaC_{Sm}$ und deren Punktmutanten H27A, H31A, H68A, H105A und H149A wurden auf AC-Aktivität getestet. Dabei ergaben sich folgende Fragestellungen:

- Bleibt isolierte $CyaC_{Sm}$ ohne Membranintegration weiterhin aktiv?
- Ist Häm-B, das durch die vier hochkonservierten Histidine als prosthetische Gruppe gebunden wird, für die Bildung von cAMP erforderlich?
- Wird die Aktivität des Enzyms durch RedOx-Reagenzien, insbesondere durch das Chinon Q_0 und das Chinol Q_0H_2, reguliert?

Sollten sich diese Hypothesen bestätigen, würde der zugrundeliegende Mechanismus dem des lichtempfindlichen heptahelikalen Opsinrezeptors ähneln. Dabei handelt es sich um ein Sehpigment im Inneren von Netzhautzellen, das im inaktiven Zustand 11-*cis*-Retinal bindet und in den Diskmembranen verankert ist. Nach der Aktivierung durch Licht in einem festgelegten Wellenlängenbereich, isomerisiert 11-*cis*-Retinal zu all-*trans*-Retinal, was nicht nur zu einer veränderten Raumstruktur des Moleküls, sondern auch zu Konformationsänderungen im Opsinrezeptor führt (61).

2.2 Humane AC Isoform 5

In Mammalia werden alle membrangebundenen ACn über GPCRs mittels der $G_s\alpha$-Untereinheit der G_s-Proteine aktiviert, eine direkte Regulation über den Membrananker ist bisher unbekannt. Die membrangebundenen Isoformen 1-9 sind in allen Geweben vertreten. Geht man von einer Regulierung über einen isoformspezifischen Liganden aus, so müsste dieser den Hormonen und Neurotransmittern ähnlich im Blutkreislauf zu finden sein, um alle Gewebe erreichen zu können.
Es wurden daher folgende Untersuchungen durchgeführt:

- Wird die hAC5 im aktivierten Zustand (durch $G_s\alpha$) von einem bereits bekannten Hormon oder Neurotransmitter reguliert?
- Wird die Aktivität der hAC5 durch Stoffe, die an der Regulierung des Blutzuckerspiegels beteiligt sind, beeinflusst?
- Haben Bestandteile im Humanserum regulatorische Eigenschaften?

Die Expression der hAC5 erfolgte dabei zunächst in HEK293-Zellen und anschließend in Sf9-Zellen (letzteres durch M. Finkbeiner), deren Kultivierung in serumfreiem Medium möglich ist.

3. Material und Methoden

In diesem Abschnitt werden nur Material und Methoden zur Expression der hAC5 in HEK293 Zellen beschrieben, da für die restlichen experimentellen Arbeiten ein Methodenteil in den Veröffentlichungen vorhanden ist.

3.1 Medien und Kits

Firma, Ort	**Material**
Thermo Fischer Scientific Inc., Langenselbold	Lipofectamine™ 3000 Reagent P3000™ Reagent
Life Technologies (Thermo Fisher Scientific)	Gibco® DMEM Kulturmedium Gibco® Opti-MEM® + GlutaMAX™ Gibco® DPBS

Transfektionslösungen

Transfektionslösung A:

- 125 µl Opti-MEM
- 3,75 µl Lipofectamine® 3000

Transfektionslösung B:

- 125 µl Opti-MEM
- 10 µl P3000™ Reagent
- 24 µg DNA (Plasmid hAC5)

Selektionsmedien

Selektionsmedium #1:

- 10 ml DMEM
- 10% FBS
- 1% PenStrep
- 600 µg/ml G418

Selektionsmedium #2:

- 10 ml DMEM
- 10% FBS
- 1% PenStrep
- 300 µg/ml G418

Kulturmedien

Kulturmedium für T75 Flasche:

- 14 ml DMEM
- 10% FBS
- 1% PenStrep
- 300 µg/ml G418

Kulturmedium für T175 Flasche:

- 30 ml DMEM
- 10% FBS
- 1% PenStrep
- 300 µg/ml G418

HEK-Lysepuffer (pH 7,5):

- 20 mM HEPES
- 1 mM Na-EDTA
- 2 mM $MgCl_2$
- 250 mM Sucrose
- Ad 990 ml Wasser

Frisch zugegeben:

- 1 mM DTT
- 1 Tablette Proteaseinhibitoren (Roche) pro 50 ml Lysepuffer

HEK-Resuspensionspuffer (pH 7,5):

- 20 mM MOPS
- 0,5 mM Na-EDTA
- 2 mM $MgCl_2$
- Ad 1000 ml Wasser

3.2 Geräte

Firma, Ort	**Material**
Binder GmbH, Tuttlingen	Inkubator Modell CB60
Hera safe, Tüssling	Heraeus Laminar Air Flow (Bauart EN 12469-2000)

3.3 Plasmid

Es wurde das gleiche Plasmid verwendet wie das Ausgangsplasmid (hAC5 von GenScript in pLIB mit anschließender Amplifizierung in *E. coli* XL1blue) für die Expression der hAC5 in Sf9-Zellen.

3.4 HEK293

Verwendet wurden HEK293 Zellen Passage 6 aus dem Stock vom Arbeitskreis Ruth.

3.5 Expressionsbedingungen und Zellernte

Transfektion

Etwa 0,5 Mio. HEK293 Zellen wurden am Vortag auf einer Petrischale (Ø 3,5 cm) in Opti-MEM + PenStrep ausgebracht. Die Transfektion erfolgte gemäß der Anleitung für Lipofectamine™ 3000, sobald 70-90% der Zellen konfluent waren. Anschließend erfolgte eine zweitägige Inkubation im Brutschrank (37° C, 5% CO_2). Die Selektion wurde durch Kultivierung für 7 Tage in Selektionsmedium #1 und weiteren 7 Tagen in Selektionsmedium #2 erreicht.

Zellernte

Zur Zellernte wurde eine Anfangszellzahl von 2-8 Mio. Zellen pro T75 oder T175 Flasche in Kulturmedium ausgebracht und bei 90-100% Konfluenz geerntet. Nach dem Waschen mit 2 x 10 ml kaltem DPBS wurden diese bei 4°C und 3000 x g für 5 min abzentrifugiert und der Überstand verworfen. Der Niederschlag wurde in HEK-Lysepuffer resuspendiert und 30 min auf Eis inkubiert. Das Volumen richtete sich dabei nach der Zahl der geernteten T175 Flaschen (0,5 ml pro T175 Flasche). Die Homogenisierung erfolgte durch 20 Auf- und Ab-Bewegungen des Potters bei einer Motorleistung von 100%.

Durch Zentrifugieren bei 1000 x g und 4°C für 5 min wurden die Zellkerne abgetrennt, der Überstand abgenommen und die Membranen in der Ultrazentrifuge bei 100.000 und 4°C für 60 min abzentrifugiert. Der daraus resultierende Niederschlag wurde in 0,5 ml HEK-Resuspensionspuffer pro T175 Flasche mit einem Douncer resuspendiert und bei -80°C gelagert.

4. Referenzen

1 Karin, M. Signal transduction and gene control. *Curr. Opin. Cell Biol.* **3**, 467-473, doi:10.1016/0955-0674(91)90075-a (1991).

2 Linder, J. U. & Schultz, J. E. Versatility of signal transduction encoded in dimeric adenylyl cyclases. *Curr. Opin. Struct. Biol.* **18**, 667-672, doi:10.1016/j.sbi.2008.11.008 (2008).

3 Linder, J. U. & Schultz, J. E. The class III adenylyl cyclases: multi-purpose signalling modules. *Cell. Signal.* **15**, 1081-1089, doi:10.1016/s0898-6568(03)00130-x (2003).

4 Linder, J. U. Class III adenylyl cyclases: molecular mechanisms of catalysis and regulation. *Cell. Mol. Life Sci.* **63**, 1736-1751, doi:10.1007/s00018-006-6072-0 (2006).

5 Bassler, J., Schultz, J. E. & Lupas, A. N. Adenylate cyclases: Receivers, transducers, and generators of signals. *Cell. Signal.* **46**, 135-144, doi:10.1016/j.cellsig.2018.03.002 (2018).

6 Tesmer, J. J., Sunahara, R. K., Gilman, A. G. & Sprang, S. R. Crystal structure of the catalytic domains of adenylyl cyclase in a complex with Gsalpha.GTPgammaS. *Science* **278**, 1907-1916, doi:10.1126/science.278.5345.1907 (1997).

7 Steegborn, C., Litvin, T. N., Levin, L. R., Buck, J. & Wu, H. Bicarbonate activation of adenylyl cyclase via promotion of catalytic active site closure and metal recruitment. *Nat. Struct. Mol. Biol.* **12**, 32-37, doi:10.1038/nsmb880 (2005).

8 Tews, I., Findeisen, F., Sinning, I., Schultz, A., Schultz, J. E. & Linder, J. U. The structure of a pH-sensing mycobacterial adenylyl cyclase holoenzyme. *Science* **308**, 1020-1023, doi:10.1126/science.1107642 (2005).

9 Cann, M. J., Hammer, A., Zhou, J. & Kanacher, T. A defined subset of adenylyl cyclases is regulated by bicarbonate ion. *J. Biol. Chem.* **278**, 35033-35038, doi:10.1074/jbc.M303025200 (2003).

10 Motaal, A. A., Tews, I., Schultz, J. E. & Linder, J. U. Fatty acid regulation of adenylyl cyclase Rv2212 from Mycobacterium tuberculosis H37Rv. *FEBS J.* **273**, 4219-4228, doi:10.1111/j.1742-4658.2006.05420.x (2006).

11 Lory, S., Wolfgang, M., Lee, V. & Smith, R. The multi-talented bacterial adenylate cyclases. *Int. J. Med. Microbiol.* **293**, 479-482, doi:10.1078/1438-4221-00297 (2004).

12 Gorke, B. & Stulke, J. Carbon catabolite repression in bacteria: many ways to make the most out of nutrients. *Nat. Rev. Microbiol.* **6**, 613-624, doi:10.1038/nrmicro1932 (2008).

13 Narang, A. Quantitative effect and regulatory function of cyclic adenosine 5'-phosphate in Escherichia coli. *J. Biosci.* **34**, 445-463, doi:10.1007/s12038-009-0051-1 (2009).

14 Makman, R. S. & Sutherland, E. W. Adenosine 3',5'-Phosphate in Escherichia coli. *J. Biol. Chem.* **240**, 1309-1314, doi:https://www.ncbi.nlm.nih.gov/pubmed/14284741 (1965).

15 Ullmann, A. Catabolite repression: a story without end. *Res. Microbiol.* **147**, 455-458, doi:10.1016/0923-2508(96)83999-4 (1996).

16 Chen, Y., Cann, M. J., Litvin, T. N., Iourgenko, V., Sinclair, M. L., Levin, L. R. & Buck, J. Soluble adenylyl cyclase as an evolutionarily conserved bicarbonate sensor. *Science* **289**, 625-628, doi:10.1126/science.289.5479.625 (2000).

17 Sunahara, R. K. & Taussig, R. Isoforms of mammalian adenylyl cyclase: multiplicities of signaling. *Mol. Interv.* **2**, 168, doi:10.1124/mi.2.3.168 (2002).

18 Sunahara, R. K., Dessauer, C. W. & Gilman, A. G. Complexity and diversity of mammalian adenylyl cyclases. *Annu. Rev. Pharmacol. Toxicol.* **36**, 461-480, doi:10.1146/annurev.pa.36.040196.002333 (1996).

19 Hurley, J. H. Structure, mechanism, and regulation of mammalian adenylyl cyclase. *J. Biol. Chem.* **274**, 7599-7602, doi:10.1074/jbc.274.12.7599 (1999).

20 Baldwin, T. A., Li, Y., Brand, C. S., Watts, V. J. & Dessauer, C. W. Insights into the Regulatory Properties of Human Adenylyl Cyclase Type 9. *Mol. Pharmacol.* **95**, 349-360, doi:10.1124/mol.118.114595 (2019).

21 Qi, C., Sorrentino, S., Medalia, O. & Korkhov, V. M. The structure of a membrane adenylyl cyclase bound to an activated stimulatory G protein. *Science* **364**, 389-394, doi:10.1126/science.aav0778 (2019).

22 Sunahara, R. K. & Taussig, R. Isoforms of mammalian adenylyl cyclase: multiplicities of signaling. *Mol. Interv.* **2**, 168-184, doi:10.1124/mi.2.3.168 (2002).

23 Beavo, J. A. & Brunton, L. L. Cyclic nucleotide research -- still expanding after half a century. *Nat. Rev. Mol. Cell Biol.* **3**, 710-718, doi:10.1038/nrm911 (2002).

24 Wahl-Schott, C. & Biel, M. HCN channels: structure, cellular regulation and physiological function. *Cell. Mol. Life Sci.* **66**, 470-494, doi:10.1007/s00018-008-8525-0 (2009).

25 Langan, T. A. Histone phosphorylation: stimulation by adenosine 3',5'-monophosphate. *Science* **162**, 579-580, doi:10.1126/science.162.3853.579 (1968).

26 Capela, D., Barloy-Hubler, F., Gouzy, J., Bothe, G., Ampe, F., Batut, J., Boistard, P., Becker, A., Boutry, M., Cadieu, E., Dreano, S., Gloux, S., Godrie, T., Goffeau, A., Kahn, D., Kiss, E., Lelaure, V., Masuy, D., Pohl, T., Portetelle, D., Puhler, A., Purnelle, B., Ramsperger, U., Renard, C., Thebault, P., Vandenbol, M., Weidner, S. & Galibert, F. Analysis of the chromosome sequence of the legume symbiont Sinorhizobium meliloti strain 1021. *Proc. Natl. Acad. Sci. U.S.A.* **98**, 9877-9882, doi:10.1073/pnas.161294398 (2001).

27 Beltz, S., Bassler, J. & Schultz, J. E. Regulation by the quorum sensor from Vibrio indicates a receptor function for the membrane anchors of adenylate cyclases. *elife* **5**, doi:10.7554/eLife.13098 (2016).

28 Ackrell, B. A. Progress in understanding structure-function relationships in respiratory chain complex II. *FEBS Lett.* **466**, 1-5, doi:10.1016/s0014-5793(99)01749-4 (2000).

29 Cecchini, G., Schröder, I., Gunsalus, R. P. & Maklashina, E. Succinate dehydrogenase and fumarate reductase from Escherichia coli. *Biochim. Biophys. Acta* **1553**, 140-157, doi:10.1016/s0005-2728(01)00238-9 (2002).

30 Hederstedt, L. Succinate: quinone oxidoreductase in the bacteria Paracoccus denitrificans and Bacillus subtilis. *Biochim. Biophys. Acta* **1553**, 74-83, doi:10.1016/s0005-2728(01)00231-6 (2002).

31 Wissig, J. Charakterisierung und funktionelle Untersuchung der Adenylatzyklase SMc01818 aus Sinorhizobium meliloti, Master thesis, Johannes Gutenberg-Universität, (2016).

32 Ziegler, M., Bassler, J., Beltz, S., Schultz, A., Lupas, A. N. & Schultz, J. E. Characterization of a novel signal transducer element intrinsic to class IIIa/b adenylate cyclases and guanylate cyclases. *FEBS J.* **284**, 1204-1217, doi:10.1111/febs.14047 (2017).

33 Wei, Y., Ng, W. L., Cong, J. & Bassler, B. L. Ligand and antagonist driven regulation of the Vibrio cholerae quorum-sensing receptor CqsS. *Mol. Microbiol.* **83**, 1095-1108, doi:10.1111/j.1365-2958.2012.07992.x (2012).

34 Ng, W. L., Perez, L. J., Wei, Y., Kraml, C., Semmelhack, M. F. & Bassler, B. L. Signal production and detection specificity in Vibrio CqsA/CqsS quorum-sensing systems. *Mol. Microbiol.* **79**, 1407-1417, doi:10.1111/j.1365-2958.2011.07548.x (2011).

35 Simpson, J., Palvolgyi, A. & Antoni, F. A. Direct stimulation of adenylyl cyclase 9 by the fungicide imidazole miconazole. *Naunyn Schmiedebergs Arch Pharmacol* **392**, 497-504, doi:10.1007/s00210-018-01610-1 (2019).

36 Scully, T. Diabetes in numbers. *Nature* **485**, S2-3, doi:10.1038/485s2a (2012).

37 Henquin, J. C., Ishiyama, N., Nenquin, M., Ravier, M. A. & Jonas, J. C. Signals and pools underlying biphasic insulin secretion. *Diabetes* **51 Suppl 1**, S60-67, doi:10.2337/diabetes.51.2007.s60 (2002).

38 Curry, D. L., Bennett, L. L. & Grodsky, G. M. Dynamics of insulin secretion by the perfused rat pancreas. *Endocrinology* **83**, 572-584, doi:10.1210/endo-83-3-572 (1968).

39 Lacy, P. E. The secretion of insulin. *Diabetes* **21**, 510, doi:10.2337/diab.21.2.s510 (1972).

40 Cerasi, E. & Luft, R. The plasma insulin response to glucose infusion in healthy subjects and in diabetes mellitus. *Acta Endocrinol.* **55**, 278-304, doi:10.1530/acta.0.0550278 (1967).

41 Porte, D., Jr. & Pupo, A. A. Insulin responses to glucose: evidence for a two pool system in man. *J. Clin. Investig.* **48**, 2309-2319, doi:10.1172/JCI106197 (1969).

42 Blackard, W. G. & Nelson, N. C. Portal and peripheral vein immunoreactive insulin concentrations before and after glucose infusion. *Diabetes* **19**, 302-306, doi:10.2337/diab.19.5.302 (1970).

43 Fu, Z., Gilbert, E. R. & Liu, D. Regulation of insulin synthesis and secretion and pancreatic Beta-cell dysfunction in diabetes. *Curr. Diabetes Rev.* **9**, 25-53, doi:https://www.ncbi.nlm.nih.gov/pubmed/22974359 (2013).

44 McCulloch, L. J., van de Bunt, M., Braun, M., Frayn, K. N., Clark, A. & Gloyn, A. L. GLUT2 (SLC2A2) is not the principal glucose transporter in human pancreatic beta cells: implications for understanding genetic association signals at this locus. *Mol. Genet. Metab.* **104**, 648-653, doi:10.1016/j.ymgme.2011.08.026 (2011).

45 Tarasov, A. I., Semplici, F., Li, D., Rizzuto, R., Ravier, M. A., Gilon, P. & Rutter, G. A. Frequency-dependent mitochondrial Ca(2+) accumulation regulates ATP synthesis in pancreatic beta cells. *Pflügers Arch.* **465**, 543-554, doi:10.1007/s00424-012-1177-9 (2013).

46 Ashcroft, S. J. & Ashcroft, F. M. Properties and functions of ATP-sensitive K-channels. *Cell. Signal.* **2**, 197-214, doi:10.1016/0898-6568(90)90048-f (1990).

47 Grapengiesser, E., Gylfe, E. & Hellman, B. Glucose-induced oscillations of cytoplasmic Ca2+ in the pancreatic beta-cell. *Biochem. Biophys. Res. Commun.* **151**, 1299-1304, doi:10.1016/s0006-291x(88)80503-5 (1988).

48 Rorsman, P., Eliasson, L., Renstrom, E., Gromada, J., Barg, S. & Gopel, S. The Cell Physiology of Biphasic Insulin Secretion. *News Physiol. Sci.* **15**, 72-77, doi:10.1152/physiologyonline.2000.15.2.72 (2000).

49 da Silva Xavier, G., Leclerc, I., Varadi, A., Tsuboi, T., Moule, S. K. & Rutter, G. A. Role for AMP-activated protein kinase in glucose-stimulated insulin secretion and preproinsulin gene expression. *Biochem. J.* **371**, 761-774, doi:10.1042/BJ20021812 (2003).

50 Kashyap, S., Belfort, R., Gastaldelli, A., Pratipanawatr, T., Berria, R., Pratipanawatr, W., Bajaj, M., Mandarino, L., DeFronzo, R. & Cusi, K. A sustained increase in plasma free fatty acids impairs insulin secretion in nondiabetic subjects genetically predisposed to develop type 2 diabetes. *Diabetes* **52**, 2461-2474, doi:10.2337/diabetes.52.10.2461 (2003).

51 Henquin, J. C. Regulation of insulin secretion: a matter of phase control and amplitude modulation. *Diabetologia* **52**, 739-751, doi:10.1007/s00125-009-1314-y (2009).

52 Tengholm, A. Cyclic AMP dynamics in the pancreatic beta-cell. *Ups. J. Med. Sci.* **117**, 355-369, doi:10.3109/03009734.2012.724732 (2012).

53 Seino, S. & Shibasaki, T. PKA-dependent and PKA-independent pathways for cAMP-regulated exocytosis. *Physiol. Rev.* **85**, 1303-1342, doi:10.1152/physrev.00001.2005 (2005).

54 Fatehi-Hassanabad, Z., Chan, C. B. & Furman, B. L. Reactive oxygen species and endothelial function in diabetes. *Eur. J. Pharmacol.* **636**, 8-17, doi:10.1016/j.ejphar.2010.03.048 (2010).

55 Altarejos, J. Y. & Montminy, M. CREB and the CRTC co-activators: sensors for hormonal and metabolic signals. *Nat. Rev. Mol. Cell Biol.* **12**, 141-151, doi:10.1038/nrm3072 (2011).

56 Dupuis, J., Langenberg, C., Prokopenko, I., Saxena, R., Soranzo, N., Jackson, A. U., Wheeler, E., Glazer, N. L., Bouatia-Naji, N., Gloyn, A. L., Lindgren, C. M., Magi, R., Morris, A. P., Randall, J., Johnson, T., Elliott, P., Rybin, D., Thorleifsson, G., Steinthorsdottir, V., Henneman, P., Grallert, H., Dehghan, A., Hottenga, J. J., Franklin, C. S., Navarro, P., Song, K., Goel, A., Perry, J. R., Egan, J. M., Lajunen, T., Grarup, N., Sparso, T., Doney, A., Voight, B. F., Stringham, H. M., Li, M., Kanoni, S., Shrader, P., Cavalcanti-Proenca, C., Kumari, M., Qi, L., Timpson, N. J., Gieger, C., Zabena, C., Rocheleau, G., Ingelsson, E., An, P., O'Connell,

J., Luan, J., Elliott, A., McCarroll, S. A., Payne, F., Roccasecca, R. M., Pattou, F., Sethupathy, P., Ardlie, K., Ariyurek, Y., Balkau, B., Barter, P., Beilby, J. P., Ben-Shlomo, Y., Benediktsson, R., Bennett, A. J., Bergmann, S., Bochud, M., Boerwinkle, E., Bonnefond, A., Bonnycastle, L. L., Borch-Johnsen, K., Bottcher, Y., Brunner, E., Bumpstead, S. J., Charpentier, G., Chen, Y. D., Chines, P., Clarke, R., Coin, L. J., Cooper, M. N., Cornelis, M., Crawford, G., Crisponi, L., Day, I. N., de Geus, E. J., Delplanque, J., Dina, C., Erdos, M. R., Fedson, A. C., Fischer-Rosinsky, A., Forouhi, N. G., Fox, C. S., Frants, R., Franzosi, M. G., Galan, P., Goodarzi, M. O., Graessler, J., Groves, C. J., Grundy, S., Gwilliam, R., Gyllensten, U., Hadjadj, S., Hallmans, G., Hammond, N., Han, X., Hartikainen, A. L., Hassanali, N., Hayward, C., Heath, S. C., Hercberg, S., Herder, C., Hicks, A. A., Hillman, D. R., Hingorani, A. D., Hofman, A., Hui, J., Hung, J., Isomaa, B., Johnson, P. R., Jorgensen, T., Jula, A., Kaakinen, M., Kaprio, J., Kesaniemi, Y. A., Kivimaki, M., Knight, B., Koskinen, S., Kovacs, P., Kyvik, K. O., Lathrop, G. M., Lawlor, D. A., Le Bacquer, O., Lecoeur, C., Li, Y., Lyssenko, V., Mahley, R., Mangino, M., Manning, A. K., Martinez-Larrad, M. T., McAteer, J. B., McCulloch, L. J., McPherson, R., Meisinger, C., Melzer, D., Meyre, D., Mitchell, B. D., Morken, M. A., Mukherjee, S., Naitza, S., Narisu, N., Neville, M. J., Oostra, B. A., Orru, M., Pakyz, R., Palmer, C. N., Paolisso, G., Pattaro, C., Pearson, D., Peden, J. F., Pedersen, N. L., Perola, M., Pfeiffer, A. F., Pichler, I., Polasek, O., Posthuma, D., Potter, S. C., Pouta, A., Province, M. A., Psaty, B. M., Rathmann, W., Rayner, N. W., Rice, K., Ripatti, S., Rivadeneira, F., Roden, M., Rolandsson, O., Sandbaek, A., Sandhu, M., Sanna, S., Sayer, A. A., Scheet, P., Scott, L. J., Seedorf, U., Sharp, S. J., Shields, B., Sigurethsson, G., Sijbrands, E. J., Silveira, A., Simpson, L., Singleton, A., Smith, N. L., Sovio, U., Swift, A., Syddall, H., Syvanen, A. C., Tanaka, T., Thorand, B., Tichet, J., Tonjes, A., Tuomi, T., Uitterlinden, A. G., van Dijk, K. W., van Hoek, M., Varma, D., Visvikis-Siest, S., Vitart, V., Vogelzangs, N., Waeber, G., Wagner, P. J., Walley, A., Walters, G. B., Ward, K. L., Watkins, H., Weedon, M. N., Wild, S. H., Willemsen, G., Witteman, J. C.,

Yarnell, J. W., Zeggini, E., Zelenika, D., Zethelius, B., Zhai, G., Zhao, J. H., Zillikens, M. C., Consortium, D., Consortium, G., Global, B. C., Borecki, I. B., Loos, R. J., Meneton, P., Magnusson, P. K., Nathan, D. M., Williams, G. H., Hattersley, A. T., Silander, K., Salomaa, V., Smith, G. D., Bornstein, S. R., Schwarz, P., Spranger, J., Karpe, F., Shuldiner, A. R., Cooper, C., Dedoussis, G. V., Serrano-Rios, M., Morris, A. D., Lind, L., Palmer, L. J., Hu, F. B., Franks, P. W., Ebrahim, S., Marmot, M., Kao, W. H., Pankow, J. S., Sampson, M. J., Kuusisto, J., Laakso, M., Hansen, T., Pedersen, O., Pramstaller, P. P., Wichmann, H. E., Illig, T., Rudan, I., Wright, A. F., Stumvoll, M., Campbell, H., Wilson, J. F., Anders Hamsten on behalf of Procardis, C., investigators, M., Bergman, R. N., Buchanan, T. A., Collins, F. S., Mohlke, K. L., Tuomilehto, J., Valle, T. T., Altshuler, D., Rotter, J. I., Siscovick, D. S., Penninx, B. W., Boomsma, D. I., Deloukas, P., Spector, T. D., Frayling, T. M., Ferrucci, L., Kong, A., Thorsteinsdottir, U., Stefansson, K., van Duijn, C. M., Aulchenko, Y. S., Cao, A., Scuteri, A., Schlessinger, D., Uda, M., Ruokonen, A., Jarvelin, M. R., Waterworth, D. M., Vollenweider, P., Peltonen, L., Mooser, V., Abecasis, G. R., Wareham, N. J., Sladek, R., Froguel, P., Watanabe, R. M., Meigs, J. B., Groop, L., Boehnke, M., McCarthy, M. I., Florez, J. C. & Barroso, I. New genetic loci implicated in fasting glucose homeostasis and their impact on type 2 diabetes risk. *Nat. Genet.* **42**, 105-116, doi:10.1038/ng.520 (2010).

57 Dayeh, T. A., Olsson, A. H., Volkov, P., Almgren, P., Ronn, T. & Ling, C. Identification of CpG-SNPs associated with type 2 diabetes and differential DNA methylation in human pancreatic islets. *Diabetologia* **56**, 1036-1046, doi:10.1007/s00125-012-2815-7 (2013).

58 Hodson, D. J., Mitchell, R. K., Marselli, L., Pullen, T. J., Gimeno Brias, S., Semplici, F., Everett, K. L., Cooper, D. M., Bugliani, M., Marchetti, P., Lavallard, V., Bosco, D., Piemonti, L., Johnson, P. R., Hughes, S. J., Li, D., Li, W. H., Shapiro, A. M. & Rutter, G. A. ADCY5 couples glucose to insulin secretion in human islets. *Diabetes* **63**, 3009-3021, doi:10.2337/db13-1607 (2014).

59 Krupinski, J., Coussen, F., Bakalyar, H. A., Tang, W. J., Feinstein, P. G., Orth, K., Slaughter, C., Reed, R. R. & Gilman, A. G. Adenylyl cyclase amino acid sequence: possible channel- or transporter-like structure. *Science* **244**, 1558-1564, doi:10.1126/science.2472670 (1989).

60 Seebacher, T., Linder, J. U. & Schultz, J. E. An isoform-specific interaction of the membrane anchors affects mammalian adenylyl cyclase type V activity. *Eur. J. Biochem.* **268**, 105-110, doi:10.1046/j.1432-1327.2001.01850.x (2001).

61 Khorana, H. G. Rhodopsin, photoreceptor of the rod cell. An emerging pattern for structure and function. *J. Biol. Chem.* **267**, 1-4, doi:https://www.ncbi.nlm.nih.gov/pubmed/1730574 (1992).

62 Wissig, J. Persönliche Kommunikation *E-Mail "WG: Stämme, CyaC"* an Grischin, J. am 19.06.2017

63 Slaunwhite, W. R., Jr. & Sandberg, A. A. Transcortin: a corticosteroid-binding protein of plasma. *J. Clin. Investig.* **38**, 384-391, doi:10.1172/JCI103812 (1959).

64 Mutschler, E., Geisslinger, G., Kroemer, H. K., Ruth, P. & Schäfer-Korting, M. Mutschler Arzneimittelwirkungen: Lehrbuch der Pharmakologie, der klinischen Pharmakologie und Toxikologie: mit einführenden Kapiteln in die Anatomie, Physiologie und Pathophysiologie. Vol. 9., vollständig überarbeitete und erweiterte Auflage (Wissenschaftliche Verlagsgesellschaft, 2013).

65 Rosenbaum, W., Christy, N. P. & Kelly, W. G. Electrophoretic evidence for the presence of an estrogen-binding beta-globulin in human plasma. *J. Clin. Endocrinol. Metab.* **26**, 1399-1403, doi:10.1210/jcem-26-12-1399 (1966).

66 Pearlman, W. H. & Crepy, O. Steroid-protein interaction with particular reference to testosterone binding by human serum. *J. Biol. Chem.* **242**, 182-189, doi:https://www.ncbi.nlm.nih.gov/pubmed/6066733 (1967).

67 Rosner, W. & Deakins, S. M. Testosterone-binding globulins in human plasma: studies on sex distribution and specificity. *J. Clin. Investig.* **47**, 2109-2116, doi:10.1172/JCI105896 (1968).

68 Anderson, D. C. Sex-hormone-binding globulin. *Clin. Endocrinol.* **3**, 69-96, doi:10.1111/j.1365-2265.1974.tb03298.x (1974).

69 Rosner, W., Hryb, D. J., Kahn, S. M., Nakhla, A. M. & Romas, N. A. Interactions of sex hormone-binding globulin with target cells. *Mol. Cell. Endocrinol.* **316**, 79-85, doi:10.1016/j.mce.2009.08.009 (2010).

70 Kleine, B. & Rossmanith, W. Hormone und Hormonsystem - Lehrbuch der Endokrinologie. Vol. 3., vollständig überarbeitete und erweiterte Auflage (Springer Spektrum, 2014).

71 Hammes, A., Andreassen, T. K., Spoelgen, R., Raila, J., Hubner, N., Schulz, H., Metzger, J., Schweigert, F. J., Luppa, P. B., Nykjaer, A. & Willnow, T. E. Role of endocytosis in cellular uptake of sex steroids. *Cell* **122**, 751-762, doi:10.1016/j.cell.2005.06.032 (2005).

72 ESAP 2015 Laboratory Reference Ranges, https://education.endocrine.org/system/files/ESAP%202015%20Laboratory%20Reference%20Ranges.pdf (2015) Abgerufen am 17. Februar 2020.

73 Elhomsy, G. Dopamine, https://emedicine.medscape.com/article/2088959-overview (27. November 2019) Abgerufen am 17. Februar 2020.

74 Krause, R. S. Epinephrine, https://emedicine.medscape.com/article/2088959-overview (20. November 2019) Abgerufen am 17. Februar 2020.

75 Ferkany, J., Smith, L., Seifert Jr, W., Caprioli, R. & Enna, S. Measurement of gamma-aminobutyric acid (GABA) in blood. *Life Sci.* **22**, 2121-2128, doi:10.1016/0024-3205(78)90456-3 (1978).

76 Wilczynski, C. Glucagon, https://emedicine.medscape.com/article/2089114-overview (24. Juli 2019) Abgerufen am 17. Februar 2020.

77 Al Gawwam, G. & Sharquie, I. K. Serum Glutamate Is a Predictor for the Diagnosis of Multiple Sclerosis. *Sci. World J.* **2017**, 9320802, doi:10.1155/2017/9320802 (2017).

78 Rehn, D., Reimann, H. J., von der Ohe, M., Schmidt, U., Schmel, A. & Hennings, G. Biorhythmic changes of plasma histamine levels in healthy volunteers. *Agents Actions* **22**, 24-29, doi:10.1007/bf01968812 (1987).

79 Rizzo, V., Memmi, M., Moratti, R., Melzi d'Eril, G. & Perucca, E. Concentrations of L-dopa in plasma and plasma ultrafiltrates. *J. Pharm. Biomed. Anal.* **14**, 1043-1046, doi:10.1016/s0731-7085(96)01753-0 (1996).

80 De Peretti, E. & Mappus, E. Pattern of plasma pregnenolone sulfate levels in humans from birth to adulthood. *J. Clin. Endocrinol. Metab.* **57**, 550-556, doi:10.1210/jcem-57-3-550 (1983).

81 Lechin, F., Van Der Dijs, B. & Benaim, M. Stress versus depression. *Prog. Neuro-Psychopharmacol. Biol. Psychiatry* **20**, 899-950, doi:10.1016/0278-5846(96)00075-9 (1996).

82 Teuscher, A. Gut leben mit Diabetes Typ 2. Vol. 2. überarbeitete Auflage (Karl F. Haug Fachbuchverlag, 2006).

83 Zawalich, W. S., Karl, R. C., Ferrendelli, J. A. & Matschinsky, F. M. Factors governing glucose induced elevation of cyclic 3', 5' AMP levels in pancreatic islets. *Diabetologia* **11**, 231-235, doi:10.1007/bf00422327 (1975).

84 Charles, M. A., Lawecki, J., Pictet, R. & Grodsky, G. M. Insulin secretion. Interrelationships of glucose, cyclic adenosine 3:5-monophosphate, and calcium. *J. Biol. Chem.* **250**, 6134-6140, doi:https://www.ncbi.nlm.nih.gov/pubmed/168208 (1975).

5. Wissig et al

5.1 Eigenanteil

Molecular microbiology, July 2019, p. 16-28 Volume 112, Issue 1
doi:10.1111/mmi.14251

CyaC, a redox-regulated adenylate cyclase of *Sinorhizobium meliloti* with a quinone responsive diheme-B membrane anchor domain

Juliane Wissig[1], Julia Grischin[2], Jens Bassler[2], Christopher Schubert[1], Thorsten Friedrich[3], Heike Bähre[4], Joachim E. Schultz[5*], Gottfried Unden[1*]

[1] Microbiology and Wine Research, Institute for Molecular Physiology, Johannes Gutenberg-University of Mainz, Becherweg 15, 55099, Mainz, Germany
[2] Max-Planck-Institut für Entwicklungsbiologie, Abt. Proteinevolution, Max-Planck-Ring 5, 72076, Tübingen, Germany.
[3] Institute of Biochemistry, University of Freiburg, 79104, Freiburg, Germany.
[4] Medizinische Hochschule Hannover, Hannover, Germany.
[5] Pharmazeutisches Institut der Universität Tübingen, Auf der Morgenstelle 8, 72076, Tübingen, Germany.

Für diese Publikation habe ich die Adenylatcyclase $CyaC_{Sm}$ und deren Histidinmutanten in *E. coli* BTH101 *ΔcyaA* exprimiert und daraus Membranpräparationen hergestellt. Diese wurden anschließend von mir unter den beschriebenen Reduktions- oder Oxidationsbedingungen auf ihre Aktivität getestet, die Ergebnisse ausgewertet und grafisch dargestellt (Fig. 5B, Fig. 7A). Juliane Wissig hat das Protein kloniert, transformiert und aufgereinigt. Juliane Wissig hat auch die Messung des Häm-B-Anteils und den *in vivo* AC-Test durchgeführt sowie sowohl SDS PAGE als auch Western Blots hergestellt und grafisch dargestellt.

Jens Bassler hat das Sequenzlogo erstellt und die bioinformatische Auswertung vorgenommen. Christopher Schubert hat das Homologiemodel erstellt. Thorsten Friedrich hat die EPR-Messung durchgeführt. Heike Bähr hat die Guanylatcyclase-Aktivität von *CyaC*$_{Sm}$ getestet.
Prof. Dr. J. E. Schultz und Prof. Dr. G. Unden haben die Arbeiten beaufsichtigt, waren an der Planung und Interpretation der Ergebnisse beteiligt und haben die Endversion des Manuskripts verfasst.

5.2 Publikation

Molecular Microbiology (2019) 112(1), 16–28

doi:10.1111/mmi.14251
First published online 10 April 2019

CyaC, a redox-regulated adenylate cyclase of *Sinorhizobium meliloti* with a quinone responsive diheme-B membrane anchor domain

Juliane Wissig,[1] Julia Grischin,[2] Jens Bassler,[2] Christopher Schubert,[1] Thorsten Friedrich,[3] Heike Bähre,[4] Joachim E. Schultz[5]* and Gottfried Unden [1]*

[1] *Microbiology and Wine Research, Institute for Molecular Physiology, Johannes Gutenberg-University of Mainz, Becherweg 15, 55099, Mainz, Germany.*
[2] *Max-Planck-Institut für Entwicklungsbiologie, Abt. Proteinevolution, Max-Planck-Ring 5, 72076, Tübingen, Germany.*
[3] *Institute of Biochemistry, University of Freiburg, 79104, Freiburg, Germany.*
[4] *Medizinische Hochschule Hannover, Hannover, Germany.*
[5] *Pharmazeutisches Institut der Universität Tübingen, Auf der Morgenstelle 8, 72076, Tübingen, Germany.*

Summary

The nucleotide cyclase CyaC of *Sinorhizobium meliloti* is a member of class III adenylate cyclases (AC), a diverse group present in all forms of life. CyaC is membrane-integral by a hexahelical membrane domain (6TM) with the basic topology of mammalian ACs. The 6TM domain of CyaC contains a tetra-histidine signature that is universally present in the membrane anchors of bacterial diheme-B succinate-quinone oxidoreductases. Heterologous expression of *cyaC* imparted activity for cAMP formation from ATP to *Escherichia coli,* whereas guanylate cyclase activity was not detectable. Detergent solubilized and purified CyaC was a diheme-B protein and carried a binuclear iron-sulfur cluster. Single point mutations in the signature histidine residues caused loss of heme-B in the membrane and loss of AC activity. Heme-B of purified CyaC could be oxidized or reduced by ubiquinone analogs (Q_0 or Q_0H_2). The activity of CyaC in bacterial membranes responded to oxidation or reduction by Q_0 and O_2, or NADH and Q_0H_2 respectively. We conclude that CyaC-like membrane anchors of bacterial ACs can serve as the input site for chemical stimuli which are translated by the AC into an intracellular second messenger response.

Accepted 19 March, 2019. *For correspondence. E-mails Joachim.schultz@uni-tuebingen.de; Tel. +49 7071-2972475 (J. E. Schultz); unden@uni-mainz.de; Tel. +49-6131-3923550; Fax +49-6131-3926695 (G. Unden).

Introduction

Adenylate cyclases (ACs) generate cyclic AMP (cAMP), probably the most ubiquitous and versatile second messenger. Therefore, ACs are present in all domains of life (Gancedo *et al.*, 1985). Based on distinct sequence differences in the catalytic domains, ACs have been categorized into six classes with all but one limited to prokaryotes. Class III AC stand out as their members are present in eukaryotic and most bacterial species (Linder and Schultz, 2003; 2008; Baker and Kelly, 2004). A striking difference between bacterial and eukaryotic class III ACs is that the former are monomers and require homodimerization to form a productive catalytic center whereas the latter are pseudoheterodimers with two complementary catalytic half domains, probably the result of gene duplication. Bacterial class III ACs display a large variety in domain compositions with the catalytic domain usually at the C-terminus (Schultz and Natarajan, 2013; Bassler *et al.*, 2018). Many bacterial class III ACs are membrane-delimited by transmembrane spans, reminiscent of mammalian class III ACs that comprise a 2x6TM anchor. Strikingly, despite the significance of ACs for cell physiology, the role of the membrane anchor in function and regulation of the bacterial ACs is currently unknown. Mammalian pseudoheterodimeric ACs containing the 2x6TM anchors are regulated by G-protein α subunits (Chen-Goodspeed *et al.*, 2005; Linder and Schultz, 2008). Concerning the 6TM anchors, no intrinsic functional property beyond membrane anchoring is currently known. Indications exist from chimeras generated from class III ACs and

sensory membrane receptors that in principle the catalytic domains may be subject to direct regulation by extracellular receptor signals (Kanchan *et al.*, 2010; Beltz *et al.*, 2016; Ziegler *et al.*, 2017).

Surprisingly, the membrane anchor of the putative AC CyaC (or SMc01818 protein; $CyaC_{Sm}$) of *Sinorhizobium meliloti* was shown by cluster analysis to be closely related to the membrane-integral subunits FrdC or SdhC of bacterial diheme-B fumarate reductases and succinate dehydrogenases (Beltz *et al.*, 2016). The enzymes, also termed succinate: quinone oxidoreductases (SQOR) catalyze the reversible succinate + quinone ↔ fumarate + quinol interconversion which is either part of succinate oxidation in aerobic respiration, or of fumarate reduction in fumarate respiration (Lancaster, 2002). The FrdC and SdhC subunits catalyze the redox reaction with the quinones which involves a transmembrane electron transfer by two heme-B molecules integral to the membrane subunits (Unden and Kröger, 1986; Hägerhäll and Hederstedt, 1996; Schirawski and Unden, 1998; Lancaster *et al.*, 1999; 2000; Matsson *et al.*, 2000; Madej *et al.*, 2006a; 2006b). The heme-B molecules are coordinated by histidine (His) residues that form axial ligands to the heme iron.

$CyaC_{Sm}$ is one of 28 putative nucleotide cyclases of *S. meliloti* (Capela *et al.*, 2001; Krol *et al.*, 2016) but the individual cyclases have not been differentiated for their role as adenylate or guanylate cyclases. Currently, physiological roles for any of the nucleotide cyclases of *S. meliloti* and their individual target genes or their stimuli are unknown (Capela *et al.*, 2001; Garnerone *et al.*, 2018). The bioinformatic data pose the question whether $CyaC_{Sm}$ is a diheme-B protein. In answering this question, we provide the first demonstration of a distinct sensory function for a 6TM membrane anchor of a canonical class III AC going beyond membrane anchoring. The results may well have broader implications for the regulation of this populated class of 6TM ACs including the pseudoheterodimeric mammalian congeners.

Results

CyaC is a membrane-bound heme-B containing AC

The *cyaC* (or *smc01818*) gene of *S. meliloti* encodes a putative class III AC, $CyaC_{Sm}$, with a predicted mass of 60.5 kDa. The function of *cyaC* was tested in *E. coli* BTH101 which is deficient of AC (Karimova *et al.*, 1998). For heterologous *in vivo* studies CyaC was fused to a $Flag_3$-tag (termed CyaC-F, Table 1). Induction of *cyaC-F* expression increased β-galactosidase activity by up to 300 MU (Fig. 1A). The β-galactosidase activity depends on the formation of cAMP by CyaC which then activates in complex with the cAMP receptor protein CRP the expression of the *lac* operon and β-galactosidase production. In membranes isolated from BTH101 and the recombinant strain, AC activity increased from very low background levels (< 10 pmol cAMP × mg protein^{-1} min^{-1}) to 3.0 nmol cAMP × mg protein^{-1} min^{-1}. The activity for cGMP production from GTP was less than 5% of the adenylate cyclase activity demonstrating that CyaC has no significant guanylate cyclase activity. The adenylate cyclase activities of a strain producing CyaC without the $Flag_3$-tag were similar to the strain with CyaC-F, indicating that the $Flag_3$-tag has insignificant effect on CyaC activity.

Table 1. Strains and plasmids used.

Strains	Genotype or characteristics	
BTH101	*F- cya-99, araD139, galE15, galK16, rpsL1, str*^{R}*, hsdR2, mcrA1, mcrB1*	(Karimova *et al.*, 1998; Pakarian and Pawelek, 2016)
C43(DE3)	Mutant of BL21(DE3), for expression of membrane proteins	(Miroux and Walker, 1996)
Plasmids		
pWBT	Low-copy plasmid with IPTG inducible T5 promoter, *gent*^{R}	(Khan *et al.*, 2008; Krol *et al.*, 2016)
pCyaC-F	pWBT-*cyaC*-$Flag_3$, pWBT encoding $CyaC_{Sm}$-$Flag_3$	(Khan *et al.*, 2008; Krol *et al.*, 2016)
pCyaC(H27A)-F	Derivative of pCyaC-F encoding CyaC(H27A)-$Flag_3$	This study
pCyaC(H31A)-F	Derivative of pCyaC-F encoding CyaC(H31A)-$Flag_3$	This study
pCyaC(H68A)-F	Derivative of pCyaC-F encoding CyaC(H68A)-$Flag_3$	This study
pCyaC(H105A)-F	Derivative of pCyaC-F encoding CyaC(H105A)-$Flag_3$	This study
pCyaC(H149A)-F	Derivative of pCyaC-F encoding CyaC(H149A)-$Flag_3$	This study
pET28a	Expression vector, pBR *ori*, IPTG inducible T7 promoter, H_6-tag, kan^R	Novagen
pCyaC-S	pET28a encoding H_6-*cyaC*-$Flag_3$-Strep(CyaC-S)	This study
pCyaC(H27A)-S	Derivative of pCyaC-S, encoding CyaC(H27A)-S	This study
pCyaC(H31A)-S	Derivative of pCyaC-S, encoding CyaC(H31A)-S	This study
pCyaC(H68A)-S	Derivative of pCyaC-S, encoding CyaC(H68A)-S	This study
pCyaC(H105A)-S	Derivative of pCyaC-S, encoding CyaC(H105A)-S	This study
pCyaC(H149A)-S	Derivative of pCyaC-S, encoding CyaC(H149A)-S	This study

A

Sample	Miller U	nmol cAMP x mg protein^{-1} x min^{-1}
BTH101(pCyaC-F) – IPTG	0	0.08 (+/– 0.004)
BTH101(pCyaC-F) + IPTG	300 (+/–154)	3.0 (+/– 0.7)
CyaC-S		250 (+/– 45)

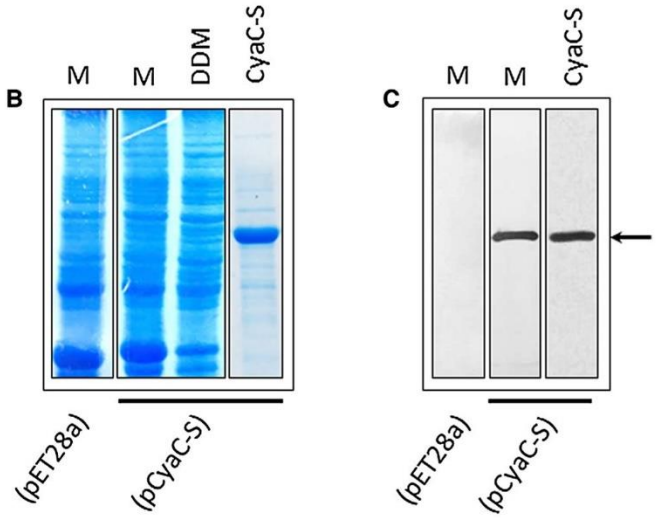

Fig. 1. Expression of CyaC in *E. coli* (A) and purification (SDS-PAGE (B) and Western Blot(C)). (A) Activity of recombinant CyaC-F (Table 1) was measured in *E. coli* BTH101(pCyaC-F) without and with IPTG induction by the β-galactosidase assay (Miller U) or in the membrane fraction of the bacteria by [^{32}P]cAMP production from [α-^{32}P]ATP (nmol cAMP × mg protein^{-1} × min^{-1}). Background activity of the empty vector was subtracted for the activities obtained for the strain with pCyaC-F. For (B) and (C) CyaC-S (Table 1) was overproduced in *E. coli* C43(DE3)(pCyaC-S). Strain C43(DE3)(pET28a) with empty vector serves as the reference. Membranes (M) and the dodecyl maltoside (DDM) extract of the membrane fraction (20 µg protein each), or the *d*-desthiobiotin eluate (3.4 µg protein) of purified CyaC-S from the Streptactin column were applied to the SDS-PAGE and stained for protein (B). For the Western blot, 5 µg of membrane proteins (M) and 0.2 µg purified CyaC-S were applied. CyaC-S (66,975 Da) has the mobility of a M_r 68 kDa protein (arrow).

For purification and detection of $CyaC_{Sm}$ the protein was tagged with an N-terminal His_6 and C-terminal $Flag_3$ and Strep tags (termed CyaC-S, Table 1). Cell homogenates or membranes of induced bacteria showed no visible additional protein band in SDS-PAGE at the expected position, indicating rather moderate expression. After membrane solubilization by 1% dodecylmaltoside (DDM) CyaC-S was affinity-purified on a Streptactin column. The purified protein had high AC activity (250 nmol cAMP × mg protein^{-1} min^{-1}) and consisted to 90 to 93% of a protein with M_r 68 kDa (Fig. 1B) which is very close to the predicted mass of 66 975 Da for CyaC-S. The protein reacts with anti-Strep in Western blots (Fig. 1C) and had the tryptic peptide pattern of CyaC-S. From 0.5 g membrane protein, 1 mg purified CyaC-S was obtained corresponding to an approx. 500-fold enrichment from the membrane based on protein contents.

Solutions of CyaC-S were colored reddish and had an absorbance spectrum typical for heme-B proteins with maxima at 560 and 530 nm for the α- and β-bands respectively (Fig. 2). Reduction of the protein by dithionite resulted in an increase in the α-band by factors of 1.7 to 3.3 depending on the redox state of the preparation, whereas oxidation by ferricyanide abrogated the α-band. The absorption spectrum of a pyridine extract of the CyaC preparation showed in the reduced state maxima of absorption at 556 and 524 nm (Fig. S1) which is characteristic for protoheme IX (Berry and Trumpower, 1987; Barr and Guo, 2015). Addition of dithionite abolished the maxima. Therefore CyaC-S is a heme-B protein, and 30 to 60% of the heme-B was in the reduced state after purification. The spectrum and the response to redox agents are similar to membrane-bound heme-B proteins such as fumarate reductase of *Wolinella* (formerly *Vibrio*) *succinogenes* (Unden *et al.*, 1980; Unden and Kröger, 1981).

CyaC is a diheme-B protein

From the protoheme IX content and the reduced *versus* oxidized heme-B spectrum, the extinction coefficient $\Delta\varepsilon_{560-580\,nm}$ (oxidized versus reduced) was determined for CyaC to be 21.5 mM^{-1} cm^{-1}. The value is very close to values of *W. succinogenes* fumarate reductase (Unden and Kröger, 1981). From the proportion of CyaC in the

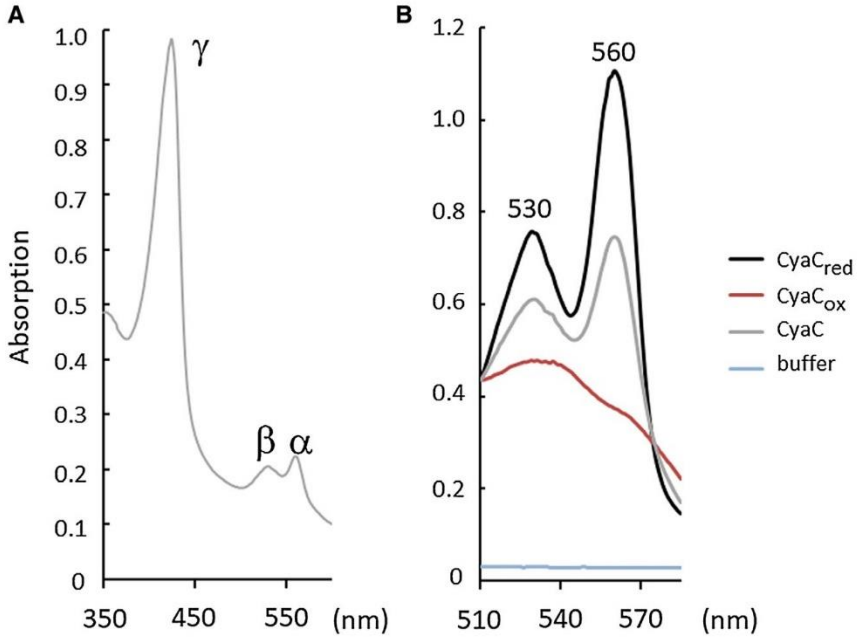

Fig. 2. UV-Vis spectra of isolated CyaC-S. (A) Spectrum with maxima for the γ, β and α bands at 410, 530 and 560 nm respectively. The sample contained 1.35 mg/ml of CyaC-S in elution buffer as isolated. (B) Spectrum of the α- and β-band region for CyaC-S (preparation as for (A) but at a concentration of 2.7 mg/ml) as isolated (gray), after oxidation with ferricyanide (red), or fully reduced with dithionite (black). The heme-B content of the preparation was 1.08 µmol × g protein, or 1.21 mol × mol^{-1} of CyaC-S using the molecular extinction coefficient ($\Delta\varepsilon_{556nm}$ (reduced minus oxidized state) = 21.5 mM^{-1} cm^{-1}) of CyaC (see Fig. S1), the molar mass of CyaC-S (67 kDa), and the purity of the preparation of CyaC-S (90%) which was determined by quantitative proteome analysis of the sample using LC-MS analysis (Distler *et al.*, 2014; 2016).

protein preparation and the heme-B content, a specific content of 1.21 mol heme/mol CyaC-S can be calculated (Fig. 2).

The heme-B contents indicate that CyaC-S is a diheme-B protein like the FrdABC and SdhABC enzyme complexes of *W. succinogenes* and *B. subtilis* respectively (Unden and Kröger, 1981; Hägerhäll and Hederstedt, 1996; Lancaster *et al.*, 1999; Lancaster, 2002). Alignment of the CyaC 6TM region with the membrane anchors of the SQOR enzymes showed high similarity between the five N-terminal transmembrane spans of CyaC and the domain of the SQOR proteins. The corresponding SQOR enzymes contain type B anchors according to (Lancaster, 2002) with 5 TMs. The histidine residues coordinating the heme molecules in FrdC and SdhC (Hägerhäll and Hederstedt, 1996; Gross *et al.*, 1998; Lancaster *et al.*, 1999) were conserved and placed individually in TM1 to TM4 of CyaC (Fig. 3). The shared Frd/Sdh/CyaC 4-His signature sequence has high significance. Of note is the tryptophan residue at position 147 that is fully conserved in CyaC proteins but missing in the membrane anchors of the SQOR enzymes.

For testing the importance of the His signature for heme coordination and CyaC AC activity, the conserved His residues were individually substituted by Ala residues (Fig. 4). The proteins were first produced as variants of CyaC-F representing CyaC with a Flag$_3$-tag (Table 1). The variants are all membrane-integral as shown by Western blotting of isolated membranes (Fig. S2). The corresponding His variants of CyaC-S were isolated by DDM extraction from the membrane as described for CyaC-S. For all variants the heme-B spectra were strongly decreased even when fully reduced (Fig. 4), and the heme-B contents were in the range from 3 to 20% of the wild type (Table S1). Substitution of the not-conserved His residue H31A had no significant effect on the heme-B content, but there is a small shift in the spectrum. It is concluded that the four conserved His residues are important for coordinating the heme in CyaC. Maximally two axial His ligands are required for coordination of one heme which is in favor of two heme molecules in CyaC, but substitution of any of the conserved His residues affected binding of both heme groups.

CyaC requires heme-B to form active enzyme

The AC activity of the wild-type and of the His point mutants were assayed in *E. coli* BTH101 and in membranes with variants of CyaC-F (Fig. 5). When testing the β-galactosidase that is produced in the BTH101 reporter strain substitutions H27A and H105A in CyaC-F indicated loss

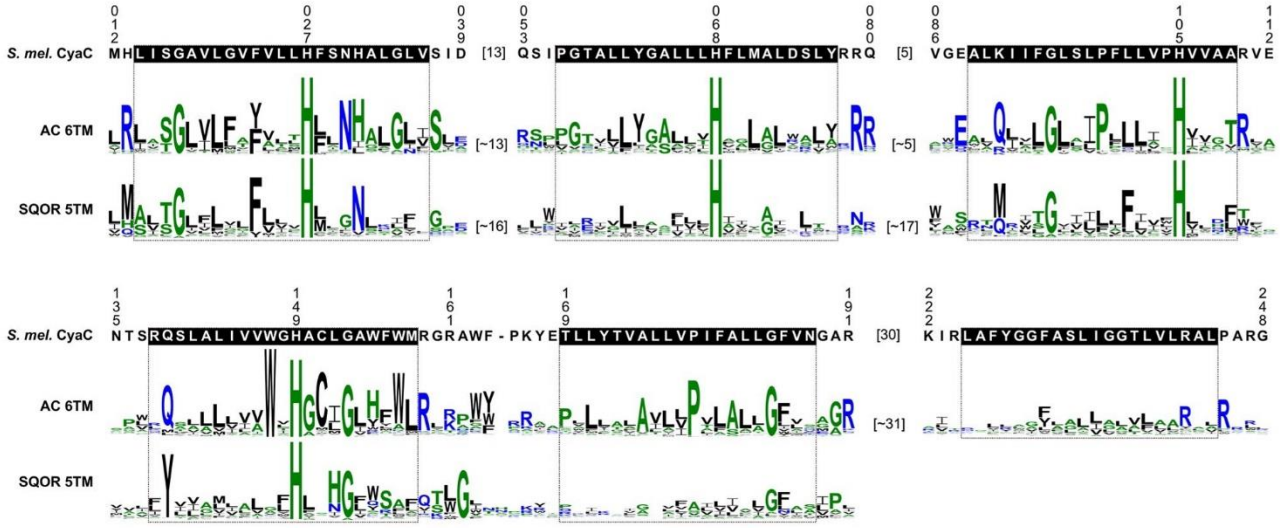

Fig. 3. Conserved His residues in the 6TM anchor of CyaC. The sequences of the $CyaC_{Sm}$ 6TM domains and the 5TM domains of bacterial SQORs (SdhCD and FrdC subunits) are aligned. The sequence logos were created from 151 representative AC sequences and 971 representative SQOR sequences, selected from a comprehensive data set of appx. 12700 SQOR-transmembrane domain proteins. Numbering on top refers to the positions in $CyaC_{Sm}$ (Uniprot entry Q92MZ6). Black highlighting in the CyaC sequence and boxed logo segments indicate the extent of the transmembrane spans. Loop segments between the transmembrane spans are left out for clarity. Numbers in brackets indicate the most common number of left-out residues.

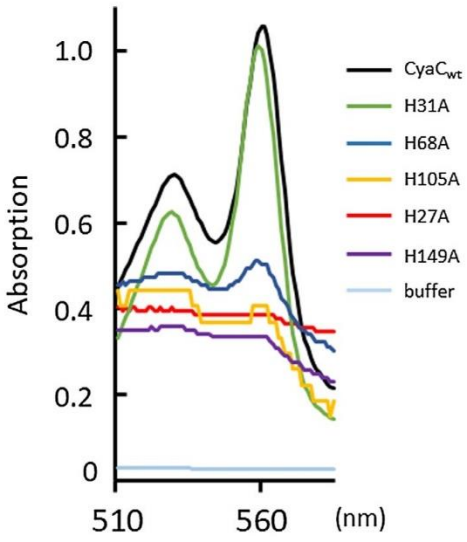

Fig. 4. Significance of conserved His residues in the 6TM region of CyaC for heme-B binding. UV-Vis spectra of purified CyaC-S (wild-type and His variants H27A, H31A, H68A, H105A, H149A) were recorded from purified protein in the dithionite-reduced state. The protein contents of the samples are adjusted to 2 mg CyaC/ml, protein purity was determined from the stain in 10% SDS-PAGE. Heme-B contents calculated from the reduced-oxidized UV-Vis spectra are given in Table S1 for CyaC and His variants.

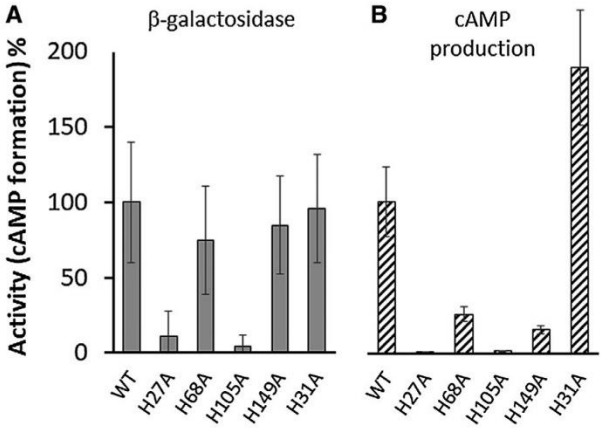

Fig. 5. Activity of wild-type CyaC and His mutants expressed in *E. coli* BTH101. (A) AC activity was tested in BHT101pCyaC-F by measuring the cAMP-dependent β-galactosidase activity. The strains encoded CyaC-F or variants mutated in the His signature sequence. The 100% activity (wild type) corresponds to 300 MU (+/– 154). Background activity of the empty vector (70 MU) was substracted from the strain with pCyaC-F (370 MU). Activity was tested in 5 to 7 replicates. (B) Activity of cAMP production with isolated membranes of wild type and mutant CyaC-F expressed in *E. coli* BTH101 from pCyaC-F or the His variants. The data were obtained from three independent experiments each ($p < 0.002$ for the wild type and variants H27A, H68A, H149A and H149A of CyaC-F). The number of 100% activity (wild type) corresponds to the production of 3 (±0.7) nmol of cAMP·min^{-1} mg^{-1}. Western blots confirmed the presence of comparable amounts of CyaC-F in cells producing the wild-type and the His variants H31A, H68A, H105A, and H149A (Fig. S3).

of AC activity (Fig. 5A). Substitutions H68A and H149A had only slight effects on activity, whereas mutation of the non-conserved residue H31A was inconspicuous. Response of cAMP production to mutation was basically the same but more marked when tested in membrane preparations (Fig. 5B). Substitutions H27A and H105A resulted in loss of cAMP production whereas substitutions H68A and H149A retained some activity. The differing assay modes for cAMP production in bacteria (indirect

via induction of β-galactosidase without linear correlation of activity to cAMP levels) and in the membranes (direct cAMP measurement) may explain the differences.

Oxidation and reduction of CyaC heme-B by quinones

In the membrane anchor subunits of SQOR enzymes heme-B is close to the quinone-reactive site and responds to the quinones (Cecchini *et al.*, 1986; Lancaster *et al.*, 2000; Madej *et al.*, 2006b; Ruprecht *et al.*, 2009). Redox responses of CyaC heme-B to quinones was tested spectroscopically with purified CyaC-S (Fig. 6). Heme-B was fully reduced by dithionite that was supplied in slight molar excess (Fig. 6A). Sequential addition of Q_0 (2,3-dimethoxy-5-methyl-1,4-benzoquinone) resulted in a stepwise and rapid oxidation of the heme-B. The residual (approx. 8%) was oxidized by ferricyanide, indicating that most of the heme-B is accessible to oxidation by Q_0. Decyl-Q (Q_0 with a decyl residue in position 6) oxidized the heme-B under equivalent conditions to similar extents (approx. 92%, not shown) whereas the menaquinone analog menadione (MD, or 2-methyl-1,4-naphthoquinone) oxidized the heme-B only to low extents (approx. 12%, Fig. 6A). The degree of oxidation is related to the midpoint potentials E_0' of Q_0, decyl-Q and MD (+160 mV, +110 mV, and –1 mV (32) respectively), and indicates that heme-B is rather positive (> 0 mV).

In the reverse reaction (Fig. 6B) oxidized heme-B is nearly completely reduced by Q_0H_2. Taken together, the data show that heme-B of CyaC is efficiently oxidized or reduced by quinones. Ubiquinone represents the major respiratory quinone in *S. meliloti* (Daniel, 1979; Collins and Jones, 1981).

Control of AC activity by oxidation and reduction

Based on the finding that the redox state of heme-B responds to Q_0 and Q_0H_2 (Fig. 6), the response of CyaC-F activity (cAMP production) to quinones was tested in membranes of *E. coli* BTH101 (Fig. 7). The experimental conditions of Fig. 7A were set to oxidize or reduce the heme-B by the quinone. Oxidation of the membranes by Q_0 caused a significant 1.6-fold increase in the AC activity when the membranes were prepared in the presence of DTT (Fig. 7A, left). Q_0H_2 reduced AC activity by 50% when membranes were prepared in the absence of a reductant (Fig. 7A, right). Reduction of the membranes by $NaBH_4$ which is able to reduce the membrane-integral quinone similarly caused a 40% reduction in AC activity (Fig. 7A right). The data indicate that (i) the state of AC reduction was dependent on the experimental condition during membrane preparation, i.e. in presence or absence of the reducing agent DTT (1mM); (ii) oxidation and reduction have opposite effects on AC activity. Overall, the activity of fully reduced CyaC was increased almost threefold by oxidation (Fig. 7A).

The second part of the experiments (Fig. 7B) tested whether the effects of oxidized and reduced quinone or reduction by $NaBH_4$ can be verified by physiological electron donors of respiration. Here, O_2 and NADH were

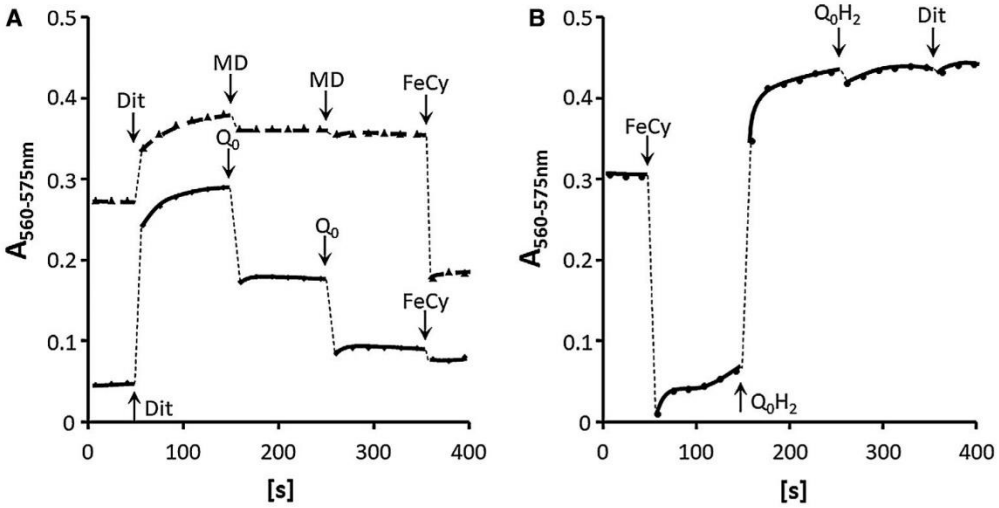

Fig. 6. Oxidation (A) and reduction (B) of purified CyaC-S by quinone analogs.
A. Purified CyaC-S (15 to 18 μM) was first fully reduced by addition of small amounts of dithionite (Dit, 220 μM). Then Q_0 (solid line) or menadione (MD, dashed line) were added stepwise (170 μM each). After two additions, ferricyanide (FeCy, 60 μM) was applied for full oxidation of the heme-
B. At each time point shown, spectra of the solution were recorded and the $A_{560-575nm}$ values were calculated. B. Purified CyaC-S (15 to 18 μM) was first fully oxidized by the addition of ferricyanide (FeCy, 30 μM), and then Q_0H_2 (reduced Q_0, 170 μM each addition) was added. Finally, full reduction was achieved by dithionite (220 μM). The Q_0H_2 applied was depleted of surplus reductant KBH_4 by intermediate acidification of the Q_0H_2 (Unden and Kröger, 1986), and Q_0-deficient sample yielded only slow reduction of the heme-B.

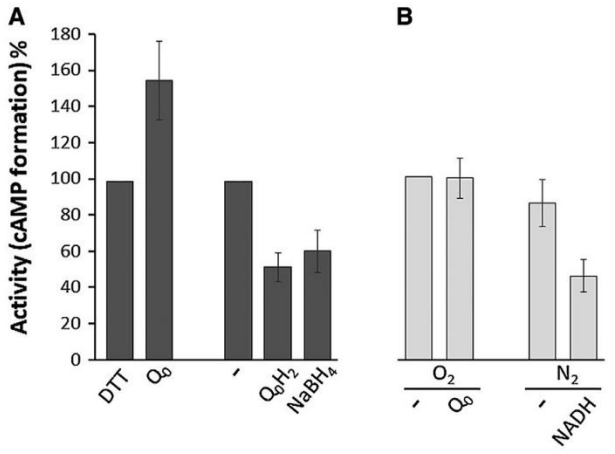

Fig. 7. Effect of Q_0 (A) and respiratory electron donors or acceptors (NADH or O_2) (B) on CyaC activity in membranes. Membranes were prepared from *E. coli* BTH101(pCyaC-F) expressing CyaC-F as in Fig. 5. (A) Membranes were prepared without (left) or with 1 mM DTT in the buffer. cAMP production was tested with and without addition of Q_0, Q_0H_2 or $NaBH_4$. Q_0H_2 was prepared as described in the methods section. The 100% activity for the membranes (25 µg protein per assay) prepared under reducing and oxidizing conditions corresponds to (1.36 (±0.39) and 2.3 (±0.39) nmol of cAMP·min^{-1} mg^{-1}. The number of separate membrane preparations (assayed in duplicates) was 7 for the left and 4 for the right part, the significance $p < 0.02$. The significance for the comparison between the $NaBH_4$- and Q H_2-treated samples was $p < 0.05$. The membranes for (B) were prepared from *E. coli* BTH101(pCyaC-F) expressing CyaC-F. Membranes were prepared without DTT in the buffer and incubated without or with Q_0 aerobically or with NADH anaerobically. cAMP production was tested as in Fig. 7A. 100% activity for the membranes (50 µg per sample) correspond to 3.4 (±0.2) nmol of cAMP·min^{-1} mg^{-1}.

applied as the physiological electron acceptors and donors for respiration that are supposed to oxidize or reduce, respectively, the respiratory chain and the ubiquinone. Under aerobic conditions, addition of Q_0 had no further stimulating effect on the AC activity, whereas anoxic conditions (i.e. absence of O_2) and particularly NADH caused inhibition up to 60%. Overall, reduction by NADH caused inhibition by a factor of 2.2 relative to the aerobic or oxidized state (Fig. 7B) which is similar to the effects of oxidation or reduction by quinone or reducing agents (Fig. 7A).

CyaC contains a [2Fe2S] cluster

TM6 of CyaC is followed by a cytoplasmic ferredoxin type (FD) domain with a Cys cluster (Cys283-X_5-Cys-X_2-Cys-X_{34}-Cys327) similar to [2Fe-2S]-type ferredoxins (Iwasaki *et al.*, 2011). The presence of iron-sulfur (Fe-S) clusters in the preparation was monitored by EPR-spectroscopy. The preparation was either used as isolated (oxidized form) or after reduction with a few grains of dithionite (reduced form). No signal of a Fe-S cluster was detectable in the oxidized sample either at 40 K (Fig. 8) or 13 K (data not shown). However, the reduced sample showed a clear signal at 40 K and 5 mW microwave power (Fig. 8). The signal was easily saturated at lower temperature indicating the presence of a binuclear cluster. The signal exhibits axial symmetry with $g_{//,\perp} = 2.024$ and 1.94. Thus, the EPR data are in agreement with the proposal that CyaC contains one Fe-S cluster of the [2Fe2S] type.

Discussion

$CyaC_{Sm}$ comprises a quinone reactive diheme-B membrane anchor of the Frd or Sdh type

CyaC is an AC with a diheme-B membrane anchor. The close similarity of the membrane anchor domain to the FrdC subunit of *W. succinogenes* (Madej *et al.*, 2006b) allows modeling of the 6TM region using FrdC as the template (Fig. 8A). CyaC has to be present in the dimeric state since purified CyaC has high catalytic activity, and the catalytic site of bacterial ACs is located in a cleft between the monomers of the homodimer (Linder and Schultz, 2008). The heme-B binding 5TM region resembles the FrdC and SdhC subunits in their topological arrangement with a distal heme-B_D close to the periplasmic and a proximal heme-B_P close to the cytoplasmic side of the membrane (Fig. 8B) (Lancaster *et al.*, 1999; Hederstedt, 2002; Madej *et al.*, 2006b). The supposed coordinates for heme-B_D of CyaC are H27 and H105 of TM1 and TM3, for heme-B_P H68 and H149 of TM2 and TM4 respectively. In CyaC, the calculated distance between the two heme molecules is very close (16 Å center to center, and 7.8 Å edge to edge) and ideal for rapid electron transfer (Lancaster *et al.*, 1999; Ohnishi *et al.*, 2000). The invariant tryptophan residue W147 is positioned in between the heme molecules with a predicted orientation outward of TM4 (Fig. 8B). A tryptophan residue of this position could be important for the quinone reactivity of the heme-B molecules (Cecchini *et al.*, 1986; Westenberg *et al.*, 1993) but other more specific roles are feasible. Overall, there is a remarkable similarity of the 6TM region of CyaC to FrdC of *W. succinogenes* (or SdhC of *B. subtilis*). The heme-B molecules may have in addition a structural role (Friden and Hederstedt, 1990; Gross *et al.*, 1998; Lancaster *et al.*, 1999; Hederstedt, 2002) resulting in destabilization of heme-B binding and loss of both heme molecules upon mutation.

The heme-B of CyaC is efficiently oxidized by the quinone analogs Q_0 (E_0' +160 mV (Schnorf, 1966)) and decyl-Q (E_0' +110 mV (Schnorf, 1966)), whereas the menaquinone analog MD (E_0' −1 mV (Schnorf, 1966)) was less efficient. Ubiquinone represents the major respiratory quinone in *S. meliloti* membranes (Daniel, 1979; Collins and Jones, 1981) implying that the function of CyaC is linked to the state of respiration. Remarkably, the heme-B responded to oxidized as well as reduced quinones which

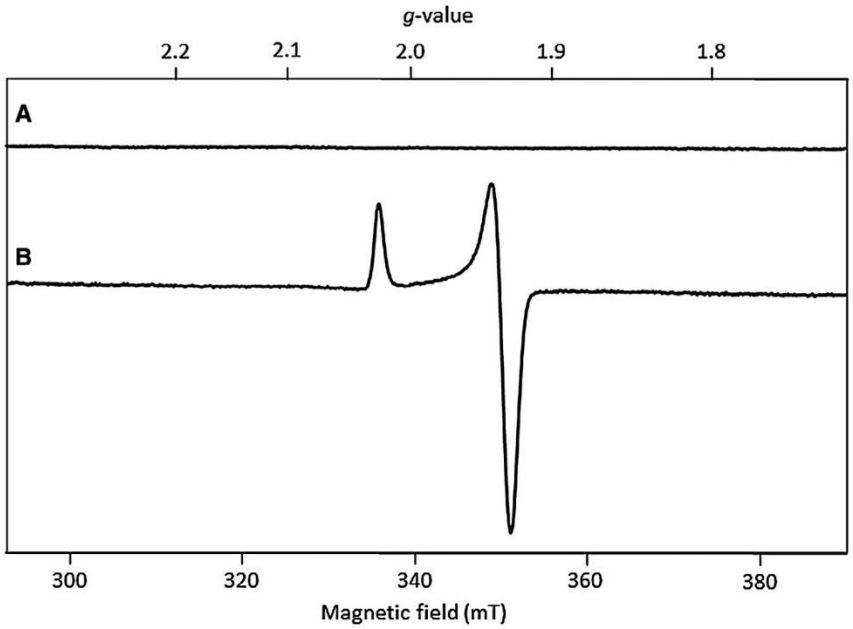

Fig. 8. EPR spectra of oxidized (A) and dithionite-reduced (B) aliquots of a 35 μM sample of CyaC at 40 K and 5 mW. Other EPR conditions were: microwave frequency, 9.47 GHz; modulation amplitude, 0.6 mT; time constant, 0.164 s; scan rate, 17.9 mT/min.

implicates a redox potential close to that of Q_0 which agrees with the poor oxidation of heme-B by MD. TM6 of CyaC which has no equivalent in FrdC links the membrane anchor to the cytoplasmic ferredoxin domain (FD) which binds a redox-sensitive [2Fe-2S] cluster (Fig. 8A).

The heme-B is quinone reactive and confers redox sensitivity to CyaC-S

The close structural and functional relation of the CyaC membrane anchor to subunits of electron transfer enzymes and the presence of a redox sensitive [2Fe-2S] cluster suggest a role for redox reactions in CyaC function although the catalytic activity of ACs involves no redox reactions. In FrdABC, the electrons supplied by the quinol (menaquinol) are used for fumarate reduction and are transferred from the heme-B (located in FrdC) to three FeS clusters in FrdB to FAD and finally to the fumarate site in FrdA (Lancaster *et al.*, 1999; Cecchini *et al.*, 2002). The catalytic activity of CyaC and ACs include no redox reaction, implicating that redox reactions of the membrane anchor and of the FD domain are involved in the regulation of AC activity. This assumption is corroborated by the response of AC activity to the redox state of the quinones. A model for CyaC activity regulation with the 6TM anchor as the sensory and the CD domain as the output site is shown in Fig. 9A. According to this model, the stimulus (redox state of the quinones) is (i) perceived by heme-B, (ii) transmitted to the [2Fe-2S] cluster which then (iii) controls the activity of CD. The first reaction (i) i.e. the redox response of the heme-B to the redox state of the quinones and a relation to CyaC activity has been shown here. The active site for quinone reactivity could be at heme-B_D or heme-B_P. The properties of CyaC (homology model in Fig. 9A,B) suggest some features of the supposed intramolecular signal transduction (ii). The predicted edge-to-edge distances for heme-B_D to heme-B_P (7.8 Å) and for heme-B_P to [2Fe2S] (16.1 Å) are in a range suited for electron transfer. The third part of the intramolecular signaling (iii) is a matter of speculation. In a working hypothesis it is supposed that the iron-sulfur cluster serves as a converter that drives a conformational switch in CD as described for the FeS clusters in the redox stress sensor SoxR (Imlay, 2015; Kobayashi, 2017). SoxR consists of a sensory domain with a $[2Fe2S]^{1+}$ cluster and a DNA-binding domain. Superoxide anion radicals oxidize the iron-sulfur cluster to the $[2Fe\text{-}2S]^{2+}$ state which distorts the SoxR dimer and alters promoter binding and transcription by RNA polymerase. Folding and unfolding are basic principles for regulating the function of the CD of ACs (Schultz and Natarajan, 2013) which could be triggered by the redox reaction in FD.

Regulation of a membrane-embedded sensor by the quinol/quinone redox state is known for the sensor kinase ArcB and related sensors. ArcB of the ArcB-ArcA two-component system of *E. coli* controls expression of aerobic and anaerobic metabolism in response to the redox state of the

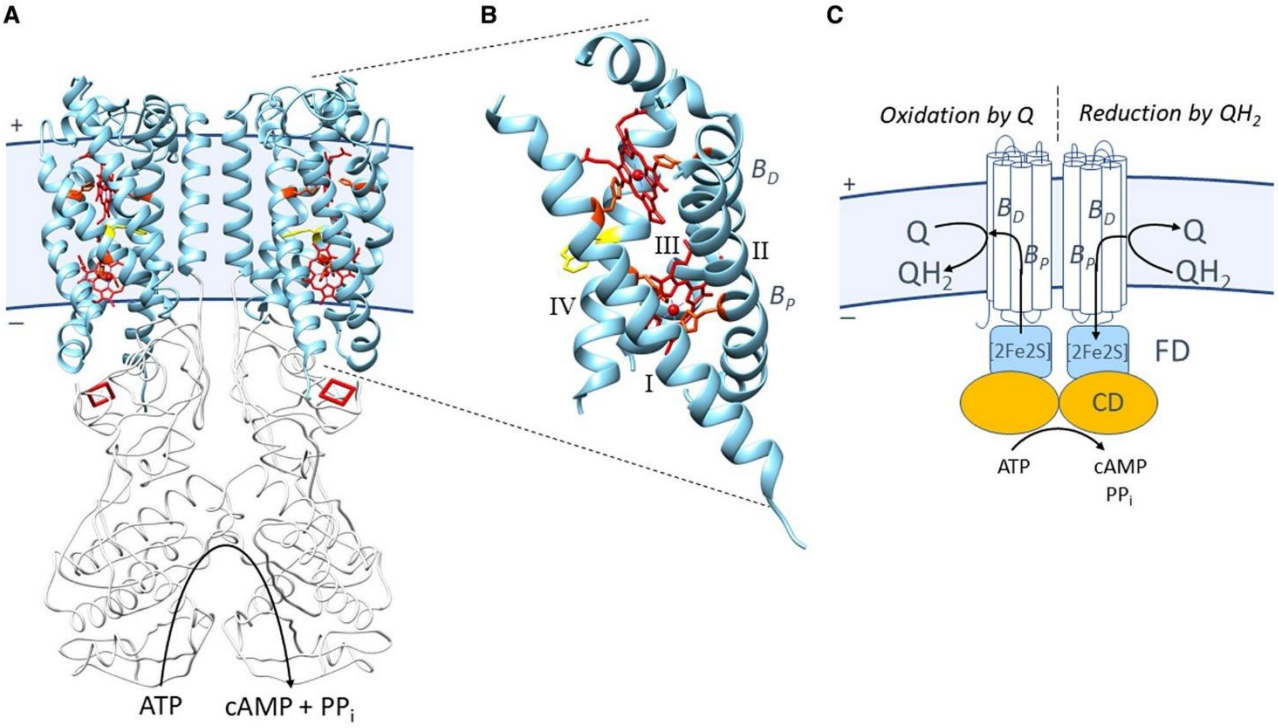

Fig. 9. Homology model of CyaC based on the crystal structure of $FrdC_{Ws}$. (A) Structure prediction for $CyaC_{Sm}$, (B) a detailed model of TM 1 to 4 of the TM region, and (C) a model for the reversible interaction of CyaC with the respiratory quinones. The three domains of $CyaC_{Sm}$ consist of the membrane anchor (light blue) including the distal and proximal heme-B, the [2Fe2S]-cluster binding domain and the catalytic CD domain (white). Modeling (see *Experimental procedures*) was based on the structures of FrdC from *W. succinogenes*, the ferredoxin of *E. coli* (FD) and the catalytic domain (CD) of CyaB of *P. aeruginosa* as the templates. The heme and the [2Fe2S] cluster are labeled in red, residues coordinating the distal and proximal heme-B (B_D and B_P) of the membrane anchor in red and W147 in yellow. Part (B) shows TM1 to TM4 of CyaC and the coordination of the heme-B molecules by TM1, TM2, TM3 and TM4 in detail. His ligands H27, H68, H105 and H149 are labeled in red, W147 in yellow. The distal heme-B (B_D) is coordinated by H27 and H105, the proximal heme-B (B_P) by H68 and H149. In (C) the heme-B molecules of the 6TM anchor are reversibly oxidized and reduced by the quinones. It is assumed that heme-B_P oxidizes and reduces the [2Fe2S] cluster of FD.

quinones (Malpica *et al.*, 2004; 2006). In ArcB, the respiratory state (i.e. the Q/QH_2 ratio) controls an intermolecular thiol/disulfide switch in the ArcB dimer and reversible activity regulation. The reversible oxidation and reduction of the heme-B of CyaC is supposed to stimulate or inhibit AC activity in a similar way in response to the redox state of the respiratory quinones (Fig. 9C), implicating a role of CyaC in the regulation of respiration-related processes.

Experimental procedures

Cloning, PCR

Standard molecular genetic methods were used (Sambrook and Russell, 2001). Plasmids (Table 1) were isolated using the GeneJET plasmid miniprep kit and PCR products (primers described in Table S2) with the GeneJET PCR purification kit (Fermentas). For transformation of *E. coli*, electroporation (Dower *et al.*, 1988) or heat shock (Froger and Hall, 2007) were used. Antibiotics (gentamicin or kanamycin) were used at 50 µg/ml.

Protein purification

6His-$CyaC_{Sm}$3Flag-Strep ('CyaC-S') was produced in *E. coli* C43(DE3)(pCyaC-S) (Table 1). A single clone from LB agar (Bertani, 1951) plates (with kanamycin) was grown in LB medium with kanamycin overnight. The main culture (0.6 l LB medium + kanamycin in 2 l baffled Erlenmeyer flasks), inoculated with 5% (vol/vol) of the pre-culture, was grown at 30°C under shaking (300 U/min) to OD_{578} of 0.9. Then expression of $CyaC_{Sm}$ was induced with 1 mM IPTG. The bacteria were grown for 5 more hours, then the culture was kept at 4°C for 16 h without shaking. The bacteria were collected by centrifugation, resuspended and centrifuged in wash buffer (50 mM Tris/HCl, pH 8, 10 mM $MgCl_2$). The bacteria (5 g wet weight in 25 ml wash buffer) were disintegrated by two passages through a French press (85 Bar). Detritus was removed (9,000 × *g* at 4°C for 20 min) and membranes were pelleted (4°C, 260,000 × g, 75 min). Membranes were resuspended in 50 mM Tris/HCl, pH 8, 10% glycerol (vol/vol), and 1 mM DTT. 1% DDM (final conc.) was added and the mixture was homogenized with a Teflon potter. After stirring for 60 min on ice, followed by centrifugation at 260,000 × *g* (60 min, 4°C), the supernatant was applied to a

streptavidin affinity column (1.5 ml volume) (IBA, Göttingen). Wash buffers contained 100 mM Tris/HCl (pH 8), 150 mM NaCl, 1 mM EDTA, 0.05% DDM and 1 mM DTT. CyaC-S was eluted from the column using 2.5 mM *d*-desthiobiotin in the same buffer. Protein in the reddish desthiobiotin eluate (main fractions 2 ml) was determined by a modified Lowry protein assay (Lowry *et al.*, 1951; Pomory, 2008). Purity and identity of the protein in the CyaC preparation was determined by a quantitative proteome analysis using LC-MS analysis (TOP3-quantification) (Distler *et al.*, 2014; Distler *et al.*, 2016). According to the MS analysis, CyaC-S amounted to 90 to 93% of the proteins with the chaperone proteins DnaK_ECOLI (2.0% of the protein) and CH60_ECOLI (0.7%) representing the major contaminations.

Heme-B measurement

UV-Vis spectra were recorded in rubber-stoppered semi-micro cuvettes. The degassed and N_2-flushed (99.999% N_2) samples (15 to 18 µM CyaC-S) were measured at 20°C. Q_0 (2,3-dimethoxy-5-methyl-1,4-benzoquinone) and menadione (MD, 2-methyl-1,4-naphthoquinone) were dissolved in 100% ethanol (20 mM). Na-Dithionite (20 mM) was freshly dissolved in cold degassed H_2O. Q_0H_2 was produced by addition of KBH_4 (two-fold excess) to Q_0. Redundant KBH_4 was destroyed by lowering the pH to 1 by HCl addition, followed by adjusting pH 7 with NaOH. Heme-B content was calculated using the molar extinction coefficient $\Delta\varepsilon_{580\text{-}560nm}$(red-ox) of 21.5 mM^{-1} cm^{-1} of CyaC, for the reduced minus oxidized state of CyaC, from the absorbance at 575 and 560 nm, and the protein concentration. The molar extinction coefficient $\Delta\varepsilon_{556\,nm}$(red-ox) of CyaC was determined from the pyridine hemochrome spectrum of CyaC (Fig. S1), the absorbance of the preparation at 580 and 560 nm and the protein concentration (Berry and Trumpower, 1987; Barr and Guo, 2015).

EPR spectroscopy

A 300-µl sample CyaC (2.3 mg/ml) was either used as isolated ('oxidized') or reduced by addition of a few grains of dithionite ('reduced'). EPR measurements were conducted with an EMX 6/1 ESR spectrometer (Bruker) operating at X-band (Uhlmann and Friedrich, 2005). The sample temperature was controlled with an ESR-9 helium flow cryostat (Oxford Instruments). Spectra of the oxidized and reduced sample were recorded at 40 K and 5 mW microwave power.

In vivo assay for cAMP production in bacteria (β-galactosidase reporter strain)

Plasmid pCyaC-F (Table 1, gift of A. Becker, Marburg) (Khan *et al.*, 2008; Krol *et al.*, 2016) was transformed into *E. coli* BTH101 (*cyaA*). cAMP production by CyaC-F was tested by the β-galactosidase production and activity after growing *E. coli* BTH101 (pCyaC-F) to OD_{578} 1 to 1.5. Cells were cultivated in 96-deep-well plates at 30°C for 24 h. Enriched mineral (eM9) medium (Lehnen *et al.*, 2002), an amino acid supplemented M9 medium (Miller, 1992) was used for growth with sodium nitrate (50 mM), glycerol (50 mM) and gluconate (3 mM) as the energy substrates (Lukas *et al.*, 2010). Nitrate was included to support anaerobic growth, glycerol and gluconate as carbon sources that support growth without strong glucose repression. For anaerobic conditions, plates were incubated under N_2 in anaerobic jars, β-galactosidase activity was determined in 96-well microtiter plates (Graf *et al.*, 2016). β-Galactosidase is given in Miller U, or MU (ΔA_{420} min^{-1} ml^{-1} $OD_{570}{}^{-1}$) (Miller, 1992; Graf *et al.*, 2016).

Adenylate cyclase activity (cAMP production)

cyaC-F was expressed from pCyaC-F in *E. coli* BTH101 (*cyaA*) in LB medium (with gentamicin, 30°C). Induction was with 30 µM IPTG at an OD_{600} of 0.7 to 0.8 for 5 h at 22°C. Cells were washed with 50 mM Tris/HCl, pH 8.0 and 1 mM EDTA and the pellet stored at −80°C. Membranes were prepared as described (Beltz *et al.*, 2016).

Adenylate cyclase activity was determined for 1 min in 100 µl at 37°C. The reactions contained 25 µg protein, 50 mM MOPS pH 8, 13% glycerol, 3 mM $MnCl_2$, 6 mM creatine phosphate and 23 µg creatine kinase, 750 µM [α-^{32}P] ATP, and 2 mM [2,8-^{3}H] cAMP to monitor yield during cAMP purification (Salomon *et al.*, 1974). Substrate conversion was kept below 10%. Respective controls were carried out throughout. All solutions (except for the membrane preparation) were degassed and flushed with N_2. The quinones were dissolved in H_2O, $NaBH_4$ in 0.1 M NaOH, Na-dithionite in cold H_2O. QH_2 was produced by a solution containing 5 mM $NaBH_4$ and Q_0. To measure the effect of QH_2 alone, the solution was kept at pH 7.5 for 10 min, >40 times the half-life of $NaBH_4$ at this pH. This reduced $NaBH_4$ concentration below 1 fM).

For the experiment of Fig. 7B, cAMP was determined by preparing the bacterial membranes without DTT in the buffers. The membranes of BTH101 (pCyaC-F) were incubated aerobically, or after degassing and followed by incubation under N_2 with 0.2 mM ATP and 0.2 mM NADH. After 2 and 5 min, samples (BTH101 (pCyaC-F) were withdrawn and samples were prepared for cAMP quantification. For measurement of guanylate cyclase activity, 0.2 mM GTP was added instead of ATP. Concentrations of cAMP and cCGMP were determined by high performance liquid chromatography coupled with tandem mass spectrometry (HPLC-MS/MS) according to the protocol described in (Beste *et al.*, 2012) with the following modifications: Chromatography was performed on a Shimadzu HPLC-system (Shimadzu, Duisburg, Germany), consisting of two HPLC-Pumps (LC-30AD), a temperature-controlled autosampler (SIL-30AC), a degasser (DGU-20A4) and a column oven (CTO-20AC). Detection and quantification of cyclic nucleotides was carried out on a 5500QTRAP® (Sciex, Framingham, Massachusetts).

SDS PAGE and Western blotting

Bacterial cells (50 µg of protein), cell homogenates (25 µg of protein) or purified CyaC-S (3.4 µg protein) were used for SDS-PAGE (10%) (Lämmli, 1970). The relative contents of the M_r 68 kD protein band was estimated by scanning of

SDS-PAGES and quantitative evaluation of protein bands by image analysis software ImageJ (https://imagej.nih.gov/ij/). For Western blotting, proteins were blotted onto nitrocellulose membrane. Flag-tag antibody as the primary antibody (M2 monoclonal, Sigma-Aldrich; dilution 1:10000 dilution) and fluorophore-conjugated rabbit anti-mouse IgG (Qiagen, dilution 1:10000) were used or Strep-tag antibody (HRP conjugate, IBA Lifesciences, dilution 1:10000).

Sequence logos

SQOR domain sequences were collected from the Uniprot reference proteomes database (2018_09; Apweiler *et al.*, 2012). SQOR proteins were identified using five iterations of jackhmmer searches (Eddy, 2011) with the transmembrane domain of *S. meliloti* CyaC (Uniprot Q92MZ6, residues 11-251) and the chicken SdhD subunit (PDB: 2H88:D) as query. The obtained sequences were clustered to 70% sequence identity using kClust (Hauser *et al.*, 2013), and then interactively grouped in CLANS (Frickey and Lupas, 2004). The sequences of AC 6TM domains and 5TM domains of Sdh and Frd proteins were extracted and converted into sequence logos using WebLogo3 (Crooks *et al.*, 2004).

Homology model of CyaC

The homology model of the $CyaC_{Sm}$ (UniProt Identifier: Q92MZ6) membrane anchor is based on the structure of FrdC from *Wolinella succinogenes* (2BS2, 82.2% coverage and 14.2% identity), TM6 was modeled as an α-helix with the boundaries predicted by TOPCONS (Tsirigos *et al.*, 2015). The sequences of the membrane anchor (aa 1 to 244 of CyaC), the [2Fe2S]-binding FD domain (a 245 to 363) and the catalytic CD domain (aa 364 to 557) were individually submitted to I-TASSER (Zhang, 2008) and joined in Chimera (Pettersen *et al.*, 2004). The FD and CD domain are structurally modeled as coils. The [2Fe2S]-cluster binding domain was modeled with ferredoxin of *E. coli* (1I7H, 85.7% coverage and 26.5% identity), the catalytic domain with the cyclase domain of CyaB of *P. aeruginosa* (3R5G, 95.9% coverage and 23.7% identity) as the main templates.

Acknowledgements

We gratefully acknowledge support by a grant of Deutsche Forschungsgemeinschaft (UN 49/20-1), SFB 766, TP B8 and institutional funds from the Max Planck Society. We are grateful to A. Becker (Marburg) for the supply of plasmid pWBT-*cyaC*-$Flag_3$, and M. Distler and S. Tenzer (Mainz) for performing the proteome analysis of the CyaC preparation.

Author contributions

JW, JG carried out experiments and analyzed data; JB was responsible for bioinformatics; CS modeled structure; TF measured EPR; GU and JES developed concept, analyzed data and wrote the ms.

References

Apweiler, R.J.M.M., O'onovan, C., Magrane, M., Alam-Faruque, Y., Antunes, R., Barrera Casanova, E., *et al.* (2012) Reorganizing the protein space at the Universal Protein Resource (UniProt). *Nucleic Acids Research*, **40**, D71–75.

Baker, D.A. and Kelly, J.M. (2004) Structure, function and evolution of microbial adenylyl and guanylyl cyclases. *Molecular Microbiology*, **52**, 1229–1242.

Barr, I. and Guo, F. (2015) Pyridine hemochromagen assay for determining the concentration of heme in purified protein solutions. *Bio-protocol*, **5**, e1594.

Bassler, J., Schultz, J.E. and Lupas, A.N. (2018) Adenylate cyclases: receivers, transducers, and generators of signals. *Cellular Signalling*, **46**, 135–144.

Beltz, S., Bassler, J. and Schultz, J.E. (2016) Regulation by the quorum sensor from Vibrio indicates a receptor function for the membrane anchors of adenylate cyclases. *eLife*, **5**, e13098. doi: 10.7554/eLife.13098

Berry, E.A. and Trumpower, B.L. (1987) Simultaneous determination of hemes a, b, and c from pyridine hemochrome spectra. *Analytical Biochemistry*, **161**, 1–15.

Bertani, G. (1951) Studies on lysogenesis. I. The mode of phage liberation by lysogenic *Escherichia coli*. *Journal of Bacteriology*, **62**, 293–300.

Beste, K.Y., Burhenne, H., Kaever, V., Stasch, J.P. and Seifert, R. (2012) Nucleotidyl cyclase activity of soluble guanylyl cyclase alpha1beta1. *Biochemistry*, **51**, 194–204.

Capela, D., Barloy-Hubler, F., Gouzy, J., Bothe, G., Ampe, F., Batut, J., *et al.* (2001) Analysis of the chromosome sequence of the legume symbiont *Sinorhizobium meliloti* strain 1021. *Proceedings of the National Academy of Sciences*, **98**, 9877–9882

Cecchini, G., Schröder, I., Gunsalus, R.P. and Maklashina, E. (2002) Succinate dehydrogenase and fumarate reductase from *Escherichia coli*. *Biochimica et Biophysica Acta*, **1553**, 140–157.

Cecchini, G., Thompson, C.R., Ackrell, B.A., Westenberg, D.J., Dean, N. and Gunsalus, R.P. (1986) Oxidation of reduced menaquinone by the fumarate reductase complex in *Escherichia coli* requires the hydrophobic FrdD peptide. *Proceedings of the National Academy of Sciences*, **83**, 8898–8902.

Chen-Goodspeed, M., Lukan, A.N. and Dessauer, C.W. (2005) Modeling of Galpha(s) and Galpha(i) regulation of human type V and VI adenylyl cyclase. *The Journal of Biological Chemistry*, **280**, 1808–1816.

Collins, M.D. and Jones, D. (1981) Distribution of isoprenoid quinone structural types in bacteria and their taxonomic implication. *Microbiological Reviews*, **45**, 316–354.

Crooks, G.E., Hon, G., Chandonia, J.M. and Brenner, S.E. (2004) WebLogo: a sequence logo generator. *Genome Research*, **14**, 1188–1190.

Daniel, R.M. (1979) The occurrence and role of ubiquinone in electron transport to oxygen and nitrate in aerobically, anaerobically and symbiotically grown rhizobium japonicum. *Journal of General Microbiology*, **110**, 333–337.

Distler, U., Kuharev, J., Navarro, P., Levin, Y., Schild, H. and Tenzer, S. (2014) Drift time-specific collision energies

enable deep-coverage data-independent acquisition proteomics. *Nature methods*, **11**, 167–170.
Distler, U., Kuharev, J., Navarro, P. and Tenzer, S. (2016) Label-free quantification in ion mobility-enhanced data-independent acquisition proteomics. *Nature Protocols*, **11**, 795–812.
Dower, W.J., Miller, J.F. and Ragsdale, C.W. (1988) High efficiency transformation of *E. coli* by high voltage electroporation. *Nucleic Acids Research*, **16**, 6127–6145.
Eddy, S.R. (2011) Accelerated profile HMM searches. *PLoS Computational Biology*, **7**, e1002195.
Frickey, T. and Lupas, A. (2004) CLANS: a Java application for visualizing protein families based on pairwise similarity. *Bioinformatics (Oxford, England)*, **20**, 3702–3704.
Friden, H. and Hederstedt, L. (1990) Role of his residues in *Bacillus subtilis* cytochrome b558 for haem binding and assembly of succinate: quinone oxidoreductase (complex II). *Molecular Microbiology*, **4**, 1045–1056.
Froger, A. and Hall, J.E. (2007) Transformation of plasmid DNA into *E. coli* using the heat shock method. *Journal of Visualized Experiments: JoVE*, 253.
Gancedo, J.M., Mazón, M.J. and Eraso, P. (1985) Biological roles of cAMP: similarities and differences between organisms. *Trends in Biochemical Sciences*, **10**, 210–212.
Garnerone, A.M., Sorroche, F., Zou, L., Mathieu-Demaziere, C., Tian, C.F., Masson-Boivin, C. and Batut, J. (2018) NsrA, a predicted beta-barrel outer membrane protein involved in plant signal perception and the control of secondary infection in *Sinorhizobium meliloti*. *Journal of Bacteriology*, **200**(11), e00019-18.
Graf, S., Broll, C., Wissig, J., Strecker, A., Parowatkin, M. and Unden, G. (2016) CitA (citrate) and DcuS (C4-dicarboxylate) sensor kinases in thermophilic *Geobacillus kaustophilus* and *Geobacillus thermodenitrificans*. *Microbiology (Reading, England)*, **162**, 127–137.
Gross, R., Simon, J., Lancaster, C.R. and Kroger, A. (1998) Identification of histidine residues in *Wolinella succinogenes* hydrogenase that are essential for menaquinone reduction by H2. *Molecular Microbiology*, **30**, 639–646.
Hägerhäll, C. and Hederstedt, L. (1996) A structural model for the membrane-integral domain of succinate: quinone oxidoreductases. *FEBS Letters*, **389**, 25–31.
Hauser, M., Mayer, C.E. and Soding, J. (2013) kClust: fast and sensitive clustering of large protein sequence databases. *BMC Bioinformatics*, **14**, 248.
Hederstedt, L. (2002) Succinate:quinone oxidoreductase in the bacteria *Paracoccus denitrificans* and *Bacillus subtilis*. *Biochimica et Biophysica Acta*, **1553**, 74–83.
Imlay, J.A. (2015) Transcription factors that defend bacteria against reactive oxygen species. *Annual Review of Microbiology*, **69**, 93–108.
Iwasaki, T., Kappl, R., Bracic, G., Shimizu, N., Ohmori, D. and Kumasaka, T. (2011) ISC-like [2Fe-2S] ferredoxin (FdxB) dimer from Pseudomonas putida JCM 20004: structural and electron-nuclear double resonance characterization. *Journal of Biological Inorganic Chemistry: JBIC: A Publication of the Society of Biological Inorganic Chemistry*, **16**, 923–935.
Kanchan, K., Linder, J., Winkler, K., Hantke, K., Schultz, A. and Schultz, J.E. (2010) Transmembrane signaling in chimeras of the *Escherichia coli* aspartate and serine chemotaxis receptors and bacterial class III adenylyl cyclases. *The Journal of Biological Chemistry*, **285**, 2090–2099.
Karimova, G., Pidoux, J., Ullmann, A. and Ladant, D. (1998) A bacterial two-hybrid system based on a reconstituted signal transduction pathway. *Proceedings of the National Academy of Sciences*, **95**, 5752–5756.
Khan, S.R., Gaines, J., Roop, R.M. 2nd and Farrand, S.K. (2008) Broad-host-range expression vectors with tightly regulated promoters and their use to examine the influence of TraR and TraM expression on Ti plasmid quorum sensing. *Applied and Environmental Microbiology*, **74**, 5053–5062.
Kobayashi, K. (2017) Sensing mechanisms in the redox-regulated, [2Fe-2S] cluster-containing, bacterial transcriptional factor SoxR. *Accounts of Chemical Research*, **50**, 1672–1678.
Krol, E., Klaner, C., Gnau, P., Kaever, V., Essen, L.O. and Becker, A. (2016) Cyclic mononucleotide- and Clr-dependent gene regulation in *Sinorhizobium meliloti*. *Microbiology (Reading, England)*, **162**, 1840–1856.
Lämmli, U.K. (1970) Cleavage of structural proteins during the assembly of the head of bacteriophage T4. *Nature*, **227**, 680–685.
Lancaster, C.R. (2002) Succinate:quinone oxidoreductases: an overview. *Biochimica et Biophysica Acta*, **1553**, 1–6.
Lancaster, C.R., Gorss, R., Haas, A., Ritter, M., Mäntele, W., Simon, J. and Kröger, A. (2000) Essential role of GluC66 for menaquinol oxidation indicates transmembrane electrochemical potential generation by *Wolinella succinogenes* fumarate reductase. *Proceedings of the National Academy of Sciences of the United States of America*, **97**, 13051–13056.
Lancaster, C.R., Kröger, A., Auer, M. and Michel, H. (1999) Structure of fumarate reductase from *Wolinella succinogenes* at 2.2 A resolution. *Nature*, **402**, 377–385.
Lehnen, D., Blumer, C., Polen, T., Wackwitz, B., Wendisch, V.F. and Unden, G. (2002) LrhA as a new transcriptional key regulator of flagella, motility and chemotaxis genes in *Escherichia coli*. *Molecular Microbiology*, **45**, 521–532.
Linder, J.U. and Schultz, J.E. (2003) The class III adenylyl cyclases: multi-purpose signalling modules. *Cellular Signalling*, **15**, 1081–1089.
Linder, J.U. and Schultz, J.E. (2008) Versatility of signal transduction encoded in dimeric adenylyl cyclases. *Current Opinion in Structural Biology*, **18**, 667–672.
Lowry, O.H., Rosebrough, N.J., Farr, A.L. and Randall, R.J. (1951) Protein measurement with the Folin phenol reagent. *The Journal of Biological Chemistry*, **193**, 265–275.
Lukas, H., Reimann, J., Kim, O.B., Grimpo, J. and Unden, G. (2010) Regulation of aerobic and anaerobic D-malate metabolism of *Escherichia coli* by the LysR-type regulator DmlR (YeaT). *Journal of Bacteriology*, **192**, 2503–2511.
Madej, M.G., Nasiri, H.R., Hilgendorff, N.S., Schwalbe, H. and Lancaster, C.R.D. (2006a) Evidence for transmembrane proton transfer in a dihaem-containing membrane protein complex. *The EMBO Journal*, **25**, 4963–4970.
Madej, M.G., Nasiri, H.R., Hilgendorff, N.S., Schwalbe, H., Unden, G. and Lancaster, C.R. (2006b) Experimental evidence for proton motive force-dependent catalysis by the diheme-containing succinate:menaquinone

oxidoreductase from the Gram-positive bacterium Bacillus licheniformis. *Biochemistry*, **45**, 15049–15055.
Malpica, R., Franco, B., Rodriguez, C., Kwon, O. and Georgellis, D. (2004) Identification of a quinone-sensitive redox switch in the ArcB sensor kinase. *Proceedings of the National Academy of Sciences*, **101**, 13318–13323.
Malpica, R., Sandoval, G.R., Rodriguez, C., Franco, B. and Georgellis, D. (2006) Signaling by the arc two-component system provides a link between the redox state of the quinone pool and gene expression. *Antioxidants & Redox Signaling*, **8**, 781–795.
Matsson, M., Tolstoy, D., Aasa, R. and Hederstedt, L. (2000) The distal heme center in *Bacillus subtilis* succinate:quinone reductase is crucial for electron transfer to menaquinone. *Biochemistry*, **39**, 8617–8624.
Miller, J.H. (1992) *A Short Course in Bacterial Genetics: A Laboratory Manual and Handbook for* Escherichia coli *and Related Bacteria*. New York: Cold Spring Harbor Laboratory Press.
Miroux, B. and Walker, J.E. (1996) Over-production of proteins in *Escherichia coli*: mutant hosts that allow synthesis of some membrane proteins and globular proteins at high levels. *Journal of Molecular Biology*, **260**, 289–298.
Ohnishi, T., Moser, C.C., Page, C.C., Dutton, P.L. and Yano, T. (2000) Simple redox-linked proton-transfer design: new insights from structures of quinol-fumarate reductase. *Structure*, **8**(2), R23–R32.
Pakarian, P. and Pawelek, P.D. (2016) Subunit orientation in the *Escherichia coli* enterobactin biosynthetic EntA-EntE complex revealed by a two-hybrid approach. *Biochimie*, **127**, 1–9.
Pettersen, E.F., Goddard, T.D., Huang, C.C., Couch, G.S., Greenblatt, D.M., Meng, E.C. *et al.* (2004) UCSF Chimera–a visualization system for exploratory research and analysis. *Journal of computational chemistry*, **25**, 1605–1612.
Pomory, C.M. (2008) Color development time of the Lowry protein assay. *Analytical Biochemistry*, **378**, 216–217.
Ruprecht, J., Yankovskaya, V., Maklashina, E., Iwata, S. and Cecchini, G. (2009) Structure of *Escherichia coli* succinate:quinone oxidoreductase with an occupied and empty quinone-binding site. *The Journal of Biological Chemistry*, **284**, 29836–29846.
Salomon, Y., Londos, C. and Rodbell, M. (1974) A highly sensitive adenylate cyclase assay. *Analytical Biochemistry*, **58**, 541–548.
Sambrook, J. and Russell, D.W. (2001) *Molecular Cloning: A Laboratory Manual*. Cold Spring Harbor, NY: Cold Spring Harbor Laboratory.
Schirawski, J. and Unden, G. (1998) Menaquinone-dependent succinate dehydrogenase of bacteria catalyzes reversed electron transport driven by the proton potential. *European Journal of Biochemistry*, **257**, 210–215.
Schnorf, U. (1966) Thesis, No 3871. Zürich: Eidgenössische Technische Hochschule.
Schultz, J.E. and Natarajan, J. (2013) Regulated unfolding: a basic principle of intraprotein signaling in modular proteins. *Trends in Biochemical Sciences*, **38**, 538–545.
Tsirigos, K.D., Peters, C., Shu, N., Kall, L. and Elofsson, A. (2015) The TOPCONS web server for consensus prediction of membrane protein topology and signal peptides. *Nucleic Acids Research*, **43**, W401–W407.
Uhlmann, M. and Friedrich, T. (2005) EPR signals assigned to Fe/S cluster N1c of the *Escherichia coli* NADH:ubiquinone oxidoreductase (complex I) derive from cluster N1a. *Biochemistry*, **44**, 1653–1658.
Unden, G., Hackenberg, H. and Kröger, A. (1980) Isolation and functional aspects of the fumarate reductase involved in the phosphorylative electron transport of Vibrio succinogenes. *Biochimica et Biophysica Acta*, **591**, 275–288.
Unden, G. and Kröger, A. (1981) The function of the subunits of the fumarate reductase complex of Vibrio succinogenes. *European Journal of Biochemistry*, **120**, 577–584.
Unden, G. and Kröger, A. (1986) Reconstitution of a functional electron-transfer chain from purified formate dehydrogenase and fumarate reductase complexes. In: Fleischer, S. and Fleischer, B. (Eds.) *Methods in Enzymology*. Amsterdam: Elsevier B.V., pp. 387–399.
Westenberg, D.J., Gunsalus, R.P., Ackrell, B.A., Sices, H. and Cecchini, G. (1993) *Escherichia coli* fumarate reductase frdC and frdD mutants. Identification of amino acid residues involved in catalytic activity with quinones. *The Journal of Biological Chemistry*, **268**, 815–822.
Zhang, Y. (2008) I-TASSER server for protein 3D structure prediction. *BMC Bioinformatics*, **9**, 40.
Ziegler, M., Bassler, J., Beltz, S., Schultz, A., Lupas, A.N. and Schultz, J.E. (2017) Characterization of a novel signal transducer element intrinsic to class IIIa/b adenylate cyclases and guanylate cyclases. *The FEBS Journal*, **284**, 1204–1217.

Supporting Information

Additional supporting information may be found online in the Supporting Information section at the end of the article

Supplementary information

CyaC, a redox-regulated adenylate cyclase of *Sinorhizobium meliloti* with a diheme-B membrane anchor domain

Juliane Wissig[1], Julia Grischin[2], Jens Bassler[2], Christopher Schubert[1], Thorsten Friedrich[3], Heike Bähre[4], Joachim E. Schultz[5] and Gottfried Unden[1]

[1]Microbiology and Wine Research, Institute for Molecular Physiology, Johannes Gutenberg-University of Mainz, Mainz, Germany

[2]Max-Planck-Institut für Entwicklungsbiologie, Abt. Proteinevolution, Max-Planck-Ring 5, 72076 Tübingen, Germany

[3]Institute of Biochemistry, University of Freiburg, 79104 Freiburg, Germany

[4]Medizinische Hochschule Hannover

[5]Pharmazeutisches Institut der Universität Tübingen, Auf der Morgenstelle 8, 72076 Tübingen, Germany

Address for correspondence:

Dr. Gottfried Unden
Institute for Molecular Physiology, Johannes Gutenberg-Universität Mainz,
Becherweg 15, 55099 Mainz, Germany
Phone +49-6131-3923550; Fax +49-6131-3926695
Email: unden@uni-mainz.de

Dr. Joachim E Schultz
Pharmazeutisches Institut der Universität Tübingen,
Auf der Morgenstelle 8, 72076 Tübingen, Germany

Phone: +49 7071-2972475, Email: Joachim.schultz@uni-tuebingen.de

Table S1. **Heme-B contents of purified CyaC-S and His variants of CyaC-S.** The heme-B contents were calculated from the oxidized-reduced UV-Vis spectra shown in Fig. 4 as described for Fig. 2.

CyaC-S	**Heme B [mol/mol CyaC-S]**
CyaC-S	1.19 (+/- 0.023)
(CyaC(H27A)-S	0.04 (+/- 0,005)
CyaC(H68A)-S	0.17 (+/- 0.08)
CyaC(H105A)-S	0.26 (+/- 0.02)
CyaC(H149A)-S	0.11 (+/- 0.016)

1

2 **Table S2. Primers used for plasmid construction and site-directed mutagenesis of *cyaC*.**

His_TM1_Ala_f	GCGTTTTCGTGCTCTTGGCCTTCTCGAATCACGCGC	pMW 2609 and pMW2591 (PCR Mutagenesis of His27 in TM1 against Alanin)
His_TM1_Ala_r	GCGCGTGATTCGAGAAGGCCAAGAGCACGAAAACGC	pMW 2609 and pMW2591 (PCR Mutagenesis of His27 in TM1 against Alanin)
His_TM1B_Ala_f	GCACTTCTCGAATGCCGCGCTCGGGCTCG	pMW2610 and pMW2592 (PCR Mutagenesis of His31 in TM1 against Alanin)
His_TM1B_Ala_r	CGAGCCCGAGCGCGGCATTCGAGAAGTGC	pMW2610 and pMW2592 (PCR Mutagenesis of His31 in TM1 against Alanin)
His_TM2_Ala_f	CGCTGCTGCTGGCTTTCCTGATGGC	pMW2611 and pMW2593 (PCR Mutagenesis of His68 in TM2 against Alanin)
His_TM2_Ala_r	GCCATCAGGAAAGCCAGCAGCAGCG	pMW2611 and pMW2593 (PCR Mutagenesis of His68 in TM2 against Alanin)
His_TM3_Ala_f	CTTTCTGCTTGTGCCTGCCGTGGTCGCCGCCCG	pMW2612 and pMW2594 (PCR Mutagenesis of His105 in TM3 against Alanin)
His_TM3_Ala_r	CGGGCGGCGACCACGGCAGGCACAAGCAGAAAG	pMW2612 and pMW2594 (PCR Mutagenesis of His105 in TM3 against Alanin)
His_TM4_Ala_f	GTCGTCTGGGGTGCCGCCTGTCTTGG	pMW2613 and pMW2595 (PCR Mutagenesis of His149 in TM4 against Alanin)
His_TM4_Ala_r	CCAAGACAGGCGGCACCCCAGACGAC	pMW2613 and pMW2595 (PCR Mutagenesis of His149 in TM4 against Alanin)
Link_Nhe1_cyaC_f	GCGGCGGCGGCTAGCATGACGATCCTATCCGCCAGCA CGCGCAAGAAG	Fragment NheI-CyaC-Flag_HindIII, amplified from pCyaC, (construction of pCyaC-S)
CyaC_Flag_Stop_HindIII _Link_r	CGCCGCCGCAAGCTTTCACTTGTCATCGTCATCCTTGTA ATCGATATCGTGATCC	Fragment NheI-CyaC-Flag_HindIII, amplified from pCyaC, (construction of pCyaC-S)
InsStrep_f	TGGAGCCACCCGCAGTTCGAAAAATGAAAGCTTGCGG CCGCACTCGAGCAC	Insertion of Strep-tag (construction of pCyaC-S)
InsStrep_r	TTTTTCGAACTGCGGGTGGCTCCACTTGTCATCGTCATC CTTGTAATCGATATCGTGATCC	Insertion of Strep-tag (construction of pCyaC-S)

3

4

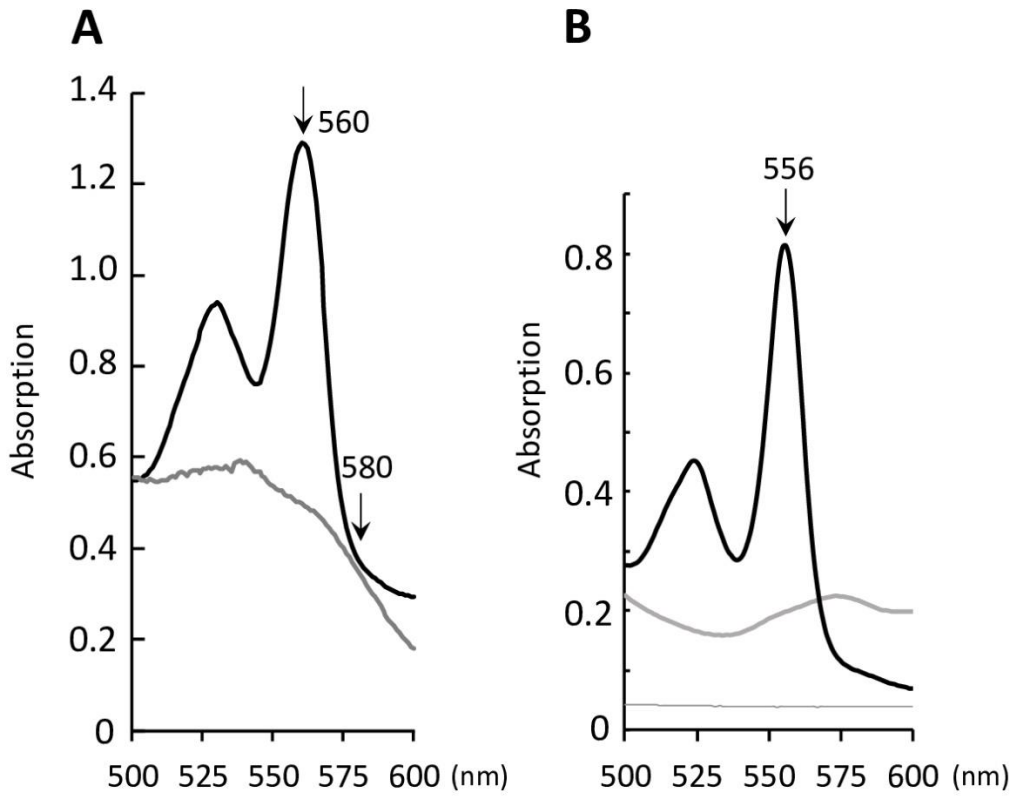

Fig. S1. UV-vis spectra of isolated CyaC heme B (A) and CyaC pyridine hemochrome (B). (A) CyaC heme-B spectrum with maxima for the β and α bands at 530 and 560 nm. The sample contained 2.7 mg/ml of CyaC-S in elution buffer, after reduction with dithionite (*black*) and oxidation with ferricyanide (red). The heme-B content of the preparation was 1.08 µmol x g protein, or 1.21 mol x mol^{-1} of CyaC-S. (B) Pyridine hemochrome spectrum in the α- and β-band region with protoheme IX maxima at 524 and 556 nm after reduction with dithionite (*black*) and oxidation with ferricyanide (red). From the pyridine hemochrome ($\Delta\varepsilon_{556nm}$ (reduced minus oxidized state; (Berry & Trumpower, 1987)) and the heme spectrum (reduced – oxidized) the molecular extinction coefficient of CyaC heme-B was calculated ($\Delta\varepsilon_{560\text{-}580nm}$ (red- ox)) = 21.5 mM^{-1} cm^{-1}.

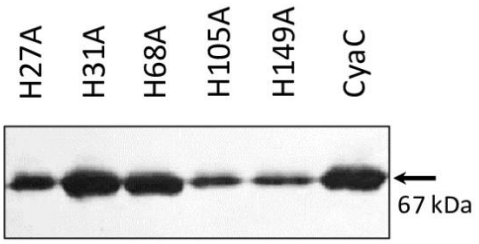

Figure S2. Localisation of CyaC-S wild-type and His-variants in *E. coli* C43 membranes. C43D3pCyaC-S and His-variants were grown aerobically in LB-medium at 30°C as for protein isolation. After induction with 1 mM IPTG (OD_{578nm} 0.9) the bacteria were incubated for 5 h at 30 °C, and then for 16 hours at 4 °C without shaking. After harvest, membranes were isolated and the membrane proteins were separated by SDS-PAGE, transferred to nitrocellulose membrane and analyzed in Western blotting. CyaC-S and the variants were detected by Flag-antibody (dilution 1:10000). Variations in the yield of CyaC protein for the different variants is in part reflected by differing yields during membrane preparation. The arrow gives the position of CyaC-S (M_r 68.000).

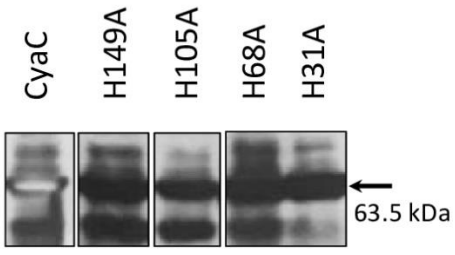

Figure S3. Expression of CyaC-F wildtype and His-variants in *E. coli* BTH101. *E. coli* BTH101(pCyaC-F) encoding CyaC-Fand His variants (50 µg cell protein) were applied to SDS-PAGE. After electrophoresis proteins were transferred to nitrocellulose membrane and detected with Flag-antibody (dilution 1:10000). The arrow shows the position of CyaC-F (M_r 63,500).

6. Seth et al

6.1 Eigenanteil

Cellular Signalling, April 2020, Volume 68
doi:10.1016/j.cellsig.2020.109538

Gsα stimulation of mammalian adenylate cyclases regulated by their hexahelical membrane anchors

Anubha Seth[a,b], Manuel Finkbeiner[b], Julia Grischin[b], Joachim E. Schultz[a,*]

[a] Pharmazeutisches Institut der Universität Tübingen, Auf der Morgenstelle 8, 72076, Tübingen, Germany.
[b] Max-Planck-Institut für Entwicklungsbiologie, Abt. Proteinevolution, Max-Planck-Ring 5, 72076, Tübingen, Germany.

Für diese Publikation hat M. Finkbeiner die humanen Adenylatcyclase-Gene in Sf9-Zellen transformiert, eine Kultur angelegt, die Zellen geerntet und anschließend die Membranpräparationen hergestellt, wobei ich die Herstellung der Membranpräparation der Isoform 5 übernommen habe. A. Seth hat die Klonierung, Transformation, Expression und Herstellung der Membranpräparationen des chimären Enzyms CqsS-hAC2 durchgeführt. Anschließend hat sie alle Aktivitätstests mit CqsS-hAC2 nach Zugabe von $G_s\alpha$, CAI-1, FBS und FSK geplant, durchgeführt, ausgewertet und grafisch dargestellt. Ebenso hat sie alle Versuche mit Proben aus der Gehirnrinde von Ratten nach Zugabe von „hitzeinaktiviertem“ HS, sowie die Wirkung von CAI-1 und FSK auf die basale und aktivierte hAC2 geplant, durchgeführt, ausgewertet und grafisch dargestellt.
Die Versuche mit den durch $G_s\alpha$ aktivierten hACn 2,3,5 und 9 unter Einfluss von hitzeinaktiviertem HS wurden von mir geplant, durchgeführt, ausgewertet und grafisch dargestellt (Fig. 4, Supplementary Figure 3). M. Finkbeiner hat die

Hemmung durch hitzeinaktiviertes HS auf die Basalaktivität der hACn 2,3,5 und 9 und den Einfluss von FBS und HSA auf hAC2 in Anwesenheit von $G_s\alpha$ geplant, durchgeführt, ausgewertet und grafisch dargestellt. Die $G_s\alpha$-Dosis-Wirkungskurve mit der hAC2 in Anwesenheit von je 5% bzw. 10% ebenso wie der Einfluss von hitzeinaktiviertem HS auf die Standardkurve wurden in Zusammenarbeit zwischen M. Finkbeiner und mir geplant, durchgeführt, ausgewertet und grafisch dargestellt (Supplementary Figure 5 links), während A. Seth die gleichen Arbeiten für die Standardkurve nach Zugabe von FSK übernommen hat.

Prof. Dr. J. E. Schultz hat die Arbeit beaufsichtigt, war an der Planung und Interpretation der Ergebnisse beteiligt und hat die Endversion des Manuskripts verfasst sowie der Graphen erstellt.

6.2 Publikation

Cellular Signalling 68 (2020) 109538

Contents lists available at ScienceDirect

Cellular Signalling

journal homepage: www.elsevier.com/locate/cellsig

Gsα stimulation of mammalian adenylate cyclases regulated by their hexahelical membrane anchors

Anubha Seth[a,b], Manuel Finkbeiner[b], Julia Grischin[b], Joachim E. Schultz[a,*]

[a] Pharmazeutisches Institut der Universität Tübingen, Tübingen, Germany
[b] Max-Planck-Institut für Entwicklungsbiologie, Tübingen, Germany

ARTICLE INFO

Keywords:
Adenylate cyclases
Cyclic AMP
Membrane anchor
Quorum-sensor
Receptor

ABSTRACT

Mammalian adenylate cyclases (ACs) are pseudoheterodimers with dissimilar hexahelical membrane-anchors, isoform-specifically conserved for more than half a billion years. We exchanged both membrane anchors of the AC isoform 2 by the quorum-sensing receptor from *Vibrio harveyi*, CqsS, which has a ligand, *Cholera*-Autoinducer-1 (CAI-1). In the chimera, AC activity was stimulated by Gsα, CAI-1 had no effect. Surprisingly, CAI-1 inhibited Gsα stimulation. We report that Gsα stimulation of human AC isoforms 2, 3, 5, and 9 expressed in Sf9 cells is inhibited by serum as is AC activity in membranes isolated from rat brain cortex. AC2 activation by forskolin or forskolin/Gsα was similarly inhibited. Obviously, serum contains as yet unidentified factors affecting AC activity. The data establish a linkage in ACs, in which the membrane anchors, as receptors, transduce extracellular signals to the cytosolic catalytic dimer. A mechanistic three state model of AC regulation is presented compatible with all known regulatory inputs into mammalian ACs. The data allow designating the membrane anchors of mammalian ACs as orphan receptors, and establish a new level of AC regulation.

1. Introduction

The first amino acid sequence of a mammalian adenylate cyclase identified two similar catalytic domains (C1 and C2) and two dissimilar hexahelical membrane anchors (TM1 and TM2) which were proposed to possess a channel or transporter-like function, properties, which were never confirmed [1]. Subsequently, nine genes for mAC isoforms were identified, indicating substantial subfunctionalization during evolution (mAC isoforms 1–9; [2,3]). Membrane-delimited ACs (mACs) are the cellular effector proteins for many hormones that signal via G-protein-coupled receptors and their regulation has received broad attention [2,3]. The catalytic center of mACs is formed at the C1/C2 dimer interface. Most biochemical studies have used the startling observation that the separately expressed C1/C2 catalytic domains are regulated by Gsα, i.e. the membrane anchors appear dispensable for catalysis and regulation [4]. Why then 2 × 6 transmembrane spans, when 1 or 2 would have been sufficient for membrane-anchoring? The evolutionary conservation of the membrane domains for more than half a billion years justifies searching for a physiological function beyond membrane-anchoring [5–7].

Recently, we replaced the 6TM domain of the mycobacterial Rv1625c AC, a monomeric progenitor of mACs, by the hexahelical quorum-sensing receptor CqsS from *Vibrio*, generating a CqsS-AC Rv1625c chimera (here and in the following, CqsS is used to denote the ligand-binding membrane domain of CqsS, not the full receptor protein [6,7]). The ligand for CqsS, *Cholera*-Auto-Inducer-1 [CAI-1; (*S*)-3-hydroxy-tridecan-4-one], stimulated AC activity in the chimera [6]. Subsequently, we characterized a family of conserved cyclase-transducing-elements (CTEs) which are indispensable for signal transduction [7]. They are isoform-specifically conserved in mACs, supporting the notion that the AC membrane domains may be ligand receptors [5–7]. Here, we asked whether AC regulation by CqsS is maintained in a chimera, in which the TM1 and TM2 domains in human AC2 (hAC2) are replaced by CqsS, generating a CqsS-hAC2 chimera. We report that stimulation by Gsα is preserved whereas the ligand CAI-1 does not, by itself, affect basal AC activity. Surprisingly, CAI-1 inhibits Gsα stimulation in CqsS-hAC2. We further show that the Gsα stimulation of the hAC2 holoenzyme is similarly inhibited by as yet unidentified factors present in human serum. Serum also inhibited Gsα activation of hAC isoforms 3, 5, and 9, and AC activity in rat brain cortical membranes indicating that the AC membrane domains are orphan ligand receptors.

Abbreviations: AC, adenylate cyclase; hAC, human adenylate cyclase; mAC, membrane-delimited adenylate cyclase; TM, hexahelical membrane domain; CTE, cyclase-transducing-element; CAI-1, *Cholera*-Autoinducer-1; CqsS, quorum-sensing receptor CqsS from *Vibrio*

* Corresponding author at: Pharmazeutisches Institut der Universität Tübingen, Auf der Morgenstelle 8, 72076 Tübingen, Germany.
E-mail address: joachim.schultz@uni-tuebingen.de (J.E. Schultz).

https://doi.org/10.1016/j.cellsig.2020.109538
Received 9 January 2020; Received in revised form 9 January 2020; Accepted 9 January 2020
Available online 10 January 2020

2. Materials and methods

2.1. Reagents and materials

CqsS of *V. harveyi* (acc. # AAT86007) and hAC2 and hAC9 (acc. # Q08462 and NM_001116.3) sequences were used. Position Phe166 in CqsS was mutated to Leu (F166 L) [6]. Radiochemicals were from Hartmann Analytic and Perkin Elmer. Enzymes were from either New England Biolabs or Roche Molecular. Other chemicals were from Sigma, Merck and Roth. CAI-1 was synthesized in-house [8]. The constitutively active GsαQ227L point mutant was from Dr. C. Kleuss, Berlin [9]. It was expressed and purified as described earlier [9–11]. Human serum (catalog # 4522 from human male AB plasma), heat-inactivated human serum (i.e. inactivated complement; catalog # H3667 from human male AB plasma), and serum albumin (catalog # A3782) were from Sigma-Aldrich, fetal bovine serum was from Gibco, Life Technologies, Darmstadt, Germany (catalog #: 10270; lot number: 42Q8269K).

2.2. Plasmid construct

CqsS-hAC2 was generated using standard methods. 5'-BamHI or *Eco*RI and 3´-*Hin*dIII sites restriction sides were used and inserted into $pQE80_L$ (Δ *Xho*I; Δ *Nco*I). Gly-Ser and Arg-Ser were introduced for internal restriction sites. An N-terminal MRGS-hexa-His-tag was used to for Western blotting. The construct boundaries were: $MRGSHis_6$-GS–CqsS $(F166L)_{1–181}$-$hAC2_{221–603}$-RS-CqsS $(F166L)_{1–181}$-$hAC2_{836–1091}$. Genes for hACs 2, 3, 5, and 9 were obtained from GenScript. For virus production, hACs were inserted into pLIB. The plasmid was amplified in *E. coli* XL1blue and transformed into *E. coli* EMBacY cells generating the bacmid for Sf9 transfection.

2.3. Protein expression

CqsS-hAC2 was expressed in *E. coli* BL21 (DE3) in Luria-Bertani broth at 30 °C with 100 μg/ml ampicillin. 200 ml medium were inoculated with a preculture (to A_{600} of 0.2) and grown at 30 °C with antibiotics. At A_{600} 0.8 expression was induced with 500 μM isopropyl β-D-1-thiogalactopyranoside (22 °C, 4 h). Cells were harvested, washed with buffer and stored at −80 °C. Cell membranes were prepared in lysis buffer (50 mM Tris/HCl, 0.021% thioglycerol, 50 mM NaCl, pH 8) after disintegrating cells in a French press (1100 psi). After removal of cell debris (4300 × g, 30 min, 4 °C) membranes were collected (100,000 × g; 1 h, 4 °C). Membranes were suspended in buffer (40 mM Tris/HCl, 0.016% thioglycerol, 20% glycerol, pH 8). Virus-infected Sf9 cells expressing hACs were grown in Sf900 III medium, harvested after three days and membranes were isolated and stored at −80 °C. Each hAC isoform was expressed once in Sf9 cells and membranes were used in multiple assays (in triplicates). Membrane preparation from rat brain cortex was according to [12].

2.4. Adenylate cyclase assay

Activity of CqsS-hAC2 was assayed for 15 min at 30 °C–37 °C in 100 μl with 40 μg membrane protein, 50 mM Tris/HCl pH 8.3, 5 mM $MnCl_2$, 6 mM creatine phosphate, 230 μg/ml creatine kinase, 750 μM [α-^{32}P]-ATP, and 2 mM [2,8-^{3}H]-cAMP to monitor yield during cAMP purification [13]. Substrate conversion was kept below 10%. CAI-1 was dissolved in DMSO. Incubations with DMSO were carried out as controls. Activity of hACs was determined in a volume of 10 μl using 1 mM ATP, 2 mM $MgCl_2$, 3 mM creatine phosphate, 60 μg/ml creatine kinase, 50 mM MOPS, pH 7.5 using an Assist-Plus pipetting robot (Integra Biosciences, Germany) and a cAMP assay kit from Cisbio (Codolet, France) according to the supplier's instructions (see controls of standard curves in Supplemental fig. 5).

2.5. Western blot analysis

For Western blotting an RGS-His_4-antibody (Qiagen) and a 1:2500 dilution of the fluorophore-conjugated secondary antibody Cy3 (ECL Plex goat-α-mouse IgG-Cy3, GE Healthcare) was used. Proteolysis was not observed.

2.6. Data analysis and statistical analysis

All incubations were in duplicates (CqsS-hAC2) or triplicates (hACs). S.E.M values are given for experiments with CqsS and refer to separately expressed and analyzed proteins. S.D. values apply hACs individually expressed once in Sf9 insect cells. Data analysis was with GraphPad prism 8.1.2.

3. Results

3.1. CqsS serves as a ligand receptor for hAC2

We generated a pseudoheterodimeric chimera of hAC2 in which both 6TMs were isosterically replaced by the 6TM quorum-sensing receptor CqsS from *Vibrio* (CqsS-hAC2). The point of transition between CqsS and hAC2 was at the respective hAC2 CTEs in front of the catalytic domains C1a and C2, thus maintaining all structural features potentially required for signaling (Fig. 1 left; [6,7,14]). Two questions were obvious: a) Is such a chimera expressed in *Escherichia coli* although bacterial expression of mammalian ACs has so far proven impossible, and b) Is regulation by Gsα and the quorum-sensing ligand CAI-1 maintained? The chimera was expressed in *E. coli* and had robust basal activity indicating that native mAC-like features were maintained (Fig. 1). AC activity was stimulated by constitutively active Gsα (Q227L, below termed Gsα [10,11]) demonstrating formation of a productive C1/C2 catalytic dimer. A concentration-response curve showed a 2.3-fold increase in activity with an EC_{50} of around 200 nM Gsα (Fig. 1). By comparison, AC2 expressed in Sf9 cells is stimulated by Gsα about 5 to 12-fold [15,16]. The quantitatively differing responses compared to AC2 may be due to the replacement of the dissimilar TM1 and TM2 domains by two identical CqsS receptors. The quorum-sensor ligand CAI-1, up to 100 μM, failed to affect AC activity. This posed two questions: a) Are the catalytic domains of mACs at all capable of operating as output domains for transmembrane signals? b) Which biochemical differences between bacterial and mammalian ACs exist, which might explain the divergent results obtained with the CqsS-Rv1625c AC chimera [6].

A crucial difference between bacterial and mammalian ACs are the dissociation constants of the catalytic domains. Bacterial catalytic domains usually have a high 'self'-affinity (Kd $\leq 10^{-7}$ M) and are active when conformationally unconstrained [5–7,17]. Similarly, the individual C1 and C2 domains of mACs have a high propensity for self-association, i.e. C1 preferentially associates with C1 and C2 with C2, as documented in the first mAC crystal structure, a C2 homodimer [18]. However, homodimers of C1 or C2 are inactive [19]. The actual affinity between the C1 and C2 catalytic domains in mACs is rather low (Kd ≥ 10^{-5} M [20–22]. AC stimulation by Gsα is tantamount to an increase in the apparent affinity of C1 and C2 for each other by approximately two orders of magnitude [20–23]. Therefore, a provocative interpretation for the lack of a CAI-1 effect would be that CqsS receptor activation causes conformational changes which interfere with Gsα stimulation. This was tested next.

3.2. The CqsS receptor regulates stimulation of hAC2 by Gsα

In presence of 5 or 10 μM CAI-1, Gsα activation of CqsS-hAC2 was significantly attenuated (Fig. 2A). Inhibition was instantaneous. The effect was ligand-specific and reversible as determined by re-assaying membranes which were stimulated, washed and re-isolated (Fig. 2B). In

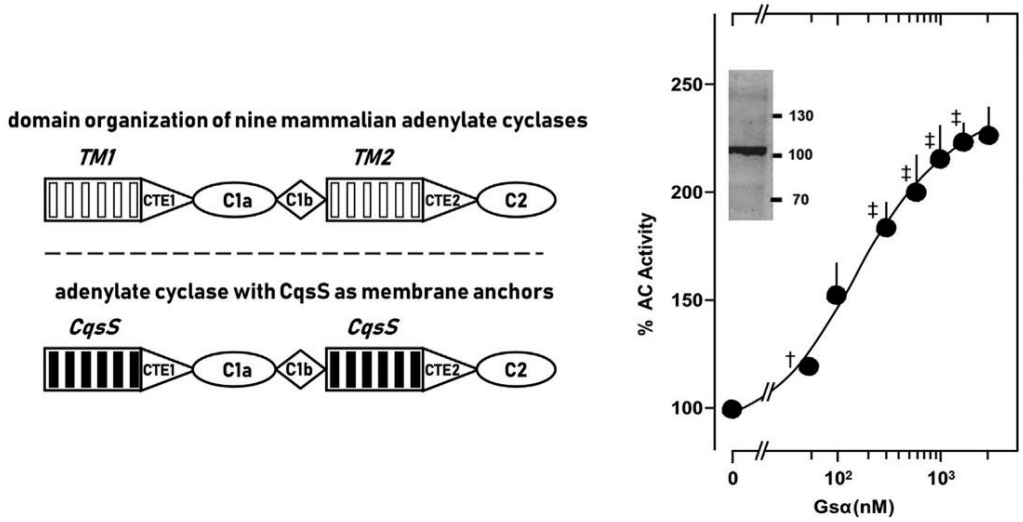

Fig. 1. Stimulation of the chimera CqsS-hAC2 by Gsα. Left: general domain organization of the membrane-delimited adenylate cyclases (top) and scheme of the chimera between CqsS as membrane anchors and hAC2 (bottom). The 6TM regions are idealized, CTE1 and CTE2 denote the cyclase-transducing-elements, indispensable for signal transduction [6,7], C1a and C2 are the respective catalytic domains, C1b connects C1a to TM2 (construct boundaries: MRGSHis$_6$-GS–CqsS (F166 L)$_{1–181}$-hAC2$_{221–603}$-RS-CqsS (F166 L)$_{1–181}$-hAC2$_{836–1091}$). Right: Gsα concentration-response curve. Basal activity (100%) was 27.2 ± 2.6 pmol cAMP·mg^{-1}·min^{1}. Half-maximal stimulation was around 200 nM Gsα. Error bars denote S.E.M. of 2–7 separate experiments (expressions). Significances: ‡: $p < .001$ compared to basal. For clarity, not all significances are marked. Insert: Western blot of the chimera with an anti-His$_6$-antibody indicating absence of proteolysis. MW standards are at right.

presence of 5 or 10 μM CAI-1, the EC_{50} concentrations for Gsα were increased 1.5- and 4-fold, respectively (Fig. 2A). Concomitantly, CAI-1 at 10 μM significantly diminished the maximal Gsα response by 20% (Fig. 2A). The data supported the hypothesis that CqsS receptor activation interfered with activation by Gsα.

Next, a concentration-response curve for CAI-1 in the presence of 1 μM Gsα was carried out. At 35 μM CAI-1, activation of the CqsS-hAC2 chimera by Gsα was almost abrogated (Fig. 3A). The IC_{50} for CAI-1 inhibition was 6.3 μM, i.e. about 15-fold higher than for the stimulatory effect of CAI-1 in the CqsS-Rv1625c AC [6]. This might be due to the fact that we went from a homodimeric CqsS-Rv1625c AC to a linked pseudoheterodimeric CqsS-hAC2 chimera. To exclude that CAI-1 might have obstructed the formation of the catalytic dimer or its interaction with Gsα, the effect of CAI-1 on Gsα stimulation of native hAC2 expressed in Sf9 cells was tested. CAI-1 neither affected basal nor Gsα-stimulated AC activity (Fig. 3B). This unequivocally demonstrated that a) CAI-1 did not interfere in formation of the catalytic dimer in the CqsS-hAC2 chimera, b) CAI-1 did not interact with Gsα and impair its function, and c) CAI-1 did not impair the interactions between the catalytic dimer and Gsα. From these data we can conclude that the effect of CAI-1 in the CqsS-hAC2 chimera was mediated via the CqsS-receptor.

3.3. Gsα stimulation of hAC2 is inhibited by human serum

The above data present a proof-of-concept experiment to demonstrate that a 2x6TM anchor domain can regulate formation of the catalytic dimer of hAC2. The data pose the questions: are mammalian

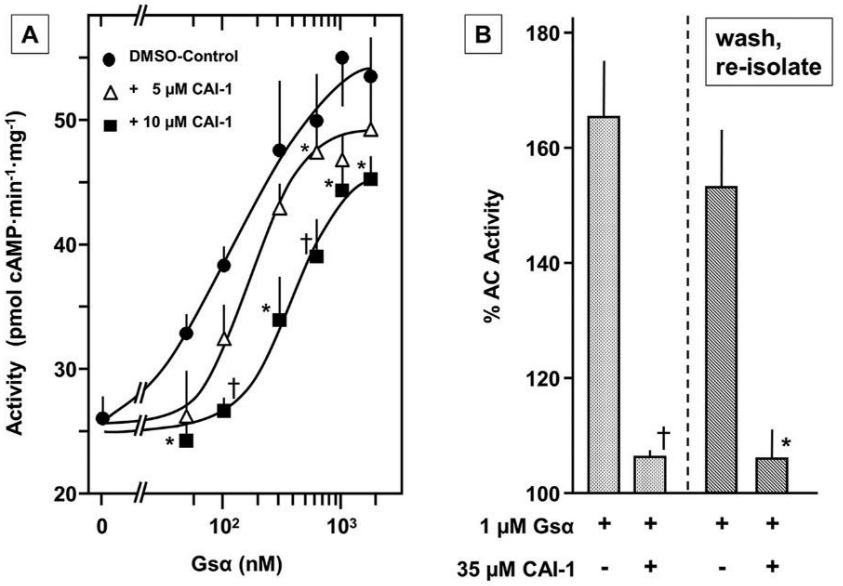

Fig. 2. A) Effect of CAI-1 on the stimulation of the chimera CqsS-hAC2 by Gsα. B) Inhibition of the Gsα response by CAI-1 is reversible. After stimulation of CqsS-hAC2 by 1 μM Gsα ± 10 μM CAI-1 for 15 min (left) membranes were washed and re-isolated by ultracentrifugation (total time required about 150 min). *Re*-stimulation was for 15 min. Basal activity (100%) corresponded to 48.2 ± 9.1 (primary stimulation) and 32.3 ± 5.1 pmol cAMP·mg^{-1}·min^{-1} (washed membranes). Error bars denote S.E.M. of 5 separate experiments. Significances: *, $p < .05$; †, $p < .01$ compared to the respective Gsα stimulation.

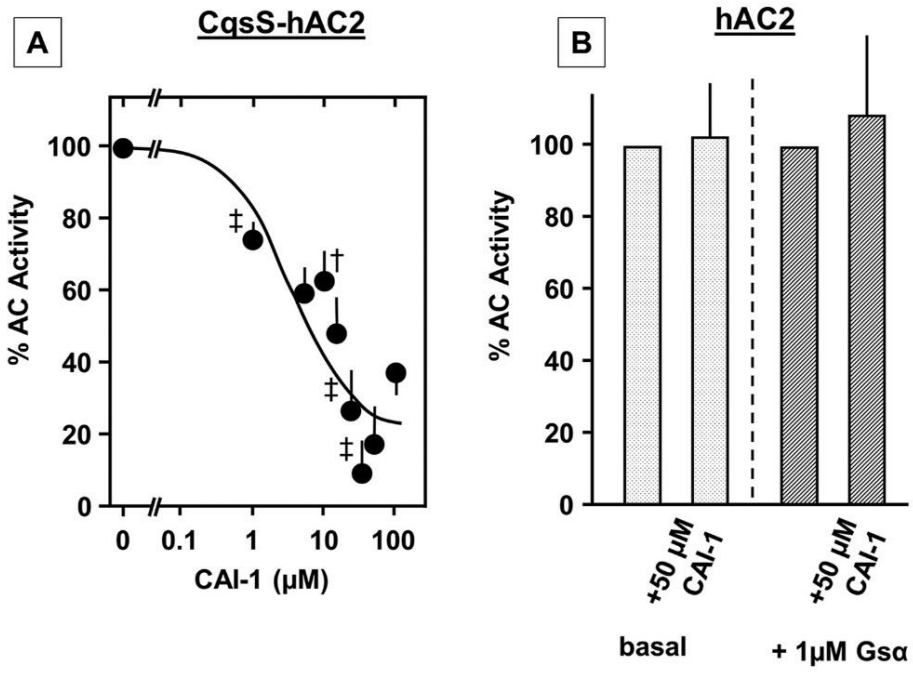

Fig. 3. A) CAI-1 concentration-response curve for the inhibition of Gsα-stimulated CqsS-hAC2. 1 μM Gsα-stimulated activity above basal (100%) was 33 ± 2.6 pmol cAMP·mg^{-1}·min^{-1}. The IC_{50} for CAI-1 was 6.3 μM. Error bars denote S.E.M. of 3–7 separate experiments. Significances: †: $p < .01$; ‡: $p < .001$ compared to Gsα-stimulated activity. For clarity, not all significances are indicated. B) CAI-1 has no effect on Gsα stimulation of hAC2. Basal (60 ± 20 pmol cAMP·mg^{-1}·min^{-1}) and 1 μM Gsα stimulated activities (2.7 ± 1.4 nmol cAMP·mg^{-1}·min^{-1}) were set at 100%, respectively; CAI-1 was dissolved in DMSO, 2% final DMSO in all assays. 5 independent assays were carried out. Error bars denote SD.

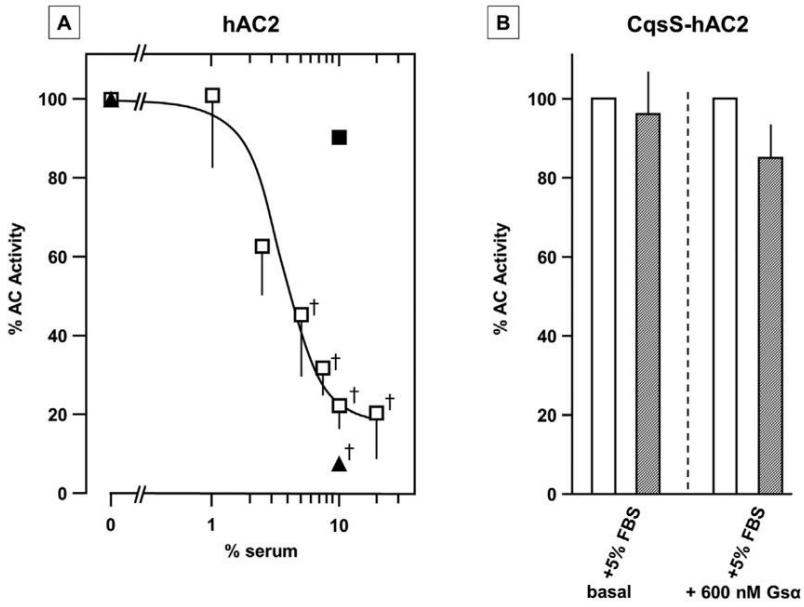

Fig. 4. A) Inhibition of Gsα stimulation (600 nM) of hAC2 by human serum (□) and FBS (▲); human serum albumin (■) at 45 μg/assay. Basal hAC2 activity was 30 pmol cAMP·mg^{-1}·min^{-1}, 100% Gsα-stimulated activity was 1.6 nmol cAMP·mg^{-1}·min^{-1}. Error bars represent SD of 3–5 experiments. †: $p < .01$ compared to control. B) Basal (open bars; 13.6 ± 2.2) and Gsα-stimulated activity (hatched bars; 27.2 ± 6.2 pmol cAMP·mg^{-1}·min^{-1}) of the CqsS-hAC2 chimera were unaffected by 5% FBS.

mACs regulated in a similar manner and what are potential ligands in mammals and where to expect them? Considering that the mAC membrane anchors are isoform-specifically conserved, prospective ligands are predicted to be similarly primordial [5,7]. Because ligands supposedly access the mACs from the extracellular solvent space, they are expected to be systemically present in the extracellular fluid system of the body. Indeed, human serum significantly inhibited stimulation of hAC2 by 600 nM Gsα (and similarly did heat-inactivated human serum in which complement is inactivated) in a concentration-dependent manner (Fig. 4A). Serum albumin had no effect (Fig. 4A). Fetal bovine serum (FBS) was even more potent indicating a higher concentration of inhibitory factors and almost excluding immunoglobulins as potential ligands because the concentration of immunoglobulins in FBS is substantially lower compared to human serum (Fig. 4 A). Although hAC2 activity with Mn^{2+}-ATP was much higher than with Mg^{2+}-ATP we preferred using Mg^{2+}-ATP as the likely physiological substrate because serum contains 1.25 mM Mg^{2+} and 2.4 mM Ca^{2+}, virtually excluding a chelating effect of divalent cations and, probably, regulatory effects of Ca^{2+} [24]. The data suggested that potential receptor ligands for hAC2 are present in serum. We also carried out concentration-response curves for Gsα stimulation of hAC2 in the absence and presence of 5 and 10% human serum (Supplemental fig. 1). In the presence of serum the efficacy of Gsα was substantially diminished, increasing the required Gsα concentrations for activation and diminishing the maximal responses (Supplemental fig. 1). This was similar to the results with the CqsS-hAC2 chimera (Fig. 2A) suggesting similar mechanisms of action for CAI-1 and specific serum factors, respectively.

Stringent controls are required to unequivocally assign the effect of

serum to the membrane anchors of hAC2: a) exclusion of a salt effect as serum contains around 120 mM NaCl, b) exclusion of an interference of serum components with the dimerization of the C1 and C2 catalytic domains, and c) exclusion of an interference in the interaction between the catalytic dimer and Gsα. 10 mM NaCl in the incubations, equivalent to 10% serum in the assays, did not impair hAC2 basal activity or Gsα stimulation. Similarly, using dialyzed serum did not abrogate inhibition of Gsα stimulation excluding interference by NaCl.

Basal activities of all mACs generally are rather low and difficult to determine reliably [25]. Therefore, we increased the amount of hAC2 membrane protein 27-fold and examined the effect of serum. It inhibited basal hAC2 activity in a concentration-dependent manner with a half-maximal inhibition at 4.9% serum whereas albumin did not (Supplemental fig. 2).

This created a critical issue because components of human or fetal bovine serum might either interfere with dimerization of C1 and C2 domains or with activation of the dimer by Gsα. This was explored using CqsS-hAC2 in which the membrane anchors are from a *Vibrio* quorum-sensor whereas the cytosolic domains are from hAC2 (scheme in Fig. 1). In the CqsS-hAC2 chimera FBS did neither interfere with basal hAC2 activity nor with Gsα stimulation (Fig. 4B). Thus we excluded an effect of serum on the catalytic hAC2 dimer or on Gsα activation of the dimer. The results demonstrated that the action of serum on basal hAC2 activity was contingent on the presence of the membrane anchor of hAC2.

3.4. Human serum inhibits Gsα stimulation of hAC 3, 5, 9 and in brain membranes

Are the above results restricted to the hAC2 isoform or are they indicative of a more general regulatory mechanism applicable to all mACs? Based on pronounced sequence features the nine mACs are subclassified into four subclasses, AC 1, 3 and 8, AC 2, 4, and 7, AC 5 and 6, and the standalone isoform AC9 [3,26,27]. We investigated hAC3, hAC5 and hAC9, i.e. one member of each subclass (including hAC2). Using appropriate enzyme concentrations, serum inhibited basal activities of hACs 3, 5, and 9 with hAC5 being less sensitive to inhibition compared to hAC3 and 9 (IC_{50} = 6.3% serum) indicating either different concentrations of specific inhibitory factors in serum or differences in affinity of a potentially common factor (Supplemental fig. 3). Similarly, Gsα stimulation of hAC isoforms 3, 5, and 9 was inhibited by human serum. The calculated IC_{50} concentrations ranged between 3 and 7% (Fig. 5A). These insignificant differences were not surprising as the commercial human serum is mixed from adult human donors, certainly presenting various physiological states while donating blood.

Next we investigated whether we might have dealt with a serum effect related to the heterologous expression of hACs in Sf9 cells. We prepared membranes from rat brain cortex which contain essentially all mAC isoforms [28]. Serum potently inhibited basal AC as well as Gsα stimulated activity, suggesting that the mACs in brain membranes are similarly regulated as individual AC isoforms expressed in Sf9 cells (Fig. 5B and Supplemental fig. 4).

3.5. Serum inhibits forskolin-stimulated AC activity

mACs are known to be regulated by a number of cytosolic effectors such as Gβγ, calcium / calmodulin, or forskolin and by several secondary modifications such as phosphorylation [3]. These factors generally have divergent, isoform-specific effects, e.g. Gβγ is reported to enhance Gsα or forskolin-stimulated activities of mACs 2, 4, 5, 6, and 7, but to have no effect alone (reviewed in [26,29]). On the other hand, Gβγ inhibits mACs 1, 3, and 8, and is even reported to inhibit AC5 and 6 [26,30,31]. Similarly, calcium and calmodulin have isoform-specific inhibitory or activating effects [26]. In contrast, the plant diterpene forskolin uniformly activates mACs 1 to 8 and it potentiates Gsα activation [3]. In crystal structures of the catalytic dimer, forskolin is bound within the catalytic cleft [21,32]. Therefore, we examined whether serum affects the action of forskolin on hAC2, either alone or in conjunction with Gsα. 25 μM Forskolin stimulated hAC2 about 2.4-fold and human serum significantly inhibited activation (Fig. 6A). 25 μM Forskolin + 300 nM Gsα resulted in a 6.6-fold potentiation of activation of hAC2 and serum was significantly inhibitory as well (Fig. 6B). Interestingly, also basal AC activity in rat cortical membranes was inhibited by serum in line with respective results of hACs 2, 3, 5, and 9 activities (Supplemental fig.'s 2, 3 and 4). This demonstrates that regulatory processes of mACs, which are mediated via direct effects on the cytosolic catalytic dimer, are affected by action of specific inhibitory factors present in serum acting via mAC membrane domains. The data support our suggestion that we were dealing with a novel general mechanism of mAC regulation.

4. Discussion

Thus far, studies of regulation of mAC activity mostly dealt with

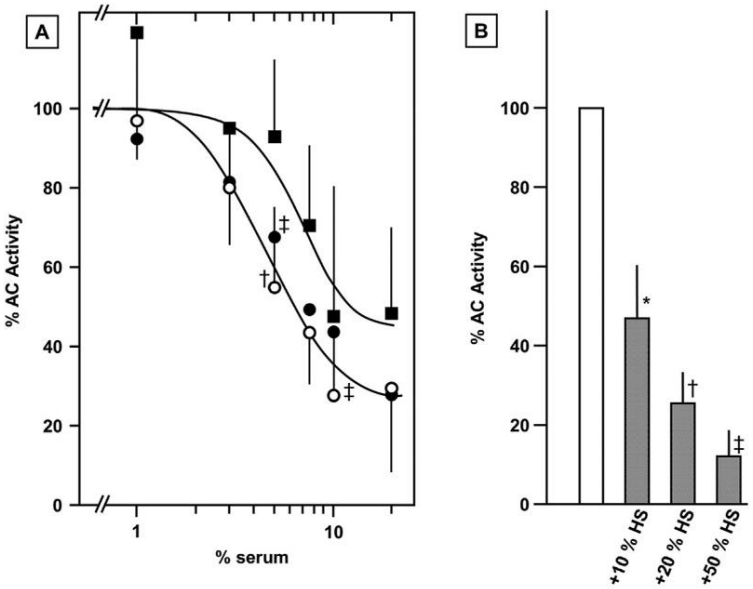

Fig. 5. A) Serum inhibition of hACs 3, 5, and 9 stimulated by 600 nM Gsα (○: hAC 3; ●: hAC5; ■: hAC9). To depict the data in a single graph, activities of hACs 3, 5, and 9 stimulated by 600 nM Gsα were taken as 100% (hAC3 = 0.7, hAC5 = 4.5, AC9 = 1.5 nmol cAMP·mg^{-1}·min^{-1}; for inhibition of basal AC activities see Supplemental fig. 3). B) Serum inhibition of AC activity in rat brain cortical membranes stimulated by 600 nM Gsα. 100% activity corresponds to 1.24 nmol cAMP·mg^{-1}·min^{-1} (3.5-fold stimulation above basal; n = 3). *: $p < .05$: †: $p < .01$: ‡: $p < .001$. Error bars denote SD of 3–4 experiments. (for inhibition of basal activity see Supplemental fig. 4). For clarity, not all significances are indicated.

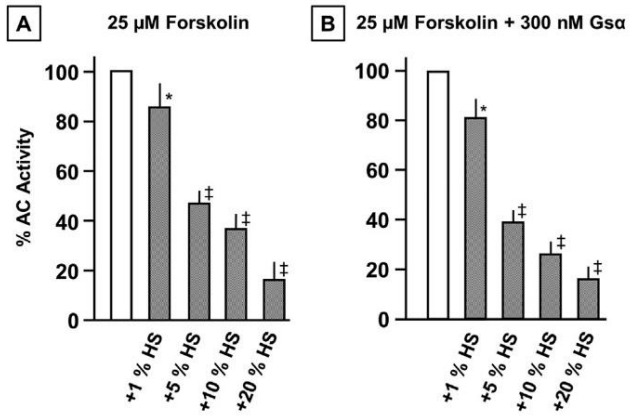

Fig. 6. Serum inhibition of hAC2 activity stimulated by forskolin and forskolin + Gsα. A) Inhibition of 25 µM forskolin stimulated hAC2 activity (100% corresponds to 0.19 nmol cAMP·mg^{-1}·min^{-1}, a 2.5-fold stimulation). B) Inhibition of hAC activity stimulated by 25 µM forskolin and 300 nM Gsα (100% corresponds to 0.5 nmol cAMP·mg^{-1}·min^{-1}, a 6.6-fold stimulation). Error bars denote SD of 4 experiments. *: $p < .05$; ‡: $p < .001$.

regulation of the cytosolic catalytic dimer, primarily by uniformly activating Gsα and, secondarily, by variable other inputs (reviewed in [3,27]). The biochemical data emanating from these studies are usually discussed by a two-state model, an active and an inactive state. In this respect, the 2x6TM anchors were considered inert. Potential roles for the membrane anchors were assigned to localization, e.g. in membrane rafts, or as potential interaction sites for scaffolding proteins [33–36]. Our data demonstrate a new level of mAC regulation which is spatially distinct from the catalytic dimer, and, for the first time, confer a regulatory function to all mAC domains. In addition, the regulatory input via the AC membrane domains immediately suggests a possible explanation for the striking evolutionary conservation of the membrane anchors in an isoform-specific manner [5] and requires expanding the previous two-state model of mAC regulation to a three-state model.

CqsS is a hexahelical quorum-sensing receptor from *Vibrio* sensing the extracellular ligand CAI-1 [8,37]. It is isosteric to a 6TM domain of the pseudoheterodimeric mACs [6]. In the CqsS-hAC2 chimera, we observed that CAI-1 attenuated Gsα stimulation in an unequivocally receptor-mediated process (Fig. 2). CAI-1 had no such effect on Gsα-stimulated activity of the hAC2 holoenzyme, because the hAC2 membrane anchor lacks the functionality to sense CAI-1 (Figs. 2, 3). However, stimulation of hAC2 by Gsα was inhibited by serum (Fig. 4A). The effect was dependent on the membrane domain from hAC2 because serum did not affect Gsα stimulation of CqsS-hAC2 as the CqsS receptor cannot sense signaling components present in mammalian serum (Fig. 4B). In addition, this demonstrated that serum did not affect dimerization of C1 and C2 (Fig. 4B). Serum albumin, the major protein in serum, had no effect suggesting the presence of specific, as yet unidentified inhibitory components in serum (Fig. 4A). Inhibition of Gsα stimulation by serum was further demonstrated for hAC isoforms 3, 5, and 9, thus covering one isoform from each mAC subclass (Fig. 5A). Likewise, serum inhibited basal and Gsα stimulated mAC activity present in rat brain cortical membranes (Fig. 5B and Supplemental fig. 4), virtually excluding the possibility of an artifact due to heterologous expression of hACs in Sf9 insect cells. Conceptually, a regulatory input from the extracellular space should affect all cytosolic regulatory inputs impinging upon the catalytic dimer. This was verified with forskolin which stimulates cytosolic catalytic dimer (exception mAC9). Forskolin activation of hAC2 ± Gsα was inhibited by serum (Fig. 6B).

4.1. A three-state model of adenylate cyclase regulation

Based on these data and equilibrium thermodynamic considerations we propose a novel formal concept of regulation of mACs which encompasses all available biochemical, pharmacological and structural data (Fig. 7). Three distinct basal states of mACs exist in equilibrium, state A (inactive), state B (inactive), and state C (active). States A and B differ in the conformational flexibility of their catalytic C1/C2 domains. In state A, the catalytic domains are conformationally constrained and cannot form an active dimer. In state B, the catalytic domains are conformationally unconstrained, yet because of their low affinity for each other, they only occasionally collapse into an active dimer (state C). The highly transient state 'C' is responsible for the very low basal activity observed in all mACs.

Constraining structural flexibility by binding of a ligand at the extracellular side shifts the equilibrium to the inactive 'A'-state (Fig. 7, far left) attenuating basal AC as well as Gsα stimulated activities in hAC2, 3, 5, 9, and in rat brain cortical membranes (Figs. 4, 5 and Supplemental Fig.'s 2–4). Forskolin reversibly increases the apparent affinity of C1 and C2 about tenfold, i.e. it stabilizes the 'C'-state. The 'C'-state is further stabilized by binding of Gsα at the cytosolic dimer thus

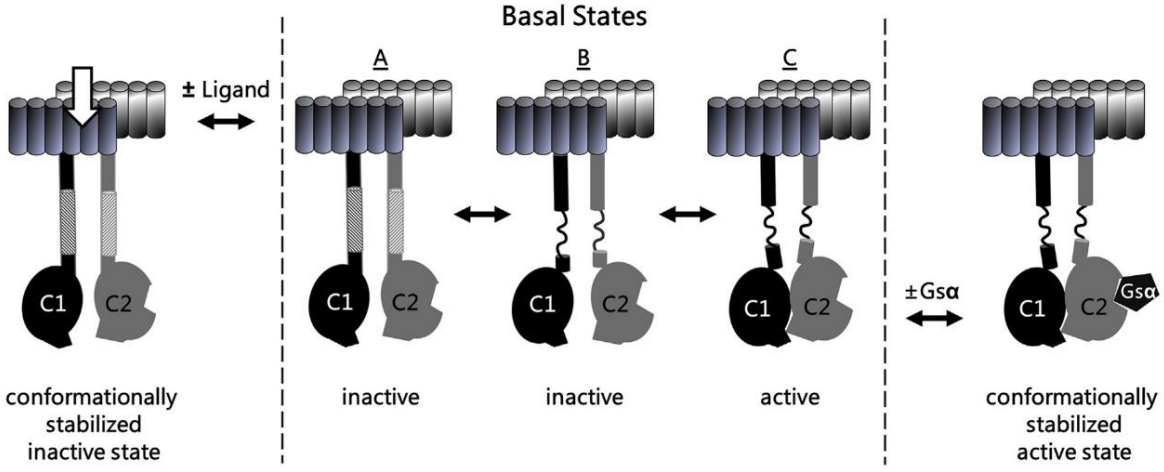

Fig. 7. Scheme of regulation of mammalian adenylate cyclases. Three basal states are in a thermodynamic equilibrium, two inactive, A and B, and one active state, C. The constant low basal enzyme activity is due to fractional formation of an active dimer as symbolized in C. Contact with Gsα in the cytosol stabilizes the active 'C'-state (conformationally stabilized active state, at far right). Conversely, binding of as yet unknown ligands at the extracellular side of the membrane anchor stabilizes the inactive state A (conformationally stabilized inactive state; at far left).

activating mACs and potentially acting in concert with forskolin (Fig. 7, far right).

The proposed three-state model suggests the existence of an allosteric linkage in mACs, in which the membrane anchors, as receptors, transduce extracellular signals across the cell membrane to the cytosolic catalytic dimer. This way, each mAC isoform can be addressed individually by an extracellular ligand and primed for a physiologically measured GPCR/Gsα response. Such a regulatory network would explain the conundrum of why often multiple Gsα-stimulated mAC isoforms are expressed in a single cell. The model is in agreement with the recently published structure of a bovine AC9 isoform which contains features compatible with signal transduction between membrane anchor and catalytic dimer [14]. We are aware of the fact that the equilibrium of states will be subject to ambient conditions such as ion and substrate concentrations, membrane charge and membrane potential. Thus, the model is open to modifications without losing its conceptual validity. Similarly, the lack of chemically identified ligands neither impaired establishing nor does it affect the validity of the three-state model. Considering the isoform-specific conservation of AC membrane anchors nine ligands are expected. These ligands in conjunction with the respective receptors will define a regulatory system which affects GPCR/Gsα actions executed via mACs. In summary then, the AC membrane anchors can now be designated as orphan receptors.

Credit author statement

Anubha Seth, Manuel Finkbeiner, Julia Grischin: Designed, carried out and analyzed experiments; Joachim E. Schultz: Conceptualization, analyzed data and wrote manuscript with all others.

Declaration of Competing Interest

None.

Acknowledgements

We thank U. Kurz for a continuous supply of Gsα (Q227L), A. Schultz for help in cloning, Dr. J. Weir, Friedrich-Miescher-Laboratory, Tübingen, for help with the Sf9 cell culture and Prof. Dr. A. Lupas for continuous encouragement. Supported by institutional funds from the Max-Planck-Society.

Appendix A. Supplementary data

Supplementary data to this article can be found online at https://doi.org/10.1016/j.cellsig.2020.109538.

References

[1] J. Krupinski, F. Coussen, H.A. Bakalyar, W.J. Tang, P.G. Feinstein, K. Orth, C. Slaughter, R.R. Reed, A.G. Gilman, Adenylyl cyclase amino acid sequence: possible channel- or transporter-like structure, Science 244 (4912) (1989) 1558–1564.
[2] S.C. Sinha, S.R. Sprang, Structures, mechanism, regulation and evolution of class III nucleotidyl cyclases, Rev. Physiol. Biochem. Pharmacol. 157 (2006) 105–140.
[3] C.W. Dessauer, V.J. Watts, R.S. Ostrom, M. Conti, S. Dove, R. Seifert, International Union of Basic and Clinical Pharmacology, CI. Structures and small molecule modulators of mammalian adenylyl cyclases, Pharmacol. Rev. 69 (2) (2017) 93–139.
[4] W.J. Tang, A.G. Gilman, Construction of a soluble adenylyl cyclase activated by Gs alpha and forskolin, Science 268 (5218) (1995) 1769–1772.
[5] J. Bassler, J.E. Schultz, A.N. Lupas, Adenylate cyclases: receivers, transducers, and generators of signals, Cell Signal. 46 (2018) 135–144.
[6] S. Beltz, J. Bassler, J.E. Schultz, Regulation by the quorum sensor from Vibrio indicates a receptor function for the membrane anchors of adenylate cyclases, elife 5 (2016).
[7] M. Ziegler, J. Bassler, S. Beltz, A. Schultz, A.N. Lupas, J.E. Schultz, A novel signal transducer element intrinsic to class IIIa and IIIb adenylate cyclases, FEBS J. 284 (2017) 1204–1217.
[8] W.L. Ng, Y. Wei, L.J. Perez, J. Cong, T. Long, M. Koch, M.F. Semmelhack, N.S. Wingreen, B.L. Bassler, Probing bacterial transmembrane histidine kinase receptor-ligand interactions with natural and synthetic molecules, Proc. Natl. Acad. Sci. U. S. A. 107 (12) (2010) 5575–5580.
[9] S. Diel, K. Klass, B. Wittig, C. Kleuss, Gbetagamma activation site in adenylyl cyclase type II. Adenylyl cyclase type III is inhibited by Gbetagamma, J. Biol. Chem. 281 (1) (2006) 288–294.
[10] M.P. Graziano, M. Freissmuth, A.G. Gilman, Expression of Gs alpha in Escherichia coli. Purification and properties of two forms of the protein, J. Biol. Chem. 264 (1) (1989) 409–418.
[11] M.P. Graziano, M. Freissmuth, A.G. Gilman, Purification of recombinant Gs alpha, Methods Enzymol. 195 (1991) 192–202.
[12] J.E. Schultz, B.H. Schmidt, Treatment of rats with thyrotropin (TSH) reduces the adrenoceptor sensitivity of adenylate cyclase from cerebral cortex, Neurochem. Int. 10 (2) (1987) 173–178.
[13] Y. Salomon, C. Londos, M. Rodbell, A highly sensitive adenylate cyclase assay, Anal. Biochem. 58 (2) (1974) 541–548.
[14] C. Qi, S. Sorrentino, O. Medalia, V.M. Korkhov, The structure of a membrane adenylyl cyclase bound to an activated stimulatory G protein, Science 364 (2019) 389–394.
[15] W.J. Tang, M. Stanzel, A.G. Gilman, Truncation and alanine-scanning mutants of type I adenylyl cyclase, Biochemistry 34 (44) (1995) 14563–14572.
[16] S. Weitmann, G. Schultz, C. Kleuss, Adenylyl cyclase type II domains involved in Gbetagamma stimulation, Biochemistry 40 (36) (2001) 10853–10858.
[17] Y.L. Guo, T. Seebacher, U. Kurz, J.U. Linder, J.E. Schultz, Adenylyl cyclase Rv1625c of mycobacterium tuberculosis: a progenitor of mammalian adenylyl cyclases, EMBO J. 20 (14) (2001) 3667–3675.
[18] G. Zhang, Y. Liu, A.E. Ruoho, J.H. Hurley, Structure of the adenylyl cyclase catalytic core, Nature 386 (6622) (1997) 247–253.
[19] S.Z. Yan, D. Hahn, Z.H. Huang, W.J. Tang, Two cytoplasmic domains of mammalian adenylyl cyclase form a Gs alpha- and forskolin-activated enzyme in vitro, J. Biol. Chem. 271 (18) (1996) 10941–10945.
[20] M.E. Hatley, B.K. Benton, J. Xu, J.P. Manfredi, A.G. Gilman, R.K. Sunahara, Isolation and characterization of constitutively active mutants of mammalian adenylyl cyclase, J. Biol. Chem. 275 (49) (2000) 38626–38632.
[21] J.J. Tesmer, R.K. Sunahara, A.G. Gilman, S.R. Sprang, Crystal structure of the catalytic domains of adenylyl cyclase in a complex with Gsalpha.GTPgammaS, Science 278 (5345) (1997) 1907–1916.
[22] C.W. Dessauer, M. Chen-Goodspeed, J. Chen, Mechanism of Galpha i-mediated inhibition of type V adenylyl cyclase, J. Biol. Chem. 277 (32) (2002) 28823–28829.
[23] M. Ritt, S. Sivaramakrishnan, Correlation between activity and domain complementation in adenylyl cyclase demonstrated with a novel fluorescence resonance energy transfer sensor, Mol. Pharmacol. 89 (4) (2016) 407–412.
[24] E. Csenker, P. Dioszeghy, I. Fekete, F. Mechler, Ion concentrations in serum and cerebrospinal fluid of patients with neuromuscular diseases, Arch. Psychiatr. Nervenkr. 231 (3) (1982) 251–258 1970.
[25] J.D. Hildebrandt, L. Birnbaumer, Inhibitory regulation of adenylyl cyclase in the absence of stimulatory regulation. Requirements and kinetics of guanine nucleotide-induced inhibition of the cyc- S49 adenylyl cyclase, J. Biol. Chem. 258 (21) (1983) 13141–13147.
[26] D. Willoughby, D.M. Cooper, Organization and Ca2+ regulation of adenylyl cyclases in cAMP microdomains, Physiol. Rev. 87 (3) (2007) 965–1010.
[27] R.K. Sunahara, R. Taussig, Isoforms of mammalian adenylyl cyclase: multiplicities of signaling, Mol. Interv. 2 (3) (2002) 168–184.
[28] C. Sanabra, G. Mengod, Neuroanatomical distribution and neurochemical characterization of cells expressing adenylyl cyclase isoforms in mouse and rat brain, J. Chem. Neuroanat. 41 (1) (2011) 43–54.
[29] C.S. Brand, R. Sadana, S. Malik, A.V. Smrcka, C.W. Dessauer, Adenylyl cyclase 5 regulation by Gbetagamma involves isoform-specific use of multiple interaction sites, Mol. Pharmacol. 88 (4) (2015) 758–767.
[30] J.J. Tesmer, S.R. Sprang, The structure, catalytic mechanism and regulation of adenylyl cyclase, Curr. Opin. Struct. Biol. 8 (1998) 713–719.
[31] D. Steiner, T. Avidor-Reiss, E. Schallmach, D. Saya, Z. Vogel, Inhibition and superactivation of the calcium-stimulated isoforms of adenylyl cyclase: role of Gbetagamma dimers, J. Mol. Neurosci. 27 (2) (2005) 195–203.
[32] J.J.G. Tesmer, R.K. Sunahara, R.A. Johnson, G. Gosselin, A.G. Gilman, S.R. Sprang, Two-metal-ion catalysis in adenylyl cyclase, Science 285 (1999) 756–760.
[33] A.J. Crossthwaite, T. Seebacher, N. Masada, A. Ciruela, K. Dufraux, J.E. Schultz, D.M. Cooper, The cytosolic domains of Ca2+ −sensitive adenylyl cyclases dictate their targeting to plasma membrane lipid rafts, J. Biol. Chem. 280 (8) (2005) 6380–6391.
[34] L.A. Piggott, A.L. Bauman, J.D. Scott, C.W. Dessauer, The A-kinase anchoring protein Yotiao binds and regulates adenylyl cyclase in brain, Proc. Natl. Acad. Sci. U. S. A. 105 (37) (2008) 13835–13840.
[35] Y. Li, L. Chen, R.S. Kass, C.W. Dessauer, The A-kinase anchoring protein Yotiao facilitates complex formation between adenylyl cyclase type 9 and the IKs potassium channel in heart, J. Biol. Chem. 287 (35) (2012) 29815–29824.
[36] T.C. Rich, K.A. Fagan, H. Nakata, J. Schaack, D.M. Cooper, J.W. Karpen, Cyclic nucleotide-gated channels colocalize with adenylyl cyclase in regions of restricted cAMP diffusion, J. Gen. Physiol. 116 (2) (2000) 147–161.
[37] W.L. Ng, L.J. Perez, Y. Wei, C. Kraml, M.F. Semmelhack, B.L. Bassler, Signal production and detection specificity in Vibrio CqsA/CqsS quorum-sensing systems, Mol. Microbiol. 79 (6) (2011) 1407–1417.

Supplementary data:

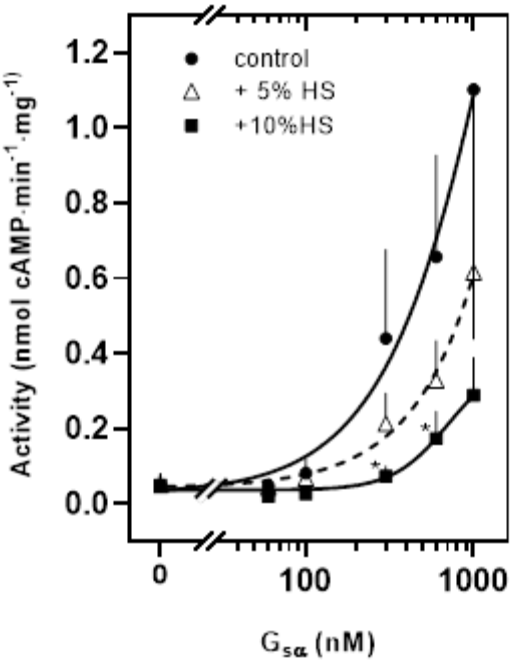

Supplementary Figure 1. Gsα concentration-response curve of hAC2 in presence of 5 and 10 % human serum, respectively. Significances: *: p≤0.05 compared to control. Error bars denote SD of 3 experiments.

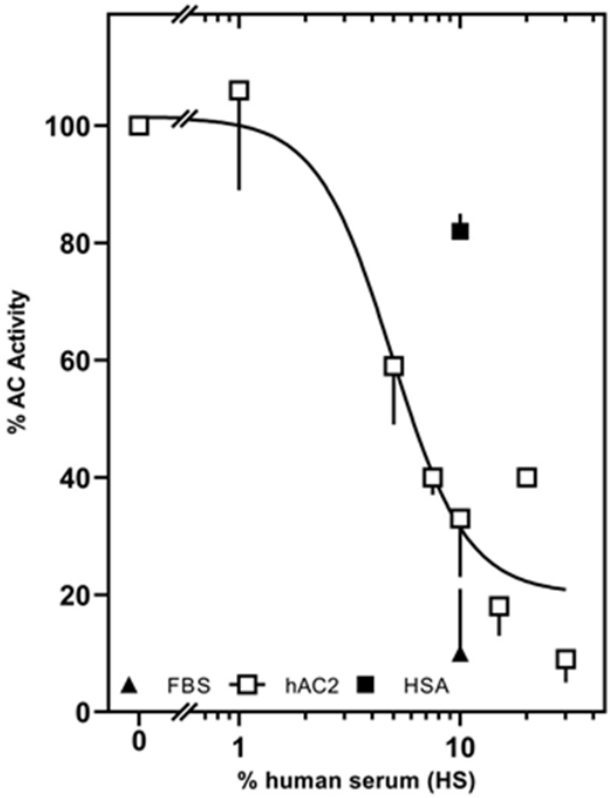

Supplementary Figure 2. Inhibition of basal activity of hAC2 by human serum. Basal activity was 0.038 ± 0.006 nmol cAMP·mg^{-1}·min^{-1}. IC_{50} concentration determined by graph-pad was: 4.9% HS. 2-5 Experiments were carried out, Error bars denote SD

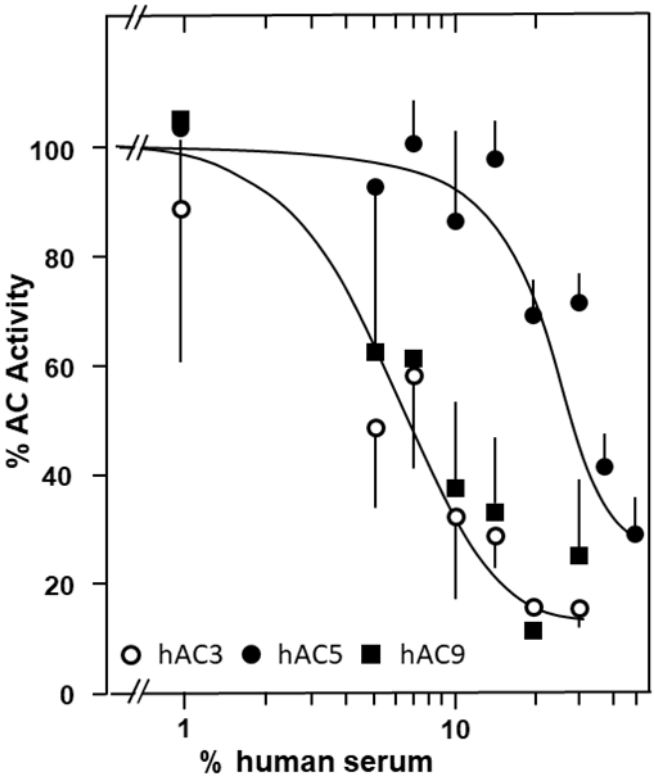

Supplementary Figure 3. Inhibition of basal activity of hACs 3, 5, and 9 by human serum. 2-5 Experiments were carried out. Error bars denote SD. Basal activities were: hAC3 0.025 ± 0.007; hAC5 0.049 ± 0.013; hAC9 0.150 ± 0.047 nmol cAMP·mg^{-1}·min^{-1} IC_{50} concentrations determined by graph-pad were: 6.0% estimated ~40% and 5.9%, respectively

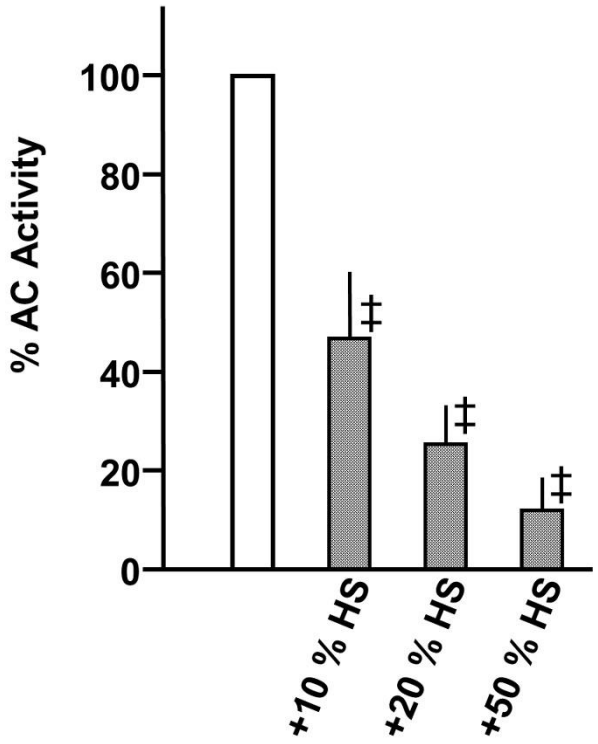

Supplementary Figure 4. Inhibition of basal AC activity in a rat brain cortical membrane preparation. Basal activity (100 %) was 325 pmol cAMP·mg1·min-1. n = 3, Error bars denote SD. Significance: ‡**:** p< 0.001

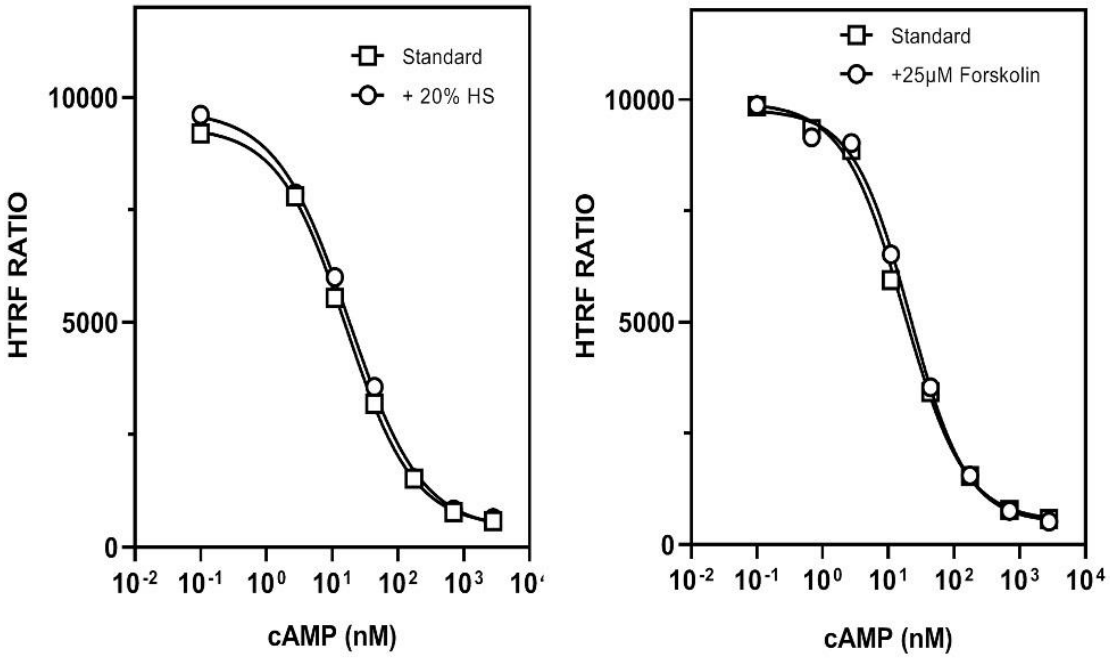

Supplementary Figure 5. Standard curves for cAMP determination generated with the homogenous-time-resolved fluorescence assay from Cisbio in presence of 20 % human serum or 25 µM forskolin. No interference of serum and forskolin (and other agents used in respective AC assays such as Gsα at 1 µM or DMSO at 2%) was observed.

7. Finkbeiner et al

7.1 Eigenanteil

International Journal of Medical Microbiology, May-June 2019, p. 245-251
Volume 309
doi:10.1016/j.ijmm.2019.03.006

In search of a function for the membrane anchors of class IIIa adenylate cyclases

Manuel Finkbeiner[a], Julia Grischin[a], Anubha Seth[a,b], Joachim E. Schultz[b,*]

[a] Max-Planck-Institut für Entwicklungsbiologie, Abt. Proteinevolution, Max-Planck-Ring 5, 72076, Tübingen, Germany.
[b] Pharmazeutisches Institut der Universität Tübingen, Auf der Morgenstelle 8, 72076, Tübingen, Germany.

Für diesen Review-Artikel wurde ein Vorschlag für ein Manuskript zu gleichen Teilen von M. Finkbeiner, A. Seth und mir verfasst, der nicht für die Publikation verwendet wurde. Prof. Dr. J. E. Schultz hat die Endfassung geschrieben, M. Finkbeiner, A. Seth und ich haben an der Endfassung Korrekturen vorgenommen.

7.2 Publikation

International Journal of Medical Microbiology 309 (2019) 245–251

Contents lists available at ScienceDirect

International Journal of Medical Microbiology

journal homepage: www.elsevier.com/locate/ijmm

In search of a function for the membrane anchors of class IIIa adenylate cyclases

Manuel Finkbeiner[a,1], Julia Grischin[a,1], Anubha Seth[b,1], Joachim E. Schultz[b,*]

[a] Max-Planck-Institut für Entwicklungsbiologie, Tübingen, Germany
[b] Pharmazeutisches Institut der Universität Tübingen, Tübingen, Germany

ARTICLE INFO

Keywords:
Adenylate cyclase
Membrane anchor
Receptor;
quorum-sensing
Chemotaxis receptor
Cyclase-transducing-element
HAMP domain

ABSTRACT

Nine pseudoheterodimeric mammalian adenylate cyclases possess two dissimilar hexahelical membrane domains (TM1 and TM2), two dissimilar cyclase-transducing-elements (CTEs) and two complementary catalytic domains forming a catalytic dimer (often termed cyclase-homology-domain, CHD). Canonically, these cyclases are regulated by G-proteins which are released upon ligand activation of G-protein-coupled receptors. So far, a biochemical function of the membrane domains beyond anchoring has not been established. For almost 30 years, work in our laboratory was based on the hypothesis that these voluminous membrane domains possess an additional physiological, possibly regulatory function. Over the years, we have generated numerous artificial fusion proteins between the catalytic domains of various bacterial adenylate cyclases which are active as homodimers and the membrane receptor domains of known bacterial signaling proteins such as chemotaxis receptors and quorum-sensors which have known ligands. Here we summarize the current status of our experimental efforts. Taken together, the data allow the conclusion that the hexahelical mammalian membrane anchors as well as similar membrane anchors from bacterial adenylate cyclase congeners are orphan receptors. A search for as yet unknown ligands of membrane-delimited adenylate cyclases is now warranted.

1. Introduction

Viability of cells, prokaryotic and eukaryotic alike depends on the ability to sense and respond to changes in the environment in a timely manner. In the late 1950s, Sutherland and colleagues identified adenosine 3′, 5′- monophosphate (cyclic AMP, cAMP) as a perspicuous intracellular second messenger in glycogen metabolism in the liver (Sutherland and Rall, 1958). In the next decades, cAMP was shown to be one of the most universal second messengers in essentially all forms of life. Generally, cAMP is formed in response to 'first messengers', i.e. primary signals such as ligands for respective membrane receptors. The proteins responsible for cAMP biosynthesis from ATP, adenylate cyclases (ACs), were identified as mostly membrane-bound proteins and the diversity of regulatory processes indicated the presence of several isoforms.

With the cloning and sequencing of the first mammalian AC in 1989, the field rapidly advanced (Krupinski et al., 1989). Quickly, it was apparent that the most populated class of AC isoforms (now termed class III ACs) was present in mammals, in most eukaryotes and throughout eubacteria (Barzu and Danchin, 1994). The divergent classes I, II, IV, V and VI ACs are restricted to bacteria. Based on specific sequence variations in class III ACs, the proteins were subclassified into class IIIa, b, c, and d (Linder and Schultz, 2003). Classes IIIc and d ACs are restricted to bacteria whereas classes IIIa and b ACs are shared among eukaryotes and prokaryotes. All class III ACs have a dimeric catalytic center which is formed at the interface of two complementary domains, often termed cyclase-homology-domain (CHD) (Linder and Schultz, 2008). X-ray structures of class III AC catalytic dimers revealed that both monomers contribute to the formation of the catalytic fold (Sinha et al., 2005; Steegborn et al., 2005; Tesmer et al., 1997; Tews et al., 2005). A crucial difference between eukaryotic and prokaryotic ACs is that bacterial isoforms generally are monomeric proteins which must dimerize for activity and form two catalytically competent centers. In contrast, nine mammalian ACs are pseudoheterodimers with two dissimilar hexahelical membrane domains (TM1 and TM2) connected via domain-specific linkers to two catalytically inactive monomers, C1 and C2. The catalytic core is formed at the interface of the two complementary domains with a single active site (Tesmer et al., 1997). Similarly, a number of bacterial congeners possess hexahelical membrane domains (6 T M), obviously much in excess of what would be

* Corresponding author at: Pharmazeutisches Institut der Universität Tübingen, Auf der Morgenstelle 8, 72076 Tübingen, Germany.
E-mail address: Joachim.schultz@uni-tuebingen.de (J.E. Schultz).
[1] Names are arranged alphabetically.

https://doi.org/10.1016/j.ijmm.2019.03.006
Received 9 January 2019; Received in revised form 8 March 2019; Accepted 21 March 2019

required for membrane anchoring. Indeed, it was initially speculated that these membrane anchoring devices might possess an ion channel- or transporter-like function (Krupinski et al., 1989). However, a possible regulatory function of these voluminous membrane domains has so far proved elusive.

Since publication of the first amino acid sequence of a mammalian AC our working hypothesis was that such large membrane anchors likely have a physiological function beyond anchoring. Over time we developed several experimental approaches to address and possibly solve this puzzling question. Initially, we were intrigued by the cAMP system in *Paramecium*. In this protozoan, a K^+-current evoked by hyperpolarization of the cell stimulates cAMP biosynthesis (Schultz et al., 1992). The purified AC protein has ion-channel properties when inserted into a black lipid membrane (Schultz et al., 1992). Cloning of the AC identified a canonical voltage-sensor in its hexahelical membrane domain and the motif of a potassium channel (Weber et al., 2004). Such an AC is also present in other protozoans such as *Tetrahymena* or the malaria pathogen *Plasmodium* (Weber et al., 2004). Sequence comparison of these protozoan ACs with mammalian isoforms established that we were most likely dealing with a molecular outlier which did not permit to generalize about such a function in other, similarly membrane-anchored ACs. Over time, the increasing number of sequenced ACs from animals and bacteria allowed well-founded bioinformatic analyses and considerably expanded the number of potential model organisms suitable for addressing the central question of this lab: is there any function of the hexahelical AC membrane anchors beyond anchoring? Below we summarize the data following the timeline since 1999.

The genome of *Mycobacterium tuberculosis HRv37* was sequenced in 1998 (Cole et al., 1998). About 15 genes were predicted to encode class III ACs. These comprise AC isoforms of many stripes, such as the soluble ACs Rv1264, Rv0386 and Rv1900 (AC class IIIc), the class IIIa AC Rv1625c with a hexahelical membrane anchor, a likely monomeric progenitor of the pseudoheterodimeric mammalian ACs, and the class IIIb ACs Rv3645, Rv1318c, Rv1319c and Rv1320c which possess 6 T M anchors and a cytosolic HAMP domain connecting to the catalytic domain (Linder and Schultz, 2003). The acronym HAMP is derived from its occurrence in **H**istidine kinases, **A**denylate cyclases, **M**ethyl-accepting chemotaxis receptors and **P**hosphatases (Aravind and Ponting, 1999). It is a ubiquitously occurring domain in many dimeric signal-transducing proteins in bacteria. HAMP domains are established as signal transducers and their concurrent presence in bacterial ACs is indicative of such a function in these AC isoforms. The hexahelical membrane anchor, the HAMP domain and the catalytic domain give these bacterial ACs an unequivocal tripartite domain organization. We have generated several chimeras between these ACs and bacterial signaling proteins such as chemotaxis receptors and quorum-sensing (QS)-receptors (Fig. 1). In conjunction with comprehensive bioinformatic studies, this has allowed us to tentatively conclude that all membrane delimited ACs are in fact primary signal-transducing proteins which translate extracellular signals into an intracellular cAMP - second messenger response (Bassler et al., 2018).

2. Chemotaxis receptors and HAMP domains as signaling devices for adenylate cyclases

Cytoplasmic HAMP domains are components of bacterial one- and two-component systems such as chemotaxis receptors and histidine kinases (Ferris et al., 2011; Hazelbauer et al., 2008; Parkinson, 2010; Ulrich et al., 2005; Ulrich and Zhulin, 2010). Signaling via chemotaxis receptors (MCPs, methyl-accepting chemotaxis proteins) has been studied extensively (Parkinson, 2010). The HAMP domain connects a two-helical membrane receptor e.g. Tsr (for serine) or Tar (for aspartate) to a methyl-accepting protein involved in the cascade to regulate swimming behavior via control of flagellar beating and in adaptation to a given level of stimulation (Hazelbauer et al., 2008; Parkinson, 2010). In 2006, the predicted coiled-coil structure of the archaebacterial protein Af1503 from *Archaeoglobus fulgidus* was determined by NMR (Hulko et al., 2006). N-terminally, Af1503 has a two-helical membrane anchor of unknown function followed by a cytoplasmic HAMP domain. Somewhat surprisingly, it lacks an output domain (Fig. 1A). We have replaced the HAMP domain in the Rv3645 AC from *M. tuberculosis* by the Af1503 HAMP and introduced several point mutations at a critical alanine position in the HAMP core (Hulko et al., 2006; Fig. 1B, construct 1). The data suggest rotation of the α-helices by 26° in signal transduction (Ferris et al., 2011, 2014; Hulko et al., 2006). Next, we replaced the hexahelical membrane anchor and the HAMP domain of the Rv3645 AC by the Tsr receptor from *E. coli* (Fig. 1B; construct 2). The point of connection in the chimera was based on the alignment of the two HAMP domains (Kanchan et al., 2010). The protein is expressed in *E. coli* and inserted into the membrane. AC activity in isolated membranes is robust (up to 20 nmol cAMP·mg^{-1} min^{-1}). Serine as Tsr receptor ligand inhibits AC activity with a half-maximal inhibitory concentration (IC_{50}) of 18.5 μM, well within the physiological range (Fig. 2). The effect is ligand-specific and depends on an unabridged receptor as demonstrated by inactivating point mutations within the extracellular loop region of the serine-binding side in Tsr (Kanchan et al., 2010). These findings strongly suggest that a bacterial catalytic AC homodimer (class IIIb AC) may be a direct target for regulation by a membrane receptor signal. Signal transmission is not fully specific for the origin of the HAMP domain. It can be either from Tsr or from Rv3645 AC (Fig. 1B, constructs 2 and 3, Fig. 2; Kanchan et al., 2010). In similar constructs with the *E. coli* chemotaxis receptor for aspartate, Tar, AC activity is specifically inhibited by aspartate (Kanchan et al., 2010). The data highlight several points: a) a molecular modularity between bacterial signal transducing proteins such as chemotaxis receptors and ACs exists which enables uncomplicated domain exchangeability between differing signaling pathways; b) the HAMP domains in bacterial ACs operate as signal transducers, i.e. they receive and transduce conformational signals from N-terminal input to C-terminal output domains; c) the catalytic activity of the class IIIb AC Rv3645 in *M. tuberculosis* is probably regulated in response to membrane receptor stimulation (Kanchan et al., 2010).

The experiments summarized above deal with a class IIIb AC. A functional extrapolation to mammalian class IIIa isoforms may be deemed adventurous. Therefore, we have used the cyanobacterial class IIIa AC CyaG from *Arthrospira platensis* as our next model. CyaG has a two-helical membrane anchor of unknown function, a canonical HAMP domain and a 25 aa long spacer between the HAMP and the catalytic domains, termed signaling-helix or S-helix (Anantharaman et al., 2006; Fig. 1A). The S-helix is modeled as a two-helical parallel coiled-coil. In the next construct (Fig. 1B, construct 4), the membrane anchor of CyaG was replaced by the Tsr receptor as above and the HAMP domain and S-helix were retained together with the catalytic domain from CyaG (Kanchan et al., 2010; Winkler et al., 2012). This chimera is inhibited by serine similarly to the Tsr-HAMP-Rv3645 chimera described above (compare Figs. 2 and 3, left). Notably, this regulation requires the presence of the cyanobacterial HAMP domain as a linker (Kanchan et al., 2010). The data establish that a canonical class IIIa AC catalytic dimer can operate as a receiver/output domain for an upstream receptor signal. Surprisingly, in constructs in which the 25 amino acid long S-helix is deleted (Fig. 1B, construct 5) the sign of the signal is inverted, i.e. serine activates (Fig. 3, right). We note that the basal AC activities in these constructs ± S-helix differ substantially. Deletion of the S-helix causes a 10-fold drop in activity from 12 to 1.25 nmol cAMP mg^{-1} min^{-1}. The data are then most plausibly rationalized by assuming two different basal states in the presence or absence of the S-helix (Schultz and Natarajan, 2013). In the presence of the S-helix, basal AC activity is high, and serine inhibits, probably constraining the conformational freedom of the catalytic domains to dimerize. In the absence of the S-helix, basal activity is low, i.e. the catalytic domains cannot properly associate with each other, and serine activates,

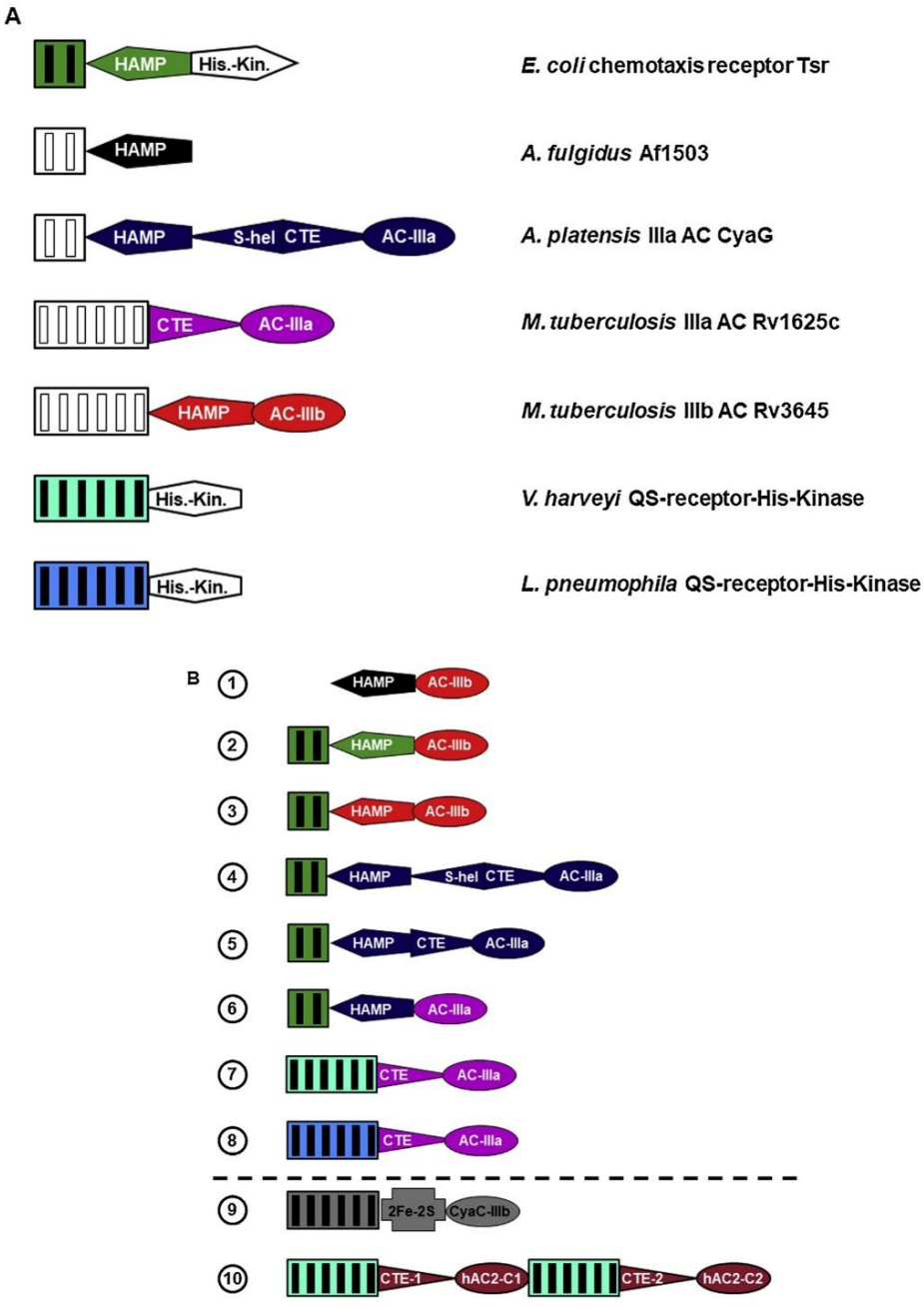

Fig. 1. A) Schematic domain organization of the reference proteins. The colored domains were used as building blocks in subsequent chimeric adenylate cyclases. The empty frames (membrane domains and histidine-kinases) denote domains not used in subsequent constructs. Transmembrane helices are symbolized by narrow vertical bars. S-hel: S-helix of AC CyaG from *A. platensis*. CTE: cyclase-transducing-element. **B) Domain organization of signaling proteins with mycobacterial class IIIb AC Rv3645, cyanobacterial class IIIa AC CyaG, mycobacterial class IIIa AC Rv1625c, and class IIIb AC CyaC from *Sinorhizobium meliloti*.** For exact domain boundaries see references (Beltz et al., 2016; Kanchan et al., 2010; Winkler et al., 2012; Ziegler et al., 2017). The numbering, color and shape coding used in this figure is maintained throughout the review. The numbering of the chimeras approximates the timeline in which they were generated.

probably by releasing the catalytic domains from a conformational constraint and allowing the formation of a productive dimer (Schultz and Natarajan, 2013; Winkler et al., 2012). Generating these slightly more complex chimeras we have noticed the necessity to use clearly defined points of transition between individual domains. The precise transition points between the S-helix and the catalytic domain of CyaG have been of particular importance (Winkler et al., 2012). The experiments summarized above demonstrate that also a class IIIa AC catalytic dimer serves as a signal output domain in response to activation of the chemotaxis receptor much like the closely related IIIb AC variant Rv3645 (Fig. 1B constructs 2–3).

In the mammalian pseudoheterodimeric ACs, HAMP domains are absent (Dessauer et al., 2017). Similarly, the mycobacterial class IIIa AC Rv1625c, a close bacterial progenitor of mammalian ACs, has no HAMP domain (Guo et al., 2001). Therefore, the next question is whether the catalytic domain of Rv1625c can in principle serve as a signal receiver/output domain for a membrane receptor signal. Accordingly, we have generated chimeras which consist of single protein modules from three bacterial species, the chemotaxis receptor Tsr from *E. coli,* the HAMP transducer domain from the AC CyaG from *A. platensis* and class IIIa catalytic domain from *M. tuberculosis* (Fig. 1B, construct 6). As reported earlier, the constructs are expressed in *E. coli* and have AC activity that is activated by serine at physiologically meaningful concentrations (Schultz et al., 2015). Including the S-helix of CyaG in such a chimera inverts the sign of the output signal (Schultz et al., 2015). Taken together, we conclude that a class IIIa AC catalytic domain without a HAMP domain in its original domain organization can also operate as an output domain for a membrane signal. In addition, our data highlight the considerable extent of modularity in these bacterial signaling systems. We have used the data to propose a receptor function for all

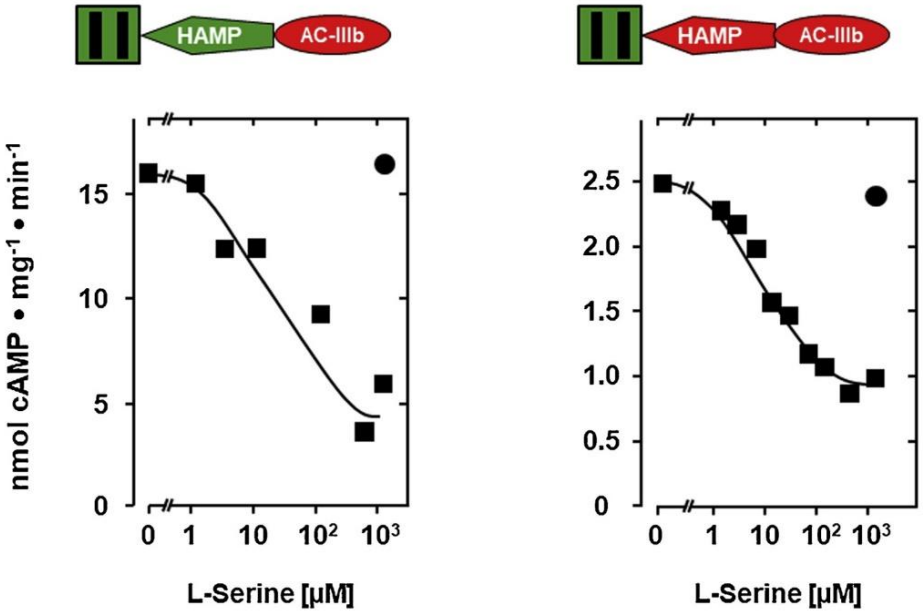

Fig. 2. l-Serine inhibits the class IIIb AC Rv3645 via the *E. coli* Tsr chemotaxis receptor for serine. Above each graph the diagram of the chimera is depicted. Left: Construct with the HAMP domain from Tsr. Maximal serine inhibition was 71 ± 3% (half maximal inhibition was at 18.5 µM). Right: The construct with the HAMP from the Rv3645 AC was inhibited by 45% (half maximal inhibition at 15 µM serine). The filled circles in both graphs are controls with 1 mM L-aspartate (figure was adapted from ref. Kanchan et al., 2010).

6 T M ACs such as AC Rv1625c or the pseudoheterodimeric mammalian ACs. However, at this point we had to acknowledge a major conceptual drawback, i.e. so far we have been dealing with a membrane signal originating from an established receptor with two transmembrane α-helices whereas Rv1625c and all mammalian ACs have hexahelical membrane anchors of unknown function. Playing Lego with protein domains in vitro is not necessarily a compelling argument for the existence of such proteins in evolution, i.e. if something can be made to function it is no proof that this functional entity must exist in nature. Therefore, following up on this point we have used the hexahelical quorum-sensing (QS) receptors from *Vibrio harveyi* and *Legionella pneumophila* which are similar to the 6 T M domains of class IIIa ACs such as Rv1625c or the mammalian congeners. Importantly and fortunately, the ligands for the QS-receptors are known (Ng et al., 2011, 2010; Spirig et al., 2008).

3. Adenylate cyclase regulation by quorum sensing receptors

The hexahelical membrane anchors of essentially all respective bacterial ACs and the nine mammalian isoforms are similar. The α-helices are connected by rather short linkers usually considered problematic for ligand-binding (Beltz et al., 2016). An almost isosteric

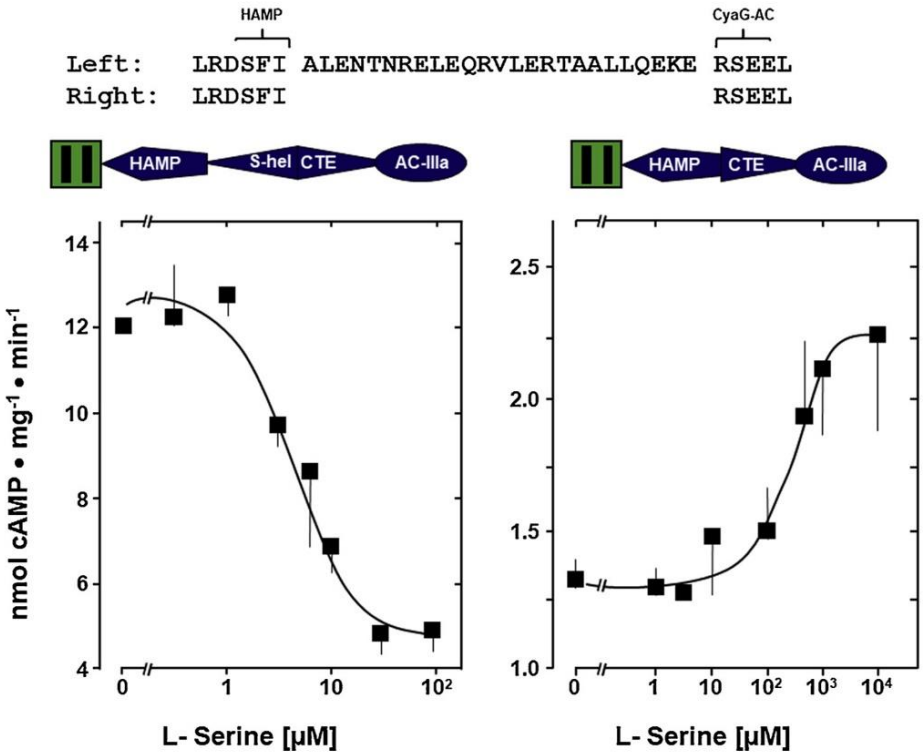

Fig. 3. Class IIIa AC CyaG from *A. platensis* is regulated by l-serine via the *E. coli* Tsr chemotaxis receptor. Left: Tsr linked to CyaG AC via HAMP and S-helix of CyaG AC is regulated by L-serine. Maximal inhibition was 58% (IC_{50} = 6 µM). Right: Removal of the 25 aa long S-helix in the chimera results in activation, i.e. the sign of the signal upon Tsr stimulation is inverted. Half-maximal activation is at 68 µM L-serine (EC_{50} = 305 µM). Top: Partial sequence of CyaG HAMP-S-helix. Error bars denote S.E.M., n = 4; figure was adapted from Winkler et al., 2012).

design, i.e. minimal-length α-helices and short connecting linkers, is known from the hexahelical QS-receptors of *Vibrio harveyi*, CqsS, and *Legionella pneumophila*, LqsS (Beltz et al., 2016). These QS-receptors are the extracellular sensing modules of canonical histidine-kinases which are active as dimers much like the class III ACs (here and in the following, CqsS is used to denote the membrane domain of the CqsS protein; Ng et al., 2012; Wei et al., 2012). For the QS-receptors, the natural ligands have been unequivocally identified. They are highly lipophilic aliphatic acyloins, i.e. ***Cholera* AutoInducer-1**, CAI-1 [(*S*)-3-hydroxytridecan-4-one] and ***Legionella* AutoInducer-1**, LAI-1 [(*S*)-3-hydroxypentadecan-4-one] (Ng et al., 2010; Spirig et al., 2008). In a somewhat daring experimental approach, we have tested whether these QS-receptors can replace the 6 T M anchor function in Rv1625c AC and possibly impose regulation by the ligands CAI-1 or LAI-1 (Beltz et al., 2016; Ziegler et al., 2017). We have generated a large number of chimeras from CqsS and the AC Rv1625c. At the QS-receptor side the optimal point of linkage is short of the canonical H-box which comprises the site of auto-phosphorylation of a critical histidine residue. For the Rv1625c AC a comparison with the above mentioned constructs between Tsr and the CyaG AC from *A. platensis* was useful (Fig. 1B, construct 4 and 5). It revealed a similar site in the Rv1625c AC that starts with the amino acids RSEALL (Winkler et al., 2012). This way, we have at last generated a chimeric class IIIa AC with a hexahelical membrane anchor/QS-receptor (Fig. 1B, construct 7) which is expressed in *E. coli* and specifically regulated, i.e. activity is stimulated by CAI-1 via of a hexahelical membrane receptor, CqsS, at nanomolar concentrations. With a point mutation at the QS-receptor membrane exit (F166 L) stimulation is enhanced up to 5-fold (Fig. 4, left) (Beltz et al., 2016). Stimulation is highly ligand specific as the chemically related LqsS ligand LAI-1 has diminished potency and the 3,4-dihydroxyderivative of CAI-1 is almost inactive (Fig. 4, left). CAI-1 also stimulates cAMP formation in vivo confirming a fully functional chimera (Beltz et al., 2016). Stimulation is irreversible probably because the lipophilic ligand binds into the membrane space of the receptor. An extended bioinformatic analysis shows that these QS-receptors may, in fact, be evolutionarily related to 6 T M anchors of ACs (Beltz et al., 2016).

In a related study using the QS-receptor LqsS from L. *pneumophila*, we have investigated in detail the points of connection between the QS-receptor and the Rv1625c AC (Fig. 1B, construct 9; Ziegler et al., 2017). The QS-receptor ligand LAI-1 significantly stimulates AC activity (Fig. 4 right). The analysis of the fusion points between the QS-receptor and the Rv1625c AC has led to the identification of a highly conserved, 19 aa long element between membrane anchor and catalytic domain which is absolutely required for functional coupling. This element is termed cyclase-transducing-element, abbreviated CTE. It is highly conserved in all class IIIa and IIIb ACs and in mammalian guanylate cyclases which

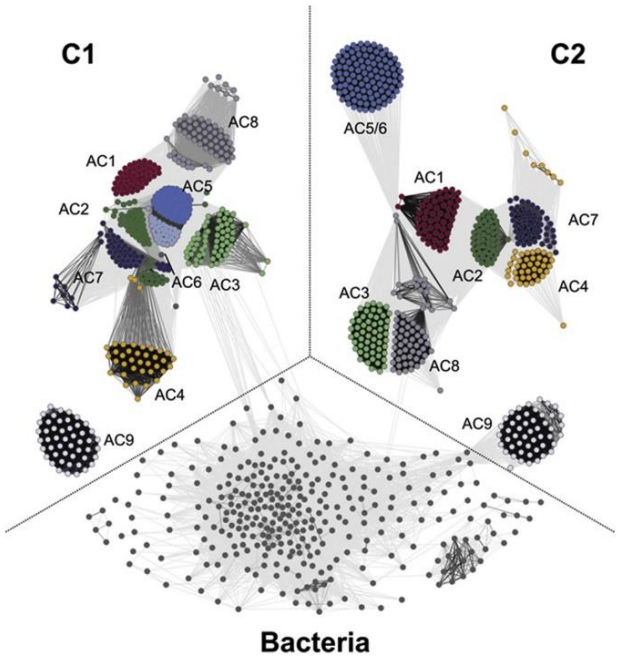

Fig. 5. Cluster map of cyclase-transducer-elements. The sequences of bacterial and vertebrate class IIIa and IIIb CTEs were analyzed using CLANS. Each dot represents a single sequence. Above threshold hits are shown as connecting lines. Darker line color indicates better pairwise blast hits. The three sectors are partitioned by broken lines. Cluster labeling indicates the AC isoform. The segregation shows that CTEs from vertebrate class IIIa ACs are highly specific for the C1- and C2-domain origins as well as for the peculiar AC isoforms. Bacterial sequences display no distinct clustering pattern. The data set comprises a total of 1265 AC sequences (figure from Ziegler et al., 2017).

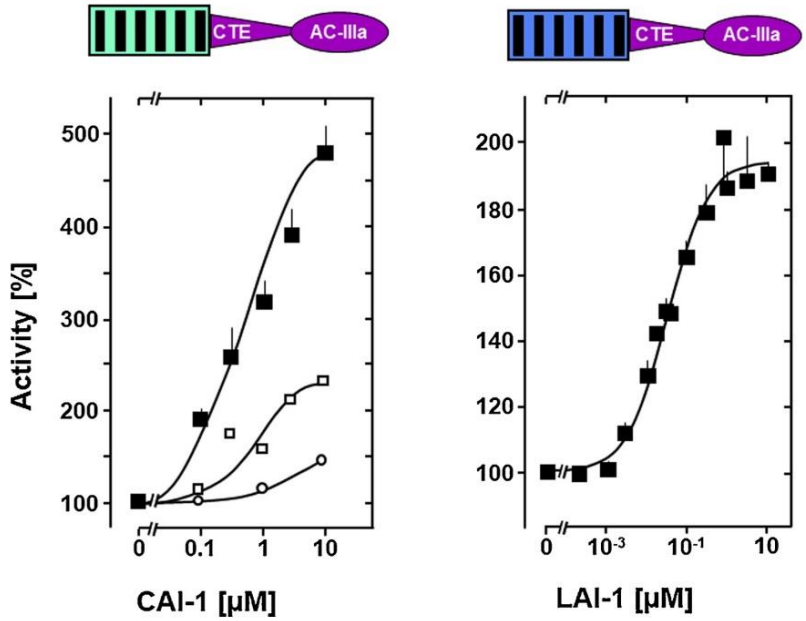

Fig. 4. Left: CqsS-Rv1625c stimulation by the QS-ligand CAI-1. Basal activity was 4 nmol cAMP·mg^{-1} min^{-1}. Filled squares, CAI-1 (n = 5–11; ± S.E.M.); open squares, LAI-1; open circles, 3,4-tridecanediol. The EC_{50} concentration for CAI-1 is 400 nM. CAI-1 stimulations were significant starting at 100 nM.
Right: LqsS-Rv1625c stimulation by the QS-ligand LAI-1. LAI-1 concentration-response curve for the LqsS construct connected to Rv1625c via Lys187. Basal activity is 20.7 nmol cAMP·mg^{-1} min^{-1}. Error bars denote S.E.M.'s. The figure was adapted from references (Beltz et al., 2016; Ziegler et al., 2017).

evolutionarily are related to the mammalian ACs (Bassler et al., 2018; Vercellino et al., 2017; Ziegler et al., 2017). These CTEs are located N-terminal with respect to the catalytic domains. They are present in all nine mammalian ACs. Recently, the structure of the cytosolic domain of the AC Cya from *Mycobacterium intracellulare* including its CTE was elucidated. Cya is 80% identical to that of Rv1625c (Vercellino et al., 2017). In the nine mammalian ACs CTEs are highly isoform specific and, in addition, specific for C1 and C2 catalytic domains as apparent from a cluster analysis (Fig. 5; Ziegler et al., 2017). In contrast, the CTEs of bacterial class IIIa and b ACs do not cluster in a respective bioinformatic analysis possibly indicating that each bacterial AC has its 'personalized' ligand and a thermodynamically optimized CTE (Fig. 5). Further experiments in which the S-helix has been placed either N-terminal or C-terminal of the CTE in an LqsS–Rv1625c chimera revealed how deeply CTEs are entrenched in signal transduction from a membrane receptor to an AC catalytic dimer. When ´N-terminal, S-helix and CTE combine into a single functional unit which inverses the sign of the signal, i.e. the QS-ligand LAI-1 inhibits cAMP formation. Positioned C-terminally of the CTE, the S-helix is without discernible function, i.e. lost its transducer function. AC activity is substantially reduced, albeit stimulation is retained (Ziegler et al., 2017). Taken together, the data can be discussed in a simple mechanistic model (Schultz and Natarajan, 2013). The two catalytic domains required for AC activity, either in homomeric bacterial or heteromeric mammalian ACs, must be conformationally free to associate into a productive dimer. Most likely, regulation by N-terminal receptors such as the chemotaxis receptors Tsr or Tar or the QS-receptors CqsS or LqsS affect the balance between constrained and unconstrained states of the catalytic domains and thus regulate activation or inhibition of ACs. In a conformationally unconstrained state, formation of a productive dimer is enabled whereas in a conformationally constrained state it is inhibited (Schultz and Natarajan, 2013). Summarizing all biochemical and bioinformatic data, one is tempted to suggest that this kind of receptor regulation is an intrinsic property of 6 T M class IIIa ACs, including the mammalian congeners. After tirelessly following many experimental trails we can reasonably conclude that the hexahelical membrane anchors of mammalian ACs in reality are orphan receptors.

4. Conclusion and outlook

In an analysis of various 6 T M domains, a small group of class IIIb ACs has been identified which obviously is an outlier and barely related to other AC membrane anchors (Beltz et al., 2016). The 6 T M domains of these ACs have a cytosolic ferredoxin in front of the catalytic domain (Fig. 1B, construct 9). Bioinformatic analysis of their membrane anchor has turned up a surprise: it is closely related to that present in fumarate reductases and succinate dehydrogenases, two proteins in the respiratory chain (Lancaster, 2002). A sequence comparison identified four fully conserved intramembranous histidine residues which axially coordinate two heme-B molecules (Wissig et al., 2019). Investigating the regulation of the CyaC AC from *Sinorhizobium meliloti*, we found that a) heme B is required for activity; b) all four histidine residues are required for heme B binding; c) AC activity is regulated via redox processes similar to those known in fumarate reductases. A somewhat unconventional interpretation of these findings would denote the heme-B molecules as membrane-integral ligands, faintly reminiscent on the membrane-integral cis-retinal in the G-protein-coupled receptor opsin that is rhodopsin. Although the conjecture might appear somewhat premature and far-fetched, CyaC AC from *S. meliloti* is the first hexahelical membrane domain of a class IIIb AC in which a clear regulatory function has been identified and characterized (Wissig et al., 2019).

Extending the above findings to mammalian ACs we have recently replaced the two dissimilar membrane anchors in the human AC2 by two necessarily identical CqsS receptors from *V. harveyi* (Fig. 1B, construct 10). In such a construct, human AC2 activity is regulated by the ligand CAI-1 and Gsα proteins which in mammalian cells are intracellularly released upon extracellular stimulation of G-protein-coupled receptors (GPCRs). The data strongly suggest that the catalytic dimers of mammalian ACs have retained the capacity to receive and translate extracellular signals from their own membrane receptor (unpublished data). The identification of ligands specific for any pro- or eukaryotic AC membrane domains/receptor remains a pressing problem and major challenge for our future work.

Acknowledgments

We thank Ursula Kurz and Anita Schultz for essential assistance throughout this work. We gratefully acknowledge most fruitful discussions with J. Bassler and A.N. Lupas, Max Planck Institute for Developmental Biology. Work in the author's laboratory was supported by the SFB 766 and institutional funds from the Max-Planck-Society.

References

Anantharaman, V., Balaji, S., Aravind, L., 2006. The signalling helix: a common functional theme in diverse signalling proteins. Bio Direct 25 (1795-), 1804.
Aravind, L., Ponting, C.P., 1999. The cytoplasmic helical linker domain of receptor histidine kinase and methyl-accepting proteins is common to many prokaryotic signalling proteins. FEMS Microbiol. Lett. 176, 111–116.
Barzu, O., Danchin, A., 1994. Adenylyl cyclases: a heterogeneous class of ATP-utilizing enzymes. Prog. Nucleic Acid Res. Mol. Biol. 49, 241–283.
Bassler, J., Schultz, J.E., Lupas, A.N., 2018. Adenylate cyclases: Receivers, transducers, and generators of signals. Cell Signal. 46, 135–144.
Beltz, S., Bassler, J., Schultz, J.E., 2016. Regulation by the quorum sensor from Vibrio indicates a receptor function for the membrane anchors of adenylate cyclases. eLife 5.
Cole, S.T., Brosch, R., Parkhill, J., Garnier, T., Churcher, C., Harris, D., Gordon, S.V., Eiglmeier, K., Gas, S., Barry 3rd, C.E., Tekaia, F., Badcock, K., Basham, D., Brown, D., Chillingworth, T., Connor, R., Davies, R., Devlin, K., Feltwell, T., Gentles, S., Hamlin, N., Holroyd, S., Hornsby, T., Jagels, K., Krogh, A., McLean, J., Moule, S., Murphy, L., Oliver, K., Osborne, J., Quail, M.A., Rajandream, M.A., Rogers, J., Rutter, S., Seeger, K., Skelton, J., Squares, R., Squares, S., Sulston, J.E., Taylor, K., Whitehead, S., Barrell, B.G., 1998. Deciphering the biology of Mycobacterium tuberculosis from the complete genome sequence. Nature 393, 537–544.
Dessauer, C.W., Watts, V.J., Ostrom, R.S., Conti, M., Dove, S., Seifert, R., 2017. International union of basic and clinical pharmacology. ci. structures and small molecule modulators of mammalian adenylyl cyclases. Pharmacol. Rev. 69, 93–139.
Ferris, H.U., Dunin-Horkawicz, S., Mondejar, L.G., Hulko, M., Hantke, K., Martin, J., Schultz, J.E., Zeth, K., Lupas, A.N., Coles, M., 2011. The mechanisms of HAMP-mediated signaling in transmembrane receptors. Structure 19, 378–385.
Ferris, H.U., Zeth, K., Hulko, M., Dunin-Horkawicz, S., Lupas, A.N., 2014. Axial helix rotation as a mechanism for signal regulation inferred from the crystallographic analysis of the E. Coli serine chemoreceptor. J. Struct. Biol.
Guo, Y.L., Seebacher, T., Kurz, U., Linder, J.U., Schultz, J.E., 2001. Adenylyl cyclase Rv1625c of Mycobacterium tuberculosis: a progenitor of mammalian adenylyl cyclases. EMBO J. 20, 3667–3675.
Hazelbauer, G.L., Falke, J.J., Parkinson, J.S., 2008. Bacterial chemoreceptors: high-performance signaling in networked arrays. Trends Biochem. Sci. 33, 9–19.
Hulko, M., Berndt, F., Gruber, M., Linder, J.U., Truffault, V., Schultz, A., Martin, J., Schultz, J.E., Lupas, A.N., Coles, M., 2006. The HAMP domain structure implies helix rotation in transmembrane signaling. Cell 126, 929–940.
Kanchan, K., Linder, J.U., Winkler, K., Hantke, K., Schultz, A., Schultz, J.E., 2010. Transmembrane signaling in chimeras of the Escherichia coli aspartate and serine chemotaxis receptors and bacterial class III adenylyl cyclases. J. Biol. Chem. 285, 2090–2099.
Krupinski, J., Coussen, F., Bakalyar, H.A., Tang, W.J., Feinstein, P.G., Orth, K., Slaughter, C., Reed, R.R., Gilman, A.G., 1989. Adenylyl cyclase amino acid sequence: possible channel- or transporter-like structure. Science 244, 1558–1564.
Lancaster, C.R., 2002. Succinate:quinone oxidoreductases: an overview. Biochim. Biophys. Acta 1553, 1–6.
Linder, J.U., Schultz, J.E., 2003. The class III adenylyl cyclases: multi-purpose signalling modules. Cell. Signal. 15, 1081–1089.
Linder, J.U., Schultz, J.E., 2008. Versatility of signal transduction encoded in dimeric adenylyl cyclases. Curr. Opin. Struct. Biol. 18, 667–672.
Ng, W.L., Wei, Y., Perez, L.J., Cong, J., Long, T., Koch, M., Semmelhack, M.F., Wingreen, N.S., Bassler, B.L., 2010. Probing bacterial transmembrane histidine kinase receptor-ligand interactions with natural and synthetic molecules. Proc. Natl. Acad. Sci. U.S.A. 107, 5575–5580.
Ng, W.L., Perez, L.J., Wei, Y., Kraml, C., Semmelhack, M.F., Bassler, B.L., 2011. Signal production and detection specificity in Vibrio CqsA/CqsS quorum-sensing systems. Mol. Microbiol. 79, 1407–1417.
Ng, W.L., Perez, L., Cong, J., Semmelhack, M.F., Bassler, B.L., 2012. Broad spectrum pro-quorum-sensing molecules as inhibitors of virulence in vibrios. PLoS Pathog. 8, e1002767.
Parkinson, J.S., 2010. Signaling mechanisms of HAMP domains in chemoreceptors and sensor kinases. Annu. Rev. Microbiol. 64, 101–122.
Schultz, J.E., Natarajan, J., 2013. Regulated unfolding: a basic principle of intraprotein

signaling in modular proteins. Trends Biochem. Sci. 38, 538–545.
Schultz, J.E., Klumpp, S., Benz, R., Schurhoff-Goeters, W.J., Schmid, A., 1992. Regulation of adenylyl cyclase from Paramecium by an intrinsic potassium conductance. Science 255, 600–603.
Schultz, J.E., Kanchan, K., Ziegler, M., 2015. Intraprotein signal transduction by HAMP domains: a balancing act. Int. J. Med. Microbiol. 305, 243–251.
Sinha, S.C., Wetterer, M., Sprang, S.R., Schultz, J.E., Linder, J.U., 2005. Origin of asymmetry in adenylyl cyclases: structures of Mycobacterium tuberculosis Rv1900c. EMBO J. 24, 663–673.
Spirig, T., Tiaden, A., Kiefer, P., Buchrieser, C., Vorholt, J.A., Hilbi, H., 2008. The Legionella autoinducer synthase LqsA produces an alpha-hydroxyketone signaling molecule. J. Biol. Chem. 283, 18113–18123.
Steegborn, C., Litvin, T.N., Levin, L.R., Buck, J., Wu, H., 2005. Bicarbonate activation of adenylyl cyclase via promotion of catalytic active site closure and metal recruitment. Nat. Struct. Mol. Biol. 12, 32–37.
Sutherland, E.W., Rall, T.W., 1958. Fractionation and characterization of a cyclic adenine ribonucleotide formed by tissue particles. J. Biol. Chem. 232, 1077–1091.
Tesmer, J.J., Sunahara, R.K., Gilman, A.G., Sprang, S.R., 1997. Crystal structure of the catalytic domains of adenylyl cyclase in a complex with Gsalpha.GTPgammaS. Science 278, 1907–1916.
Tews, Findeisen, F., Sinning, I., Schultz, A., Schultz, J.E., Linder, J.U., 2005. The structure of a pH-sensing mycobacterial adenylyl cyclase holoenzyme. Science 308, 1020–1023.
Ulrich, L.E., Koonin, E.V., Zhulin, I.B., 2005. One-component systems dominate signal transduction in prokaryotes. Trends Microbiol. 13, 52–56.
Ulrich, L.E., Zhulin, I.B., 2010. The MiST2 database: a comprehensive genomics resource on microbial signal transduction. Nucleic Acids Res. 38, D401–407.
Vercellino, I., Rezabkova, L., Olieric, V., Polyhach, Y., Weinert, T., Kammerer, R.A., Jeschke, G., Korkhov, V.M., 2017. Role of the nucleotidyl cyclase helical domain in catalytically active dimer formation. Proc. Natl. Acad. Sci. U. S. A. 114, E9821–E9828.
Weber, J.H., Vishnyakov, A., Hambach, K., Schultz, A., Schultz, J.E., Linder, J.U., 2004. Adenylyl cyclases from Plasmodium, Paramecium and Tetrahymena are novel ion channel/enzyme fusion proteins. Cell. Signal. 16, 115–125.
Wei, Y., Ng, W.L., Cong, J., Bassler, B.L., 2012. Ligand and antagonist driven regulation of the Vibrio cholerae quorum-sensing receptor CqsS. Mol. Microbiol. 83, 1095–1108.
Winkler, K., Schultz, A., Schultz, J.E., 2012. The S-helix determines the signal in a Tsr receptor/adenylyl cyclase reporter. J. Biol. Chem. 287, 15479–15488.
Wissig, J., Grischin, J., Bassler, J., Schubert, C., Schultz, J.E., Unden, G., 2019. CyaC, a redox-regulated adenylate cyclase of Sinorhizobium meliloti with a fumarate reductase-like diheme-B membrane anchor. Mol. Microbiol in revision.
Ziegler, M., Bassler, J., Beltz, S., Schultz, A., Lupas, A.N., Schultz, J.E., 2017. A novel signal transducer element intrinsic to class IIIa and IIIb adenylate cyclases. eLife 6, 1–5.

8. Ergebnisse und Diskussion

In diesem Abschnitt werden weitere Daten zusammengefasst, die nicht essenziell für die in den Publikationen gestellten Fragen waren und daher dort keinen Eingang gefunden haben.
Die Klonierung, Transfektion und Herstellung des isolierten Proteins erfolgte durch J. Wissig. Es galt $CyaC_{Sm}$ unter geeigneten Bedingungen zu exprimieren, Membranpräparationen herzustellen und anschließend deren Aktivität insbesondere in Anwesenheit von RedOx-Reagenzien zu testen. Des Weiteren wurde die membrangebundene hAC5 der Klasse IIIa in HEK und Sf9-Zellen exprimiert (Sf9-Expression erfolgte durch M. Finkbeiner), Membranpräparationen gewonnen und deren Aktivität in Anwesenheit mutmaßlicher Liganden (ausgewählte Hormone und Neurotransmitter, Glucose und andere Zucker) getestet. Für die Regulierung durch hitzeinaktiviertes Humanserum wurde je eine AC aus jeder der vier Untergruppen ausgewählt: hAC2, hAC3, hAC5 und hAC9.

8.1. Regulierung der bakteriellen AC $CyaC_{Sm}$ durch RedOx-Reagenzien

Der Einfluss von Reduktions- und Oxidationsmitteln auf die enzymatische Aktivität der AC $CyaC_{Sm}$ wurde *in vitro* getestet. Zusätzlich wurde die Aktivität der fünf Histidinmutanten H27A, H31A, H68A, H105A und H149A mit der Aktivität des Wildtyps $CyaC_{Sm}$ verglichen. Dafür wurden Membranpräparationen aus dem $CyaC_{Sm}$ enthaltenden *E. coli* Stamm BTH101 (Δ*cyaA*) in LB-Medium hergestellt.

8.1.1 Aktivität aufgereinigter $CyaC_{Sm}$

Durch die Verankerung in der Membran ergibt sich nicht nur eine vorbestimmte Position des Enzyms innerhalb der Zellstruktur, die Transmembrandomäne hat auch einen Einfluss auf die Proteinstruktur und somit auf die Position der katalytischen Domänen zueinander. Liegt das Protein ohne Membran vor, kann sich auch die Aktivität des Enzyms ändern. Daher wurde das Holoenzym von J. Wissig im pET28a Vektor mit N-terminalem His-Tag und C-terminalen Flag- und Strep-Tags in *E. coli* C43 aerob überexprimiert, mit 1% Dodecylmaltosid als Detergens löslich gemacht und über eine Strep-Tactin-Säule aufgereinigt, wobei dem Elutionspuffer entweder kein Reduktionsmittel oder 1 mM DTT zugesetzt wurden (62). Diese Proben wurden auf ihre Aktivität getestet.

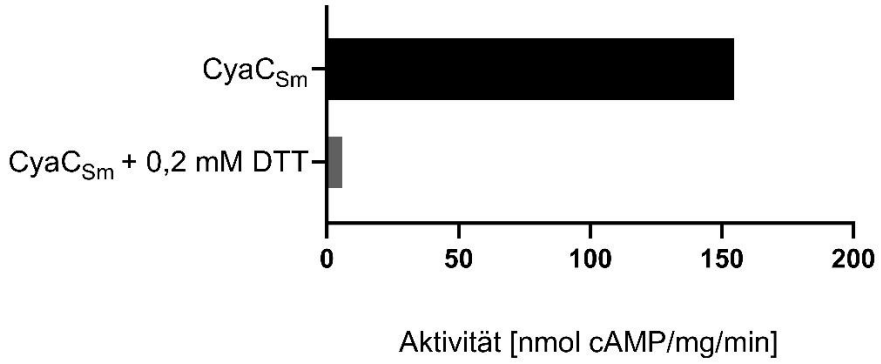

Abb. 8.1 *Aktivität der aufgereinigten $CyaC_{Sm}$ (inkl. Membrandomänen) ohne RedOx-Reagenzien (schwarzer Balken, Elutionspuffer ohne Reduktionsmittel) und in Anwesenheit von 0,2 mM DTT (grauer Balken, Elutionspuffer mit 1 mM DTT). 2 Einzelversuche aus einer Expression.*

Trotz fehlender Verankerung in der Membran bewirkt die Reduktion des Holoenzyms durch DTT eine drastische Minderung der AC-Aktivität.

8.1.2 Lagerung von $CyaC_{Sm}$ bei -80°C

Die Stabilität der meisten Proteine ist abhängig von dem sie umgebenden Medium. Änderungen der Salzkonzentration, des pH-Wertes oder der Temperatur können zur Denaturierung und zu einem erheblichen Aktivitätsverlust führen. Um Enzyme über einen längeren Zeitraum zu lagern, sollte daher nicht nur ein geeigneter Puffer, sondern auch die richtige Lagertemperatur gewählt werden. Eine kurzfristige Lagerung (< 24 h) ist meist bei 4°C möglich, wobei einige Proteine bis zu 7 Tage unter Ausschluss bakteriellen Wachstums durch Sterilfiltration oder Zugabe bakteriostatischer Wirkstoffe gelagert werden können. Für die Lagerung über einige Monate hinweg können die Proben bei -20°C unter Zugabe von 50% Glycerol zur Vermeidung von Kristallbildung gelagert werden. Friert man die Proben bei -80°C im Tiefkühlschrank oder bei -196°C in flüssigem Stickstoff ein, sind diese oft für Jahre stabil.
Auch starke Temperaturschwankungen können zur kompletten oder teilweisen Zerstörung von Proteinen führen. Es sollte daher sichergestellt werden, dass wiederholte Gefrier-Tau-Zyklen (Abb. 8.2) und die Kristallbildung bei -80°C keine oder nur geringe Auswirkungen auf die Aktivität von $CyaC_{Sm}$ haben (Abb. 8.3).

Membranpräparationen, die bei der Herstellung keinem, einem oder zwei Gefrier-Tau-Zyklen ausgesetzt waren, wurden auf Aktivitätsänderung der Cyclase untersucht. Gemessen wurde die Aktivität des Wildtyps $CyaC_{Sm}$ und dessen Histidinmutanten H27A, H31A, H68A, H105A und H149A.

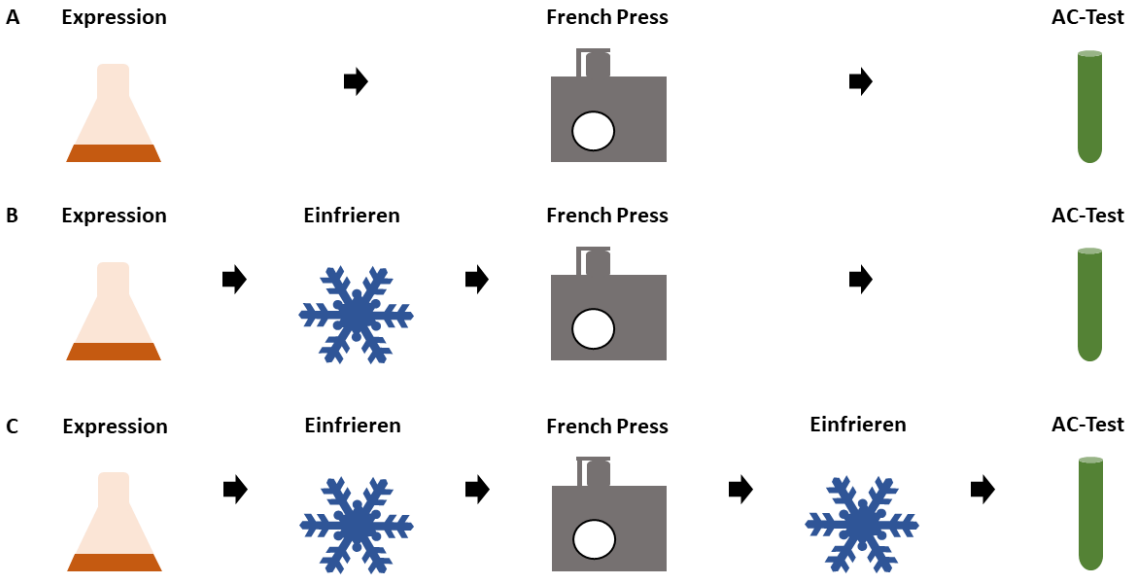

Abb. 8.2 *Unterschiedliche Behandlung der Membranpräparation mit $CyaC_{Sm}$ und deren fünf Histidinmutanten. A: Es erfolgte kein Einfrieren der Probe. B: Die exprimierten Zellen wurden vor dem Aufschluss mittels French Press bei -80°C gelagert. C: Es erfolgten zwei Gefrier-Tau-Zyklen: Jeweils einer zur Lagerung der Bakterienzellen vor dem Zellaufschluss mittels French Press und einer zur Lagerung der Membranpräparation vor dem AC-Test*.

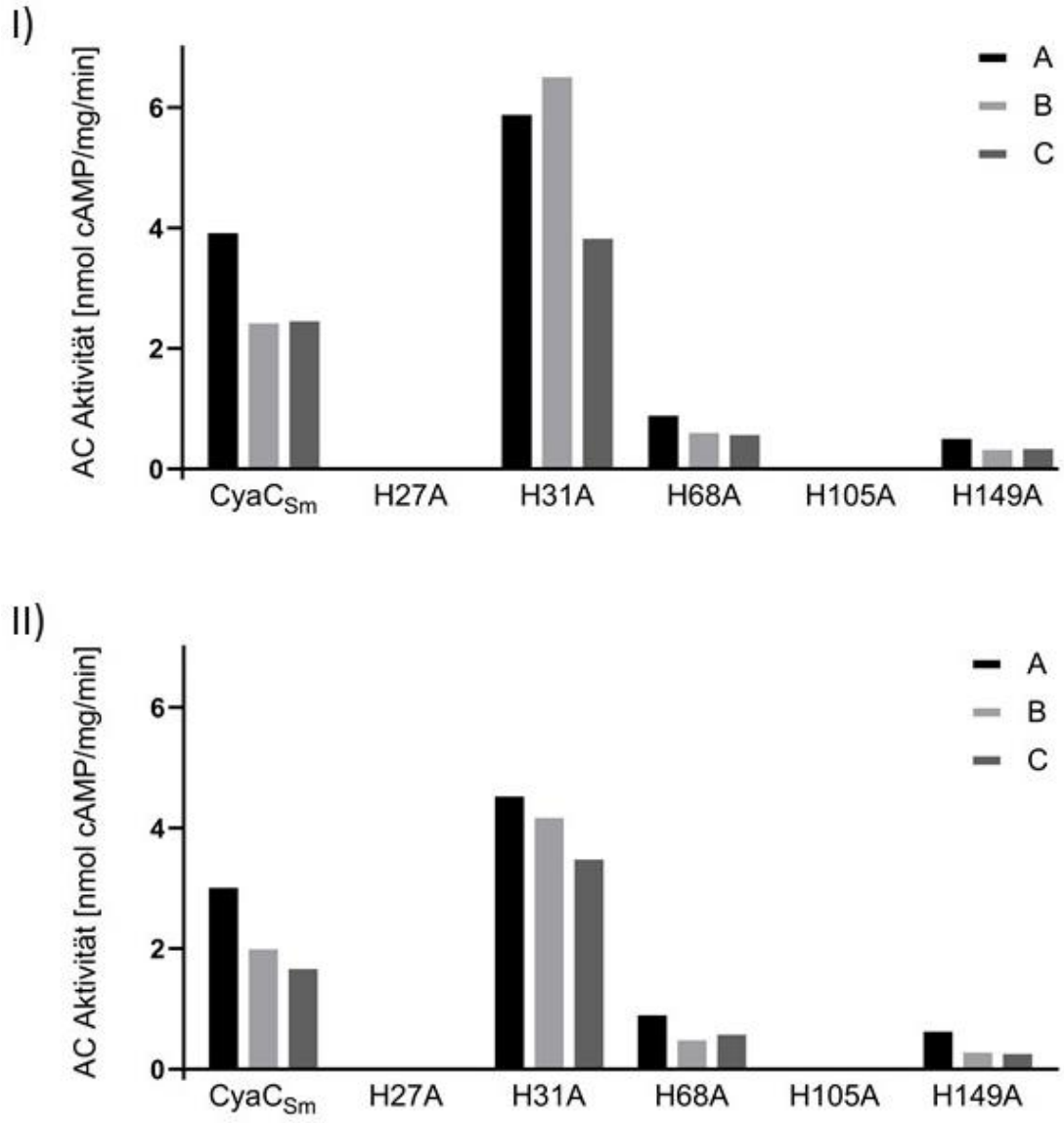

Abb. 8.3 *AC-Aktivität von Membranpräparationen von CyaC$_{Sm}$ Wildtyp und der fünf Histidinmutanten unter verschiedenen Lagerbedingungen (Einzelversuch). A: Expression, Zellaufschluss und Membranpräparation erfolgte ohne Zwischenlagerung. B: Nach der Expression wurden die Zellen bei -80°C gelagert. C: Bei -80°C gelagerte unaufgeschlossene Zellen und Membranpräparation. I) Aktivität ohne Zugabe von RedOx-Reagenzien. II) Aktivität nach Zugabe von 1 mM DTT.*

8.1.3 Stimulierung von $CyaC_{Sm}$ durch Q_0

Ubichinone sind lipophile physiologische Elektronen- und Protonenüberträger der Atmungskette. Dies erreichen sie, indem sie mit dem Membrananker der SQORs, genauer gesagt mit einem der durch vier konservierte Histidinreste gebundenen Häm-B-Moleküle, in Kontakt kommen. Da auch $CyaC_{Sm}$ über ein ähnlich gebundenes Häm-B-Molekül verfügt, lag die Vermutung für eine Regulierung durch Q_0 nahe (Abb. 8.4).

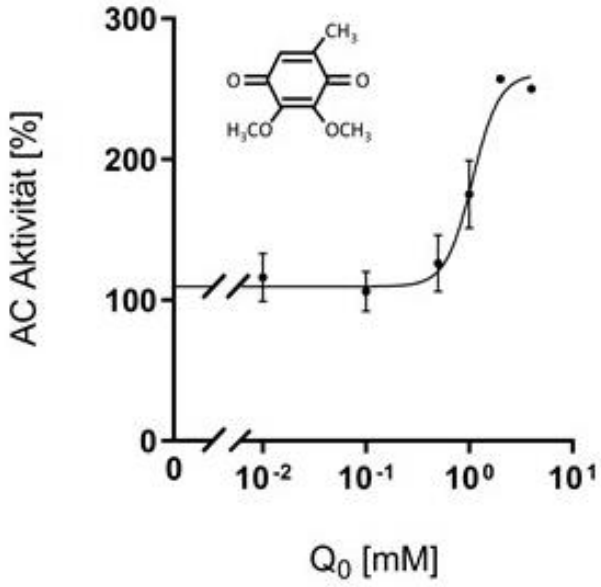

Abb. 8.4 *Q_0-Konzentrations-Wirkungskurve (3 µM – 4 mM) mit $CyaC_{Sm}$ und Q_0-Strukturformel. Für einen reduzierten Ausgangszustand enthalten alle Membranpräparationen 1 mM DTT. 100% entspricht einer Aktivität von 1,14 nmol cAMP/mg/min. Fehlerbalken kennzeichnen SEM aus 3-6 separaten Expressionen.*

8.2 Ligandensuche für die humane AC5

Es wurde der Effekt ausgesuchter Hormone und Neurotransmitter auf die hAC5 untersucht. Hierfür wurden zunächst unterschiedliche Bedingungen zur Expression der AC Isoform ausprobiert. Die Expression erfolgte zu Beginn in HEK293-Zellen, bevor Sf9-Zellen als weitaus geeigneter eingestuft wurden, da diese auch ohne Serumzugabe gezüchtet werden können.

8.2.1 Ideale Reaktionsbedingungen für den AC-Test

Für die Umwandlung von ATP zu cAMP brauchen ACn als Substrat ATP, bivalente Kationen wie Mg^{2+} oder Mn^{2+} und die richtige Reaktionstemperatur. Die Reaktionsbedingungen für die hAC5 wurden optimiert, um eine möglichst hohe Enzymaktivität zu erreichen. Getestet wurden zwei Reaktionstemperaturen (30°C und 37°C), zwei ATP-Konzentrationen (250 µM und 450 µM) und Mg^{2+} (5 mM) bzw. Mn^{2+} (2 mM) als Kationen (Abb. 8.5).

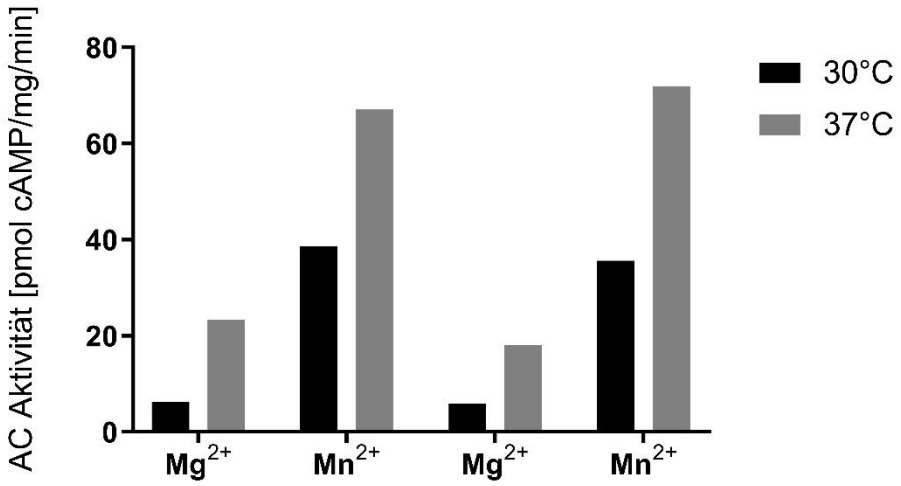

Abb. 8.5 *Optimierung der Enzymaktivität. Getestet wurde die Basalaktivität der Membranpräparation mit hAC5 bei zwei ATP-Konzentrationen (250 µM und 450 µM), bei zwei verschiedenen Temperaturen (30°C und 37°C) und unter Zugabe von Mg^{2+} (5 mM) bzw. Mn^{2+} (2 mM) als bivalente Kationen (Einzelversuch).*

8.2.2 Regulierung der hAC5 durch $G_s\alpha$, Forskolin und Ca^{2+}

Humane ACn werden über GPCRs und das pflanzliche Diterpen FSK reguliert. Beide binden an der katalytischen Domäne und stabilisieren den aktiven Zustand der Cyclase. Um zu gewährleisten, dass die in HEK293-Zellen exprimierte hAC5 ordnungsgemäß funktioniert, wurde deren Aktivierung durch $G_s\alpha$ und FSK überprüft (Abb. 8.6). Zusätzlich wird die hAC5 durch Ca^{2+}-Ionen gehemmt, was auch bei der hier exprimierten hAC5 in der Ca^{2+}-Konzentrations-Kurve der Fall ist (Abb. 8.8).
HEK293-Zellen besitzen zusätzlich zur transformierten hAC5 weitere hACn. Zur Kontrolle wurden parallel nicht-transformierte Zellen getestet (Abb. 8.7).

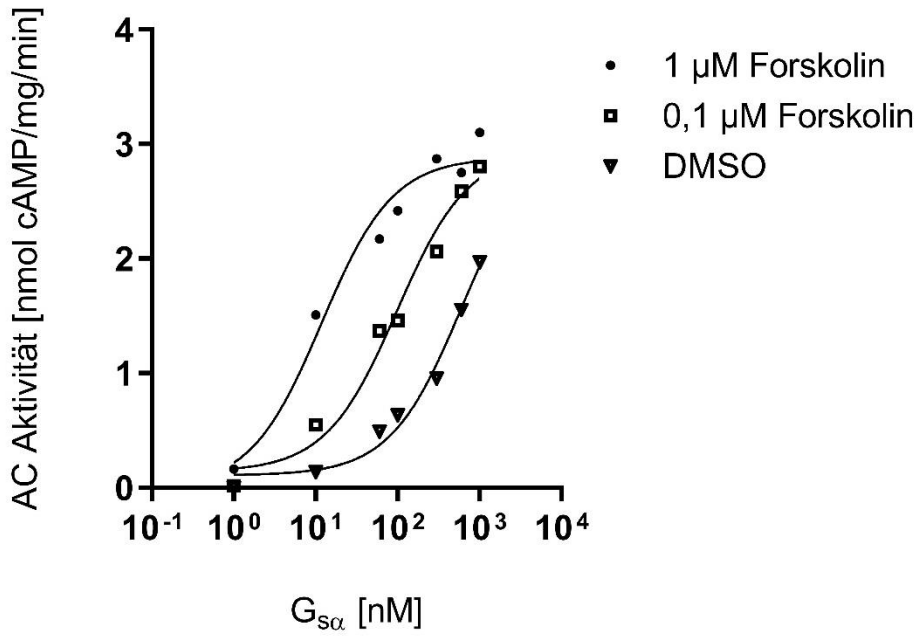

Abb. 8.6 *$G_s\alpha$-Konzentrations-Wirkungskurve (1 nM – 1000 nM) mit hAC5 nach Zugabe von ● 1 µM, □ 0,1 µM Forskolin und ▼ DMSO als Kontrolle (Einzelversuch). Proteinmenge pro Probe 25 µg. Die Membranpräparation stammt aus HEK293-Zellen.*

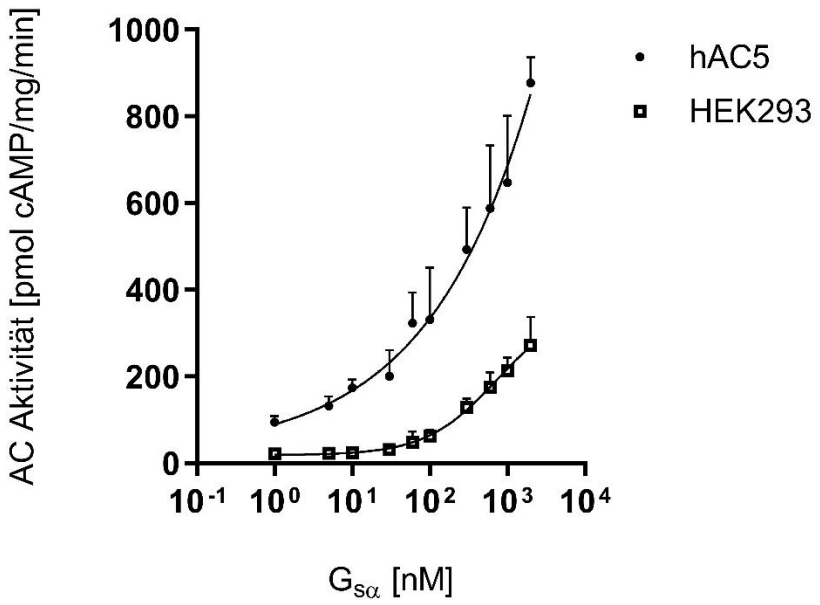

Abb. 8.7 *$G_s\alpha$-Konzentrations-Wirkungskurve (1 nM – 2000 nM) mit ● hAC5 aus transformierten HEK293-Zellen. Als Vergleich □ nicht-transformierte HEK293-Zellen. Proteinmenge pro Probe 25 µg. Die Membranpräparation stammt aus einer Expression. Fehlerbalken kennzeichnen SD aus 3 Einzelversuchen derselben Expression.*

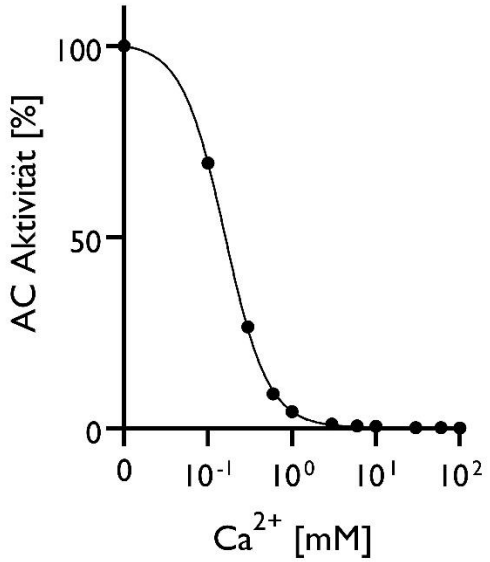

Abb. 8.8 *Ca^{2+}-Konzentrations-Wirkungskurve (0,01 – 100 mM) mit hAC5 aus transformierten HEK293-Zellen (Einzelversuch). Proteinmenge pro Probe 25 µg. 100% entspricht einer Aktivität von 12,29 nmol cAMP/mg/min (Einzelversuch).*

8.2.3 Hormone und Neurotransmitter als mögliche Liganden

Das endokrine System zeichnet sich dadurch aus, dass die Zellkommunikation auch über weite Entfernung mittels chemischer Informationsträger erfolgt. Hierfür werden Hormone und Neurotransmitter in endokrinen Drüsen synthetisiert und entweder in das Blutsystem (endokrin und neuroendokrin) oder in die Umgebung (parakrin und autokrin) sezerniert. Gerade durch die weitreichende Verteilung der Botenstoffe ist eine organübergreifende Regulierung im Organismus möglich.
Je nach Löslichkeit liegen die Signalstoffe entweder im Plasma gelöst vor oder sind an Transportproteine gebunden. Transcortin befördert lipophile Glucocorticoide (63). Triiodthyronin (T3) und Thyroxin (T4) liegen nur zu 0,5% bzw. 0,05% frei im Serum vor, während der Großteil an das Thyroxin-bindende-Globulin (60%), Thyroxin-bindende-Präalbumin (30%) und Albumin (10%) gebunden ist (64). Auch Sexualhormone wie Estradiol (65) und Testosteron (66,67) werden hauptsächlich durch das Sexualhormon-bindende Globulin (SHBG) gebunden und gelangen so an ihren Wirkort (68,69). Allein für Estrogen ergibt sich damit ein Verhältnis von 1 zu 49 von freiem zu gebundenem Hormon (70).
In der klinischen Praxis wird der Referenzbereich als Gesamtkonzentration der freien und gebundenen Hormone angegeben (Tab. 8.1).
Darüber hinaus gibt es vereinzelte Beobachtungen, dass Hormone gerade durch Bindung an Transportproteine ihre Wirkung entfalten. In einigen Zelltypen bindet SHBG im freien Zustand an den bisher nicht klonierten Rezeptor R_{SHBG} und erhöht bei Zugabe von Steroidhormonen als Agonisten die cAMP-Produktion innerhalb der Zelle (69). Auch die Aufnahme von Androgenen und Estrogenen in die Zelle soll u.a. durch den endozytotischen Rezeptor speziell nach deren Bindung an SHBG erfolgen (71).
In dieser Arbeit orientierte sich die eingesetzte Konzentration möglicher Liganden daher an den nachfolgend aufgelisteten Hormongesamtkonzentrationen im Plasma.
Während die Sekretion von Cortisol einem 24-h-Takt folgt, werden unter anderem Insulin, Noradrenalin und Aldosteron akut nur nach Bedarf ausgeschüttet. Der messbare durchschnittliche Konzentrationsbereich im Plasma ist daher meist

sehr niedrig. Gerade Neurotransmitter, deren Konzentrationen im synaptischen Spalt nur schwer messbar sind, dienen der schnellen Informationsübertragung und erreichen wohl weit höhere lokal begrenzte Konzentrationen als die im Plasma gemessenen. Für diese Stoffe wurde in den Tests eine einheitlich hohe, die Plasmakonzentration stark übersteigende Konzentration von 1 mM eingesetzt.

Tab. 8.1 *Auflistung physiologischer Konzentrationen der getesteten Substanzen.*

Hormon	*Physiologischer Konzentrationsbereich*	
Aldosteron	27,7 – 582,5 pM	(72)
Corticosteron	1,53 – 45,08 nM	(72)
Cortisol	3,6 – 689,7 nM	(72)
C-Peptid	0,30 – 1,42 nM	(72)
Deoxycorticosteron	< 0,3 nM	(72)
DHEA-S	0,41 – 12,38 µM	(72)
Dopamin	< 0,39 nM	(73)
Epinephrin	< 0,164 nM (in Ruhe)	(74)
Estradiol	36,7 – 1284,8 pM	(72)
Estron	25,9 – 739,6 pM	(72)
GABA	≈ 0,900 pM	(75)
Glucagon	0,05 – 0,1 pM	(76)
Glutamat	50 – 100 µM	(77)
Histamin	2,7 – 17,99 nM	(78)
Insulin	9,7 – 97,2 pM	(72)
Levodopa	19,3 ± 6,1 nM	(79)
L-Homocystein	< 13 µM	(72)
Pregnenolonsulfat	133,7 ± 65,6 nM	(80)
Progesteron	1,55 – 8,64 nM	(72)
Serotonin	6,8 ± 2,2 nM	(81)
T3 (frei)	3,53 – 6,45 pM	(72)
T3 (gesamt)	1,08 – 3,08 nM	(72)
T4 (frei)	10,30 – 23,17 pM	(72)
T4 (gesamt)	94,02 – 213,68 nM	(72)

Zunächst wurden drei Konzentrationen ausgesuchter Hormone unter Zusatz von 1000 nM $G_s\alpha$ getestet. Tabellarisch aufgeführt ist nur die zehnfache physiologische Konzentration.

Tab. 8.2 *Aktivität der hAC5 aus HEK293 nach Zusatz der getesteten Hormone und 1000 nM $G_s\alpha$. Die Konzentration der Hormone beträgt das Zehnfache des physiologischen Wertes (Einzelversuch).*

Probe	*Aktivität [nmol cAMP/mg/min]*	*Aktivität [%]*
Basalaktivität	**0,08**	**17**
1000 nM $G_s\alpha$	**0,47**	**100**
Aldosteron (5 nM)	0,56	119
Cortisol (5 µM)	0,69	147
Estradiol (10 nM)	0,55	117
Insulin (1 nM)	0,73	155
Progesteron (200 nM)	0,51	109
T3 (3 nM)	0,53	113
Testosteron (10 nM)	0,54	115

Die Hormone zeigen selbst in der hohen Konzentration keine deutliche hemmende oder aktivierende Wirkung. Die Vermutung liegt nahe, dass das fetale Kälberserum (FBS) in der HEK293-Zellkultur die getesteten Hormone enthält und diese unter Umständen noch in der Membranpräparation verbleiben.
Bei der nächsten Expression wurde 24 h vor der Ernte das Kulturmedium gegen FBS-freies Medium ausgetauscht, um die Hormone zu entfernen.

Aufgrund der Vermutung, dass die getesteten Substanzen nur langsam in die lipophile Membran diffundieren, wurden diese mit den Membranen in einem weiteren Versuch zuvor für 30 min auf Eis inkubiert und anschließend getestet.

Tab. 8.3 *Aktivität der hAC5 aus HEK293 nach Zusatz der getesteten Hormone und 1000 nM $G_s\alpha$ (Ohne Inkubation links) und mit 600 nM $G_s\alpha$ (30 min Inkubation auf Eis rechts). Die Hormone und Transmitter wurden in der höchsten physiologischen Konzentration eingesetzt (Einzelversuch).*

	Ohne Inkubation auf Eis		*30 min Inkubation auf Eis*	
Probe	Aktivität [nmol cAMP/mg/min]	Aktivität [%]	Aktivität [nmol cAMP/mg/min]	Aktivität [%]
Basalaktivität	**0,00**	**0**	**-**	**-**
1000 nM bzw 600 nM $G_s\alpha$ + 1 µl DMSO	**2,04**	**100**	**0,86**	**100**
Aldosteron (500 pM)	2,13	104	0,94	109
Corticosteron (50 nM)	2,16	106	0,90	105
Cortisol (500 nM)	-	-	1,07	124
Deoxycorticosteron (700 pM)	1,49	73	1,09	127
DHEA-S (20 µM)	1,82	89	1,06	123
Estradiol (1 nM)	-	-	0,90	105
Estron (1 nM)	1,81	89	0,69	80
2Insulin (100 pM)	1,92	94	1,12	130
L-Homocystein (50 µM)	1,71	84	0,99	115
Pregnenolonsulfat (15 nM)	-	-	1,06	123
Progesteron (100 nM)	1,52	75	0,99	115
T3 (5 nM)	1,69	83	0,90	105
T4 (300 pM)	1,87	92	0,65	76
Testosteron (20 nM)	1,55	76	1,07	124

Die getesteten Substanzen zeigen keinen Effekt. Um sicherzugehen, dass nach 24 h ohne FBS im Kulturmedium die Membran keine möglichen Liganden mehr

daraus enthält, wurde die Membranpräparation vor dem nächsten AC-Test 10 min bei 30°C im Resuspensionspuffer mit 30% Glycerol inkubiert, abzentrifugiert und wie gewohnt im Resuspensionspuffer aufgenommen.

Tab. 8.4 *Aktivität der hAC5 aus HEK293 nach Zusatz der getesteten Hormone und 300 nM $G_s\alpha$. Die Hormone und Transmitter wurden in der höchsten physiologischen Konzentration eingesetzt (Einzelversuch).*

	Ohne Waschen		*Waschen durch Inkubation mit Glycerol*	
Probe	Aktivität [nmol cAMP/mg/ min]	Aktivität [%]	Aktivität [nmol cAMP/mg/ min]	Aktivität [%]
Basalaktivität	**0,00**	**0**	**0,01**	**2**
300 nM $G_s\alpha$ + 1 µl DMSO	**0,45**	**100**	**0,45**	**100**
Aldosteron (500 pM)	0,46	102	0,41	91
Corticosteron (50 nM)	0,43	96	0,41	91
Cortisol (500 nM)	0,35	78	0,40	89
Deoxycorticosteron (700 pM)	0,44	98	0,45	100
DHEA-S (20 µM)	0,41	91	0,40	89
Estradiol (1 nM)	0,40	89	0,36	80
Estron (1 nM)	0,47	104	0,34	76
Insulin (100 pM)	0,45	100	0,42	93
L-Homocystein (50 µM)	0,44	98	0,39	87
Pregnenolonsulfat (15 nM)	0,33	73	0,36	80
Progesteron (100 nM)	0,45	100	0,40	89
T3 (5 nM)	0,47	104	0,45	100
T4 (300 pM)	0,41	91	0,49	109
Testosteron (20 nM)	0,40	89	0,39	87

Die Behandlung der Membran mit 30% Glycerol zeigt keine Änderungen der AC-Aktivität und keine Unterschiede zu den vorausgehenden Versuchen (Tab. 8.4). Bei der nächsten Expression von hAC5 wird 24 h vor der Zellernte 57,7 µM (0,4 g/dl) sterilfiltriertes bovines Serumalbumin (BSA) zugegeben. Diese Konzentration entspricht der Albuminkonzentration durch das vorher in der Zellkultur enthaltene FBS. Serumalbumine binden zahlreiche Hormone und andere weniger polare Stoffe im Blutplasma und es sollte überprüft werden, ob eventuell von FBS übriggebliebene Liganden, die sich in der Zellmembran befinden, durch diese Zugabe vor dem Ernten entfernen lassen.

Tab. 8.5 *Aktivität der hAC5 aus HEK293 nach Zusatz der getesteten Hormone und 300 nM $G_s\alpha$. Die Hormone und Transmitter wurden in der höchsten physiologischen Konzentration eingesetzt (Einzelversuch).*

Probe	*Aktivität [nmol cAMP/mg/min]*	*Aktivität [%]*
Basalaktivität	**0,01**	**1**
300 nM $G_s\alpha$ + 1 µl DMSO	**0,77**	**100**
Aldosteron (500 pM)	0,75	97
Corticosteron (50 nM)	0,83	108
Cortisol (500 nM)	0,82	106
Deoxycorticosteron (700 pM)	0,72	94
DHEA-S (20 µM)	0,97	126
Estradiol (1 nM)	0,67	87
Estron (1 nM)	0,82	106
Insulin (100 pM)	0,89	116
L-Homocystein (50 µM)	0,81	105
Pregnenolonsulfat (15 nM)	0,79	103
Progesteron (100 nM)	0,67	87
T3 (5 nM)	0,77	100
T4 (300 pM)	0,79	103
Testosteron (20 nM)	0,65	84

Es zeigen sich keine signifikanten Änderungen mit den bisher getesteten Substanzen. Da ein Einfluss von FBS während der Zellzucht auf die hAC5 jedoch nicht restlos ausgeschlossen werden kann, wird diese von nun an in serumfreiem Medium in Sf9-Zellen exprimiert.

Tab. 8.6 *Aktivität der hAC5 aus Sf9 nach Zusatz der getesteten Hormone bzw. Neurotransmitter und 600 nM $G_s\alpha$. Die Hormone und Transmitter wurden in folgenden Konzentrationen eingesetzt (Einzelversuch).*

Probe	*Aktivität [nmol cAMP/mg/min]*	*Aktivität [%]*
Basalaktivität	**-**	**-**
600 nM $G_s\alpha$	**4,72**	**100**
C-Peptid (100 ng/ml)	3,55	75
Dopamin (1 mM)	4,44	94
Adrenalin (1 mM)	1,75	37
GABA (1 mM)	4,21	89
Glucagon (1 µM)	2,21	47
Glutamat (1 mM)	4,68	99
Histamin (1 mM)	5,93	126
Insulin (4 µM)	3,60	76
Levodopa (1 mM)	5,66	120
Serotonin (1 mM)	4,58	97

In diesem Einzelversuch zeigt sich lediglich eine starke Hemmung von 63% bzw. 53% der hAC5 durch Adrenalin bzw. Glucagon. Bei Adrenalin handelt es sich um einen Neurotransmitter des Zentralnervensystems (ZNS) und ein im Nebennierenmark gebildetes Hormon, das vor allem über G-Protein-gekoppelte heptahelikale α_2- und β_2-Adrenozeptoren, welche die Herzaktion fördern, das ZNS stimulieren und die Glykogenolyse in den Muskelzellen aktivieren, wirkt. Interessanterweise erfolgt die Synthese von Adrenalin aus L-Tyrosin über Dopamin als Zwischenprodukt, welches in diesem Test keine Wirkung auf die hAC5 zeigt. Beide Substanzen wurden in einer Konzentration eingesetzt, die im Plasma physiologisch nicht vorkommt (1 mM), aber eventuell im synaptischen Spalt erreicht werden könnte. Die Wiederaufnahme und der schnelle Abbau

durch Catechol-O-Methyltransferase (COMT) und Monoaminooxidase (MAO), wodurch eine Halbwertszeit von wenigen Minuten zustande kommt, würden eine lokale, die Plasmakonzentration stark übersteigende Konzentration, ermöglichen.

Glucagon wird in den α-Zellen des Pankreas synthetisiert, in Sekretgranula gespeichert und hat ebenfalls eine durch den schnellen Abbau in Leber, Niere und Blut bedingte Halbwertszeit von wenigen Minuten. Ebenso wie Adrenalin stimuliert es, allerdings nur in der Leber, den Glykogenabbau und fördert die Gluconeogenese, weshalb es als Gegenspieler zu Insulin bezeichnet wird. Diese Wirkung wird durch einen membranständigen G-Protein-gekoppelten Rezeptor vermittelt. Auch hier lag die eingesetzte Menge weit über der physiologischen Konzentration im Blut und kann so theoretisch nur in direkter Nähe zu den sezernierenden Zellen erreicht werden.

8.2.4 Regulation der hAC5: Glucose und Stoffwechselprodukte des Citratzyklus

Gerade in pankreatischen β-Zellen spielt cAMP neben dem Glucose-abhängigen Ca^{2+}-Einstrom eine wichtige Rolle bei der Insulinfreisetzung. Folglich wurde zunächst der Effekt von Glucose auf die $G_s\alpha$-stimulierte hAC5 untersucht.

Um die Übersicht der Ergebnisse zu wahren, wurden nur die $G_s\alpha$-Konzentrationen 300 nM und 600 nM tabellarisch aufgeführt, sowie die höchsten eingesetzten Konzentrationen von Glucose und Ca^{2+}, da bei niedrigeren Konzentrationen keine signifikante Beeinflussung der AC-Aktivität beobachtet wurde.

Die $G_s\alpha$-Konzentration betrug 60 – 600 nM, um sowohl einen stimulierenden als auch inhibierenden Effekt erkennen zu können. Die Glucosekonzentration eines gesunden Erwachsenen liegt postprandial bei < 7,8 mM, bei Diabetes mellitus steigt diese auf Werte zwischen 11,1 – 27,7 mM (82). In den Tests wurde diese bis auf das Vierfache gesteigert.

Intrazellulär schwankt die Ca^{2+}-Konzentration periodisch, weshalb auch die Abhängigkeit der Glucosewirkung von diesem zweiwertigen Kation untersucht wurde. Zudem wird in einigen Arbeiten eine Abhängigkeit der Glucose-induzierten cAMP Erhöhung von Ca^{2+} beschrieben (83,84). Die höchste getestete Calciumkonzentration (0,1 mM) wurde so gewählt, dass die Cyclase, die durch Calcium-Ionen gehemmt wird, noch aktiv genug bleibt, um einen Effekt beobachten zu können (s. Abb. 8.8).

Tab. 8.7 *Übersicht des verwendeten Konzentrationsbereichs von $G_s\alpha$, Glucose und Ca^{2+}.*

Zugabe	*Gemessener Konzentrationsbereich*
$G_s\alpha$	60-600 nM
Glucose	5-100 mM
Ca^{2+}	10-100 µM

Tab. 8.8 *Aktivität der hAC5 aus Sf9 nach Zusatz von Glucose bzw. Ca^{2+} und 300 nM $G_s\alpha$ (Einzelversuch).*

Probe	*Aktivität [nmol cAMP/mg/min]*	*Aktivität [%]*
Basalaktivität	**0,03**	**1**
$G_s\alpha$ (300 nM)	**5,50**	**100**
+ Glucose (100 mM)	6,38	116
+ Ca^{2+} (0,1 mM)	6,01	109
+ Glucose (100 mM) + Ca^{2+} (0,1 mM)	5,37	98

Es zeigte sich keine Beeinflussung der AC-Aktivität. In einem weiteren Test sollte untersucht werden, ob Glucose in Kombination mit anderen Stoffen im Serum die hAC5 hemmen oder stimulieren kann. Dafür wurde unter Zugabe von 300 nM $G_s\alpha$ und Glucose zusätzlich Fetales Kälberserum (FBS), das Kulturmedium der HEK293-Zellen (DMEM + BSA) bzw. die Vierfache physiologische Konzentration an Insulin zugegeben.

Tab. 8.9 *Aktivität der aktiven (300 nM $G_s\alpha$) hAC5 aus Sf9 nach Zusatz von FBS, DMEM + BSA oder Insulin vor und nach Zugabe von Glucose (Einzelversuch).*

	Kontrolle *Ohne Glucose*		*Probe* *50 mM Glucose*	
Zugabe	Aktivität [nmol cAMP/mg/min]	Aktivität [%]	Aktivität [nmol cAMP/mg/min]	Aktivität [%]
Basalaktivität	**0,1**	**2**	**-**	**-**
300 nM $G_s\alpha$	**4,4**	**100**	**3,9**	**89**
+ 25% FBS	1,8	100	1,5	83
+ 25% DMEM + BSA	2,9	100	2,2	76
+ 2 nM Insulin	4,2	100	3,5	83

Auch hier zeigte sich keine veränderte cAMP-Produktion durch die Cyclase.
Da Glucose innerhalb der β-Zellen rasch zu Glucose-6-Phosphat (G-6-P) verstoffwechselt wird, wurden auch G-6-P, Fructose-6-Phosphat (F-6-P), weitere Zucker (Galactose und Fructose) als Kontrolle sowie das Endprodukt des Citratzyklus, Pyruvat, getestet.

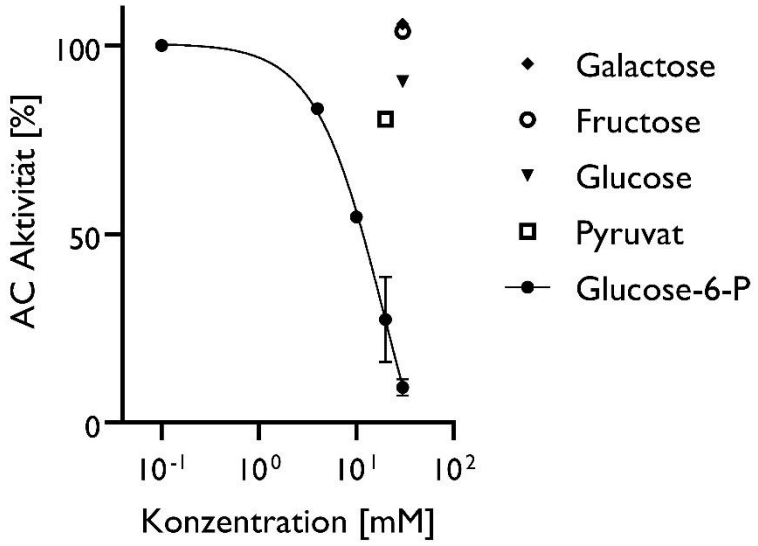

Abb. 8.9 *Hemmende Wirkung von G-6-P (0-30 mM) auf hAC5 aus Sf9-Zellen in Anwesenheit von 600 nM $G_s\alpha$. Andere Zucker wie 30 mM Glucose, 30 mM Galactose, 30 mM Fructose oder 20 mM Pyruvat zeigen keinen Effekt. Eingesetzt wurden 25 µg pro Probe aus einer Expression. Fehlerbalken kennzeichnen SD aus 3-5 Einzelversuchen aus einer Expression.*

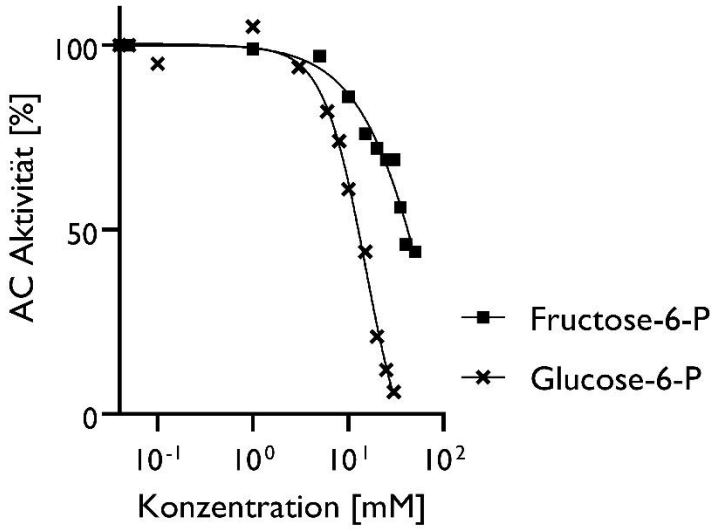

Abb. 8.10 *Hemmende Wirkung durch G-6-P (0-30 mM) und F-6-P (0-50 mM) auf hAC5 aus Sf9-Zellen in Anwesenheit von 600 nM $G_s\alpha$. Eingesetzt wurden 25 µg pro Probe aus einer Expression (Einzelversuch).*

Nur G-6-P und, in geringerem Maße, F-6-P zeigen einen hemmenden Effekt. Diese Wirkung würde vermutlich intrazellulär erfolgen, da die Stoffwechselprodukte nicht sezerniert werden und somit den Membrananker nicht als Liganden von außen erreichen können. Da Glucose und deren Stoffwechselprodukte in der Zelle schnell abgebaut werden, ist zudem nicht garantiert, dass die hemmenden Konzentrationen physiologisch erreicht werden. Am wahrscheinlichsten könnte man derart hohe Konzentrationen in pankreatischen Zellen vermuten. Die darin vorkommende Glucokinase, die Glucose in G-6-P umwandelt, wird, anders als die übrigen Hexokinasen, in ihrer Aktivität nicht durch das Produkt gehemmt.

Bei den Ergebnissen zur Hemmung durch G-6-P und F-6-P handelt es sich um vorläufige Resultate. Es sind umfassende weitere Tests erforderlich, um eine Vermutung über den möglichen Mechanismus äußern zu können. So könnte untersucht werden, ob die hAC5 auch nach Aktivierung durch FSK gehemmt wird, um eine Wechselwirkung zwischen $G_s\alpha$ und den Hexosen auszuschließen. Um einen Angriff an der katalytischen Domäne zu bestätigen, bietet sich die Klonierung einer CqsS-hAC5-Chimäre an, die nachweislich durch $G_s\alpha$ und FSK reguliert wird. Zusätzlich könnte die Wirkung von G-6-P auf andere Isoformen der hACn unter besonderer Berücksichtigung isoformspezifischer IC_{50}-Werte untersucht werden.

Auch wenn diese Beobachtung keinen Hinweis auf die Funktion des Membranankers als Rezeptor liefert, wurde dieser Effekt bisher nicht in wissenschaftlichen Arbeiten beschrieben. Weitere experimentelle Arbeiten könnten zu einem besseren Verständnis der Funktionsweise von hACn und u.U. deren Rolle in der Insulinfreisetzung beitragen.

9. Anhang

Wissig, J. Persönliche Kommunikation E-Mail "WG: Stämme, CyaC" an Grischin, J. am 19.06.2017

Die als persönliche Mitteilung (s. Referenz 62) angegebene Korrespondenz mit Frau J. Wissig im Original, da die Dissertation erst ab Oktober 2020 zugänglich ist.

Hallo Julia,

heute ist mein erster Arbeitstag:-) Die mail konnte ich dir leider nicht weiterleiten, da ich kein Internet hatte. Ich hoffe die Infos kommen noch rechtzeitig.

In der Datei "Histidinvarianten" sind ein paar Infos zu den Proteinproben. Dort findest du auch eine Sequenz, in der markiert ist welche Histidinmutanten ich euch geschickt habe (Zellen BTH101 mit Vektoren pWBT_cyaC H27_A; H31_A; H68_A; H105_A; H149_A sowie WT). Die dazugehörige Sequenz habe ich nicht als Vektorkarte, sondern nur den Insertionsbereich als Word-Dokument ("cyaC construct"), da der Ursprungsvektor von einem Kooperationspartner ist. Angeblich gibt es dazu keine Sequenz und wir konnten dazu auch nichts finden. Die Mutationen habe ich über PCR eingefügt.

Die andere Vektorkarte ist von pET28a_cyaC , mit diesem Vektor wurde das Protein in C43 überproduziert und über Strep isoliert. Das Protein verfügt über 3 Tags insgesamt (His N-term, Flag und Strep C-term).

Du wolltest ja wissen wie du die Zellen züchten musst (BTH101 mit pWBT_cyaC Histidinmutanten). Als Steffi den Wildtypen gemessen hatte, haben wir ihr eine Anleitung geschickt. Die stärkste Aktivität hatten wir in Minimalmedium, allerdings hatte sie unsere Anleitung nicht verwendet und stattdessen in LB-Medium gezüchtet. Du müsstest daher in ihren Laboraufzeichnungen nachschauen, wie genau sie das gemacht hat.

Schreib einfach, falls dir noch was fehlt!

Viele Grüße,

Juliane

Vector pWBT:
pSRKGm (Khan *et al*. (2008) Appl Environ Microbiol. 74, 5053-5062) with T5 promoter cloned into NdeI-XbaI restriction sites

Colour coding:

Genomic sequence
Restriction site used for cloning
3xFlag Tag
T5 promoter region

pWBT-cyaC-CF

CATATGCTTTCGTCTTCACCTCGAGAAATCATA
AAAAATTTATTTGCTTTGTGAGCGGATAACAATTATAATAGATTCAATTG
TGAGCGGATAACAATTTCACACAGAATTCATTAAAGAGGAGAAATCTAGA
ATGACGATCCTATCCGCCAGCACGCGCAAGAAGATGCACCTGATCTCAGG
GGCCGTACTCGGCGTTTTCGTGCTCTTGCACTTCTCGAATCACGCGCTCG
GGCTCGTCTCGATCGATGCGATGGAAACGGGCCGGCGGATATTCACCTCG
GTTTGGCAGAGCATTCCCGGAACGGCCCTCCTCTACGGCGCGCTGCTGCT
GCATTTCCTGATGGCGCTCGACAGTCTCTACCGGCGGCAAACGTTCCGCA
TGCCTGTCGGCGAAGCCCTGAAGATCATCTTCGGCCTGAGTCTGCCCTTT
CTGCTTGTGCCTCACGTGGTCGCCGCCCGCGTGGAGCCGCTTCTTTCAGG
TGTTTATCCAGACTACCCCGCGATCCTGCGCACCCTCTGGTCAAGCTCGT
TCAACACCTCTCGTCAGTCGCTTGCGCTCATCGTCGTCTGGGGTCACGCC
TGTCTTGGCGCCTGGTTCTGGATGCGAGGGCGCGCCTGGTTTCCGAAATA
CGAAACGCTGCTCTATACCGTCGCCCTGCTGGTGCCGATCTTCGCACTGC
TCGGCTTCGTCAACGGCGCCCGTTCACTGGAGCGCGACTACGCGGAACAT
GGCGGTTACGGCGACAGGGCCTATTCCAGCCAGGCACCTCGCGTCGACCC
TAACCTTCTCGATAAGATCAGGCTGGCATTCTATGGCGGCTTCGCAAGCC
TGATCGGCGGCACCCTCGTTCTGCGCGCCCTGCCGGCGCGCGGCCGTATT
CGTATTCGTTATCCGGACGGCCGGGTCGCCGCCGTCAGCCTCGGCTTCAG
CGTTCTGGAGGCCAGCCGGGCGGCCGGAATTCCTCATGTTTCCGTCTGCG
GCGGGCGCGGGCGCTGTTCCACCTGTCGCGTGCGGATAACGCAGGGGCTC
GAAGGCCAGCCGCCGCCGGAAGCTGCAGAACTCGCGACGCTGACCCGCAT
CGGCGCTCCCGAGAACGTACGCCTCGCCTGCCAGTTCCGCCCCGTGCACA
ATGTGAGCGTCGTGCCCATCCTCGACACCGACAGCCTCGGGATCAAGACG
CAGCTTGCCCGCCAGAACGCCGGCGGACGCGAGCGCCGTGTCGCCGTGCT
CTTCTGCGACCTGCGTGATTTCACCCGCATCGCCGAGCACCGGCTGCCCT
ACGACACGGTCTTTCTGCTCAACCGCTATTTCGAAGTCGTCGGCGAAGCC
GTCGAAGGTTCCGGTGGCGTCGTCGACAAGTTCATCGGCGACGGGGCGCT
CGCGATCTTCGGACTGAAGACCCCTCTGCCGGAGGCCTGCCGCCAGGCAC
TTTCGGCCGCCGCCCGGTTGTCGCAGGGAATCCGGGCGCTCAACCAGACC
TTCGAAGGGGAGCTCGAGCAGCCACTGAGGCTCGCCATCGGCCTCCACGC
GGGCCCGGCGATCATCGGCGAAATGGGCTACGGCCAGGCAACCTCGCTCA
CGGTCGTCGGCGACACGATCAATACGGCGAGCCGGCTGGAAGGTCTCGCG
AAGGAGCACGACGTCGAGCTTGCCGTTTCCGCCGAACTGGTCGAGCGCGC
CGGCCTCAGCTTCGAAGGCCACAGACGGCTGGAAATCGGCCTGCGGGGCC
GCAAGGCGACTCTGGAAACCTGGATCATCGGTGACGCGGCGCAGCTCTCG
CTTTCGCTGCCGATGCAGGGTACTAGAGATTACAAGGATCACGATGGTGA
TTACAAGGATCACGATATCGATTACAAGGATGACGATGACAAGTGAAAGC
TTATCGATACCGTCGACCTCGAGGGGGGGCCCGGTACCCAATTCGCCCTA
TAGTGAGTCGTATTACAATTCACTGGCCGTCGTTTTACAACGTCGTGACT
GGGAAAACCCTGGC

pWBT-cyaC

CATATGCTTTCGTCTTCACCTCGAGAAATCATA
AAAAATTTATTTGCTTTGTGAGCGGATAACAATTATAATAGATTCAATTG
TGAGCGGATAACAATTTCACACAGAATTCATTAAAGAGGAGAAATCTAGA
ATGACGATCCTATCCGCCAGCACGCGCAAGAAGATGCACCTGATCTCAGG
GGCCGTACTCGGCGTTTTCGTGCTCTTGCACTTCTCGAATCACGCGCTCG
GGCTCGTCTCGATCGATGCGATGGAAACGGGCCGGCGGATATTCACCTCG
GTTTGGCAGAGCATTCCCGGAACGGCCCTCCTCTACGGCGCGCTGCTGCT
GCATTTCCTGATGGCGCTCGACAGTCTCTACCGGCGGCAAACGTTCCGCA
TGCCTGTCGGCGAAGCCCTGAAGATCATCTTCGGCCTGAGTCTGCCCTTT
CTGCTTGTGCCTCACGTGGTCGCCGCCCGCGTGGAGCCGCTTCTTTCAGG
TGTTTATCCAGACTACCCCGCGATCCTGCGCACCCTCTGGTCAAGCTCGT
TCAACACCTCTCGTCAGTCGCTTGCGCTCATCGTCGTCTGGGGTCACGCC
TGTCTTGGCGCCTGGTTCTGGATGCGAGGGCGCGCCTGGTTTCCGAAATA
CGAAACGCTGCTCTATACCGTCGCCCTGCTGGTGCCGATCTTCGCACTGC
TCGGCTTCGTCAACGGCGCCCGTTCACTGGAGCGCGACTACGCGGAACAT
GGCGGTTACGGCGACAGGGCCTATTCCAGCCAGGCACCTCGCGTCGACCC
TAACCTTCTCGATAAGATCAGGCTGGCATTCTATGGCGGCTTCGCAAGCC
TGATCGGCGGCACCCTCGTTCTGCGCGCCCTGCCGGCGCGCGGCCGTATT
CGTATTCGTTATCCGGACGGCCGGGTCGCCGCCGTCAGCCTCGGCTTCAG
CGTTCTGGAGGCCAGCCGGGCGGCCGGAATTCCTCATGTTTCCGTCTGCG
GCGGGCGCGGGCGCTGTTCCACCTGTCGCGTGCGGATAACGCAGGGGCTC
GAAGGCCAGCCGCCGCCGGAAGCTGCAGAACTCGCGACGCTGACCCGCAT
CGGCGCTCCCGAGAACGTACGCCTCGCCTGCCAGTTCCGCCCCGTGCACA
ATGTGAGCGTCGTGCCCATCCTCGACACCGACAGCCTCGGGATCAAGACG
CAGCTTGCCCGCCAGAACGCCGGCGGACGCGAGCGCCGTGTCGCCGTGCT
CTTCTGCGACCTGCGTGATTTCACCCGCATCGCCGAGCACCGGCTGCCCT
ACGACACGGTCTTTCTGCTCAACCGCTATTTCGAAGTCGTCGGCGAAGCC
GTCGAAGGTTCCGGTGGCGTCGTCGACAAGTTCATCGGCGACGGGGCGCT
CGCGATCTTCGGACTGAAGACCCCTCTGCCGGAGGCCTGCCGCCAGGCAC
TTTCGGCCGCCGCCCGGTTGTCGCAGGGAATCCGGGCGCTCAACCAGACC
TTCGAAGGGGAGCTCGAGCAGCCACTGAGGCTCGCCATCGGCCTCCACGC
GGGCCCGGCGATCATCGGCGAAATGGGCTACGGCCAGGCAACCTCGCTCA
CGGTCGTCGGCGACACGATCAATACGGCGAGCCGGCTGGAAGGTCTCGCG
AAGGAGCACGACGTCGAGCTTGCCGTTTCCGCCGAACTGGTCGAGCGCGC
CGGCCTCAGCTTCGAAGGCCACAGACGGCTGGAAATCGGCCTGCGGGGCC
GCAAGGCGACTCTGGAAACCTGGATCATCGGTGACGCGGCGCAGCTCTCG
CTTTCGCTGCCGATGCAGGGTTGAAGCTTATCGATACCGTCGACCTCGAG
GGGGGGCCCGGTACCCAATTCGCCCTATAGTGAGTCGTATTACAATTCAC
TGGCCGTCGTTTTACAACGTCGTGACTGGGAAAACCCTGGCGTTACCCAA
CTTAATCG

Histidinvarianten cyaC (His_Ala)

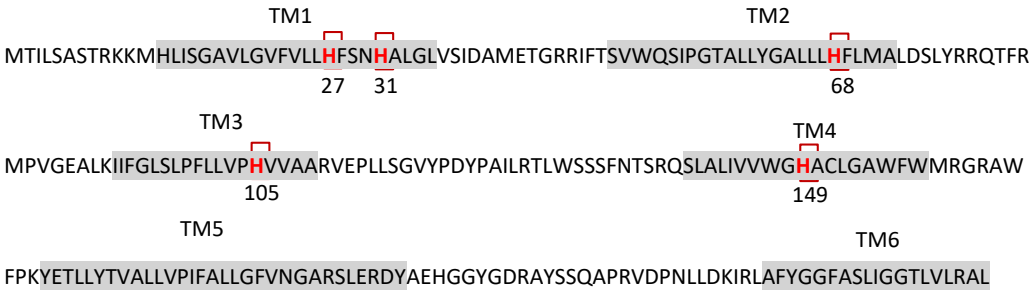

Stamm: BTH101 (Δcya), Strep^{R}
Vektor:
Wildtyp: pWBT_cyaC_3xFlag, Gent^{R}
(WT bereits zugesendet mit Stamminfo und Konstrukt)

Proteinprobe:

- Elutionsfraktion2 (11.04.17); Konz 0,86 µg/µl
(siehe Elutionspuffer)

- Elutionsfraktion4 (24.03.17); Konz 0,8 µg/µl
(ohne DTT in Elutionspuffer, nur in vorherigen Puffern mit DTT)

Solubilisierung: 1% Dodecylmaltosid

Elutionspuffer:
100mM Tris/HCl, pH: 8,0
150mM NaCl
1mM EDTA
1mM DTT
0,05% DDM
2,5mM Desthiobiotin